PB91-185090

Recommended Fine Positioning Test for the Development Test Flight (DTF-1) of the NASA Flight Telerobotic Servicer (FTS)

(U.S.) National Inst. of Standards and Technology (NEL)
Gaithersburg, MD

Feb 91

U.S. Department of Commerce
National Technical Information Service
NTIS

PB91-185090

NISTIR 4478

Recommended Fine Positioning Test for the Development Test Flight [DTF-1] of the NASA Flight Telerobotic Servicer [FTS]

Nicholas Dagalakis
Performance Measures Group

Albert J. Wavering
Intelligent Controls Group

U.S. DEPARTMENT OF COMMERCE
National Institute of Standards and Technology
Robot Systems Division
Bldg. 220 Rm. B124
Gaithersburg, MD 20899

Peter Spidaliere

National Aeronautics and Space Administration
Goddard Space Flight Center
Greenbelt, MD 20771

U.S. DEPARTMENT OF COMMERCE
Robert A. Mosbacher, Secretary
NATIONAL INSTITUTE OF STANDARDS AND TECHNOLOGY
John W. Lyons, Director

NIST

NISTIR 4478

Recommended Fine Positioning Test for the Development Test Flight [DTF-1] of the NASA Flight Telerobotic Servicer [FTS]

Nicholas Dagalakis
Performance Measures Group

Albert J. Wavering
Intelligent Controls Group

U.S. DEPARTMENT OF COMMERCE
National Institute of Standards and Technology
Robot Systems Division
Bldg. 220 Rm. B124
Gaithersburg, MD 20899

Peter Spidaliere

National Aeronautics and Space Administration
Goddard Space Flight Center
Greenbelt, MD 20771

U.S. DEPARTMENT OF COMMERCE
Robert A. Mosbacher, Secretary
NATIONAL INSTITUTE OF STANDARDS AND TECHNOLOGY
John W. Lyons, Director

NIST

Table of Contents

List of Figures

List of Tables

1.0 INTRODUCTION

The purpose of this report is to propose test procedures for the NASA DTF (Development Test Flight)-1 positioning tests of the FTS (Flight Telerobotic Servicer). The unique problems associated with the DTF-1 mission are discussed, standard robot performance tests and terminology are reviewed and a very detailed description of flight-like testing and analysis is presented.

The major technical problem associated with DTF-1 is that only one position sensor can be used, which will be fixed at one location, with a working volume which is probably smaller than some of the robot errors to be measured. Radiation heating of the arm and the sensor could also cause distortions that would interfere with the test.

Two robot performance testing committees have established standard testing procedures relevant to the DTF-1. Due to the technical problems associated with DTF-1 these procedures cannot be applied directly. These standard tests call for the use of several test positions at specific locations. Only one position, that of the position sensor, can be used by DTF-1. Off-line programming accuracy might be impossible to measure and in that case it will have to be replaced by forward kinematics accuracy.

The following flight-like tests were simulated:

1. Teach Mode Control Tests. The accuracy and repeatability of the robot was measured when it moved to a commanded position under teach mode control.
2. Coordinates Transformation Test. The objective of this test was to determine whether the transformation relationship between the sensor coordinate frame and the robot baseframe can be determined with sufficient accuracy despite the sensor small working volume. This test is necessary for any off-line programing and perhaps for the non destructive evaluation of FTS.
3. Off-Line Programming Tests. The accuracy and repeatability of the robot was measured when it moved to a commanded position under off-line programming.
4. Robot Position Resolution Tests.

The data from these tests were analyzed and the results and conclusions are reported. A Forward Kinematics Error Analysis of some of these data was also performed.

2.0 STATEMENT OF THE PROBLEM

The purpose of this report is to standardize definitions and propose test procedures for the DTF (Development Test Flight)-1 positioning tests.

The DTF-1 mission poses a number of technical problems never encountered during earth based robot performance measurements. First, although the design the DTF-1 calibration position sensor has not been decided yet it is expected that it will have a working volume smaller than the off-line programming accuracy of the robot. Second, thermal shifts during the test will cause distortions of the manipulator and sensor, possibly disturbing the tests. Regardless of the technical difficulties, the DTF-1 mission offers opportunities to understand the positioning capabilities of robots in the environment of space.

This report provides the framework about which the DTF-1 flight procedures can be developed to conduct the required fine positioning tests. First, there will be a discussion of the unique problems associated with the DTF-1 mission. This will include a standardization of terminology. Next, a very detailed description of flight-like testing, conducted at NIST, will be presented. Although the experiments conducted were performed on a robot of different design than the DTF-1, the results and techniques used can be extended to the mission. Finally, conclusions and possible future work will be presented.

3.0 DEFINITIONS AND DISCUSSION

In order to avoid confusion, the terminology and definitions for the fine positioning test must be standardized. Terminology and test procedures which were established by the ANSI/RIA (American National Standards Institute / Robotic Industries Association) R15.05 Robot Performance Subcommittee [RIA 90], and/or the ISO (International Organization for Standardization) Industrial Automation Systems Technical Committee ISO/TC 184 [ISO 90] will be maintained throughout this report whenever it is possible. This terminology differs from that in the NASA Requirements Document (SS-GSFC-0043) in the following general ways:

SS-GSFC-0043:

Accuracy - The difference between the actual position of the tool plate and the commanded position in Cartesian space.

Repeatability - The difference between the actual position of the tool plate and the commanded, previously taught position.

ISO:

Unidirectional pose accuracy expresses the deviation between a command pose and the mean of the attained poses when approaching the command pose from the same direction.

Unidirectional pose repeatability expresses the closeness of agreement between the positions and orientations of the attained poses after n repeated visits to the same command pose.

ANSI/RIA:

Static position accuracy is a statistical measure of the spatial deviation between commanded and achieved robot positions.

Positional repeatability is the measure of deviations between achieved robot positions and the mean of those positions after ordering the robot to the same pose N times from the same direction.

The term "pose", used in the above definitions, stands for position and orientation. The terms "attained" and "achieved" also used are equivalent. The term "tool plate" stands for the end of the robot arm tool mounting plate. The position or pose of the robot could be commanded by either off-line programming or teach mode control, depending on the needs of the application. Each of these modes of operation results in significantly different accuracy and repeatability errors.

The physical meaning of these definitions can be explained by using the demonstration plot of Figure 3.1. In this figure it is assumed that the test specifies that the robot moves to a single commanded position represented by point C. In the interest of simplicity we assume

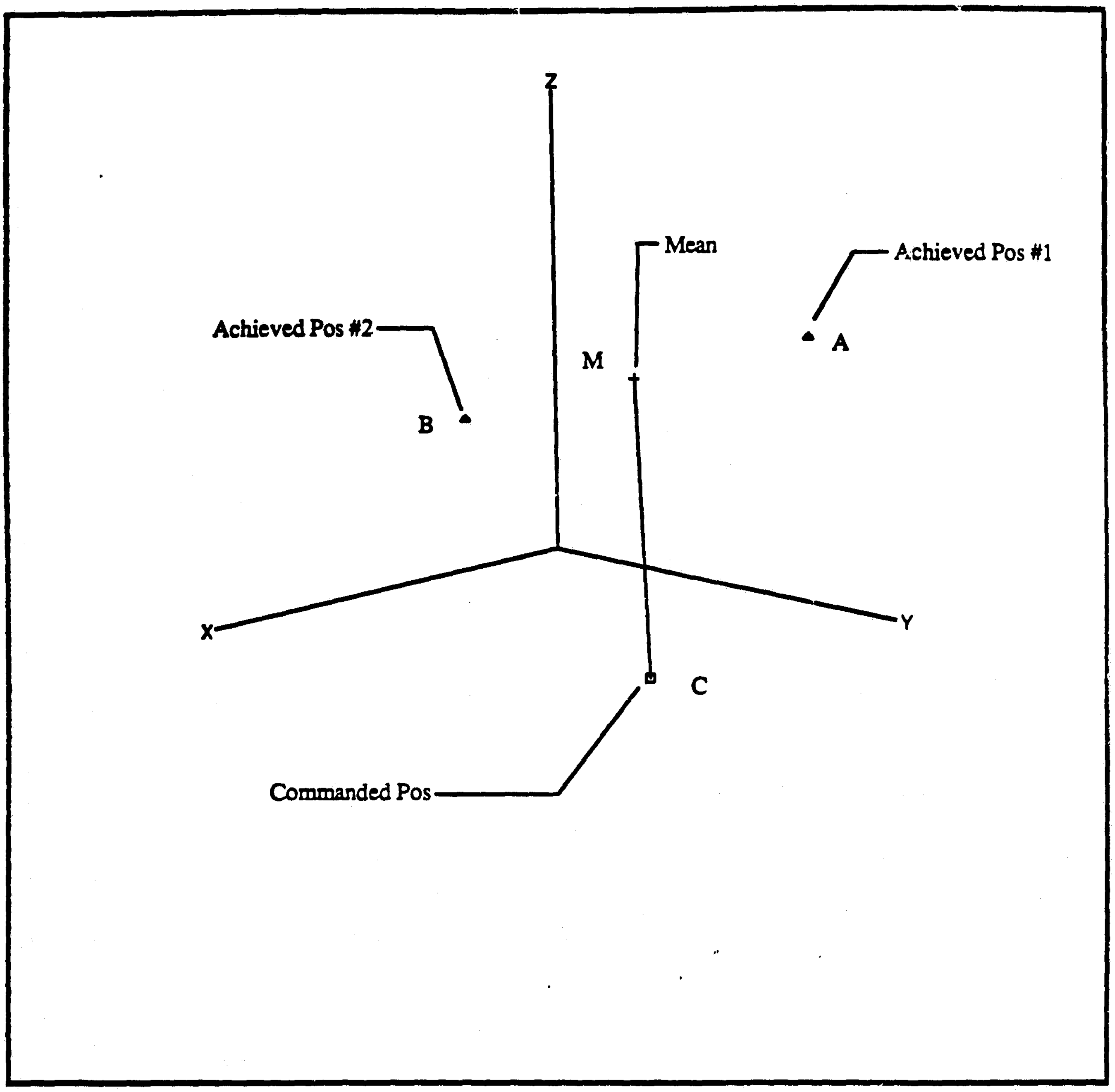

Plot of the PTP Test Achieved Positions
Each triangle is located at an achieved position
The square marks the commanded position
The cross marks the mean of the achieved positions

Figure 3.1 Test results demonstration plot.

here that the robot makes only two attempts to reach that point. During its first attempt to reach that point the robot goes to point A and during its second attempt goes to point B. The mean of those two achieved positions lies at the middle of the AB vector designated by point M in the figure. The positioning accuracy as defined by ISO, for this example, is the magnitude of the vector (CM) given by equations 4.5 and 4.9 in the next section. The positioning accuracy as defined by ANSI/RIA, for this example, is the mean of the magnitudes of the vectors (CA) and (CB) given by equations 4.2 and 4.3 in the next section. The positioning repeatability as defined by ISO, for this example, is the radius of a sphere with center M given by equations 4.13 and 4.12 in the next section, which bounds points A and B. The positioning repeatability as defined by ANSI/RIA, for this example, is the mean of the magnitudes of the vectors (MA) and (MB) given by equations 4.10 and 4.11 in the next section.

The SS-GSFC-0043 definition of accuracy matches the generalized ISO/RIA definition of accuracy under off-line programming and the SS-GSFC-0043 definition of repeatability matches the generalized ISO/RIA definition of accuracy under teach-mode control. Additionally, the generalized ISO/RIA repeatability provides information regarding the statistical behavior of the data gathered during the test.

The objective of the ISO and the ANSI/RIA proposed tests is to cover as much of the robot workspace used during common industrial applications as possible. ISO proposes to fit a cube in the workspace of the robot which is to be tested and then use five points located on one of the diagonal planes of that cube as the test commanded positions. ANSI/RIA proposes the use of the vertices of a standard test path, which is defined by the standard, as the test commanded positions. The test results from all of these commanded positions should be averaged to obtain more representative values of accuracy and repeatability. In the case of DTF-1 only one test commanded position can be used, that of the sensor nest position, and its location is dictated by considerations other than those of these standards.

The ANSI/RIA test specifications require that off-line programming is used to match the test equipment (metrology instrument) coordinate system with the robot base coordinate system for the measurement of accuracy. The ISO test specifications do not have this requirement. Ideally the accuracy capability of a robot under either off-line programming or teach mode control should be measured and be known for the portion of its workspace with the greatest anticipated use. Due to the nature of the sensors to be used during the mission to measure the fine positioning characteristic of the DTF-1 robot, a modified definition of off-line programming accuracy is required. This is due to the fact that the working volume of the sensor nest is smaller than the volume of the cluster of points and the commanded point which would result from a standard off-line accuracy test. In other words, if the robot is commanded to a Cartesian position inside the nest it could arrive outside the working volume of the sensor and, therefore, the position would not be measurable. Because of this, a modified definition of off-line programming accuracy, forward kinematics accuracy, is required. Additionally, the operator will have to initially guide the manipulator into the sensor working volume since a computer command to the location will not necessarily deliver the tool plate to the sensor working volume.

Typically, off-line programming accuracy is measured by commanding the robot to a position and measuring the difference between that command and the actual position measured by some sensor. This technique could be thought of as measuring the inverse kinematic accuracy.

GSFC (Goddard Space Flight Center) and NIST (National Institude of Standards and Technology) have developed another technique by which the same basic information can be gathered. The technique is to send the robot to a position within the working volume of the sensor to measure the tool plates actual position and simultaneously query the robot regarding its perceived position. We call this the forward kinematic accuracy. If there is good agreement between the forward and inverse kinematic solutions, the off-line accuracy using this technique should be approximately the same as the standard, inverse kinematic technique. The result will be approximate since the standard test combines the two sources of error, errors due to inaccurately modeled kinematics and errors due to servo control inaccuracies. The forward kinematic, off-line programming accuracy includes only kinematic modelling errors, which should dominate the DTF-1 errors. The two techniques should agree everywhere within the workspace except near singularities where inverse kinematic equations are not well behaved. Because of the limited range of the sensor, the forward kinematic approach will be taken during the DTF-1 mission.

In addition to what SS-GSFC-0043 refers to as accuracy and repeatability, the document specifies incremental motion requirements. Incremental motion is not defined by either ISO or RIA but is commonly referred to as resolution. For the purposes of this report incremental motion shall be defined as the smallest controllable Cartesian displacement and orientation change of the manipulator tool plate coordinate frame with respect to the manipulator base coordinate frame. Incremental motion shall be calculated using the same set of equations specifying accuracy.

4.0 EQUIPMENT SET-UP, TEST PROCEDURES, ANALYSIS AND RESULTS

4.1 Introduction

The objectives of the experimental work were to simulate the FTS performance test procedure and to develop analysis and display software. Since neither the FTS robotic arm nor the sensor nest are currently available, it was decided to use robot equipment with performance characteristics similar to those specified for FTS.

A variety of test procedures were simulated and a large number of data were collected. Based on the results of the analysis several of these tests were repeated and test conditions were modified in order to clarify questions which were raised by the analysis of the data.

For the analysis of the data and display of the results a NIST robot testing and calibration workstation was used. The workstation was interfaced with the controllers of the robot arm and the metrology instrument used in order to facilitate the collection and exchange of data. New software had to be written and old robot performance analysis programs had to be modified in order to satisfy the peculiarities of the FTS tests.

This section is organized as follows. First, the experimental equipment used to conduct the simulated performance tests is described. This is followed by a discussion of some general procedural aspects which were common to all tests. Next, details of individual test procedures, results, and analyses are presented.

4.2 Equipment Set-Up

The simulated FTS performance tests were performed in the lab of the Intelligent Controls Group (ICG) at NIST. The following equipment was used to perform the tests:

Robotics Research Corp. (RRC) K-1607[1] dextrous manipulator and controller
NIST robot control system target hardware (VME backplane and boards)
NIST control system software development and user interface workstations (Sun 3/160's)
Automated Precision, Inc. (API) Smart 310 laser tracker metrology system
Robot testing and calibration workstation (Macintosh II)

The equipment and system interconnections are shown in Figure 4.1. Each piece of equipment is discussed in detail below.

The RRC K-1607 is a 7 degree-of-freedom kinematically redundant manipulator. The manipulator base is mounted at 45-degrees to the floor, as shown in Figure 4.1. The K-1607 drive system consists of permanent-magnet dc motors with harmonic drive gear reduction. Position and velocity feedback are provided by brushless resolvers driven by anti-backlash gearing. The resolvers measure the joint output position, rather than the motor shaft position. An integral torque sensor on each joint provides output torque information which is used in a feedback loop to minimize the effects of drive nonlinearities (friction and compliance in particular). A Servo Level Interface is provided by RRC which allows an external computer system to issue joint torque, position, velocity, or motor current commands to the manipulator every 2.5 ms [Eissmann 89]. Position, velocity, and torque feedback values updated at this rate are also available. Servo Level Interface variables may be accessed via common memory locations on the Multibus backplane which resides in the RRC controller.

All motions performed during the tests were generated and controlled by the NASREM (NASA/NBS Standard Reference Model for Telerobot Control) control system being developed by the Intelligent Controls Group (ICG) at NIST [Albus 87, Fiala 89a]. This control system is being implemented in Ada, and is based on the concept of a hierarchical organization of redistributable cyclically-executing processes which communicate via common memory buffers. The system runs on (currently) five Motorola 68020-based single-board computers which reside in a VME backplane. A high-speed (225 kbaud) serial link is used to transfer command and feedback information between the ICG control

1 "Certain commercial equipment, instruments or materials are identified in this paper in order to adequately specify the experimental procedure. Such identification does not imply recommendation or endorsement by the National Institute of Standards and Technology, nor does it imply that the materials or equipment identified are necessarily the best available for the purpose".

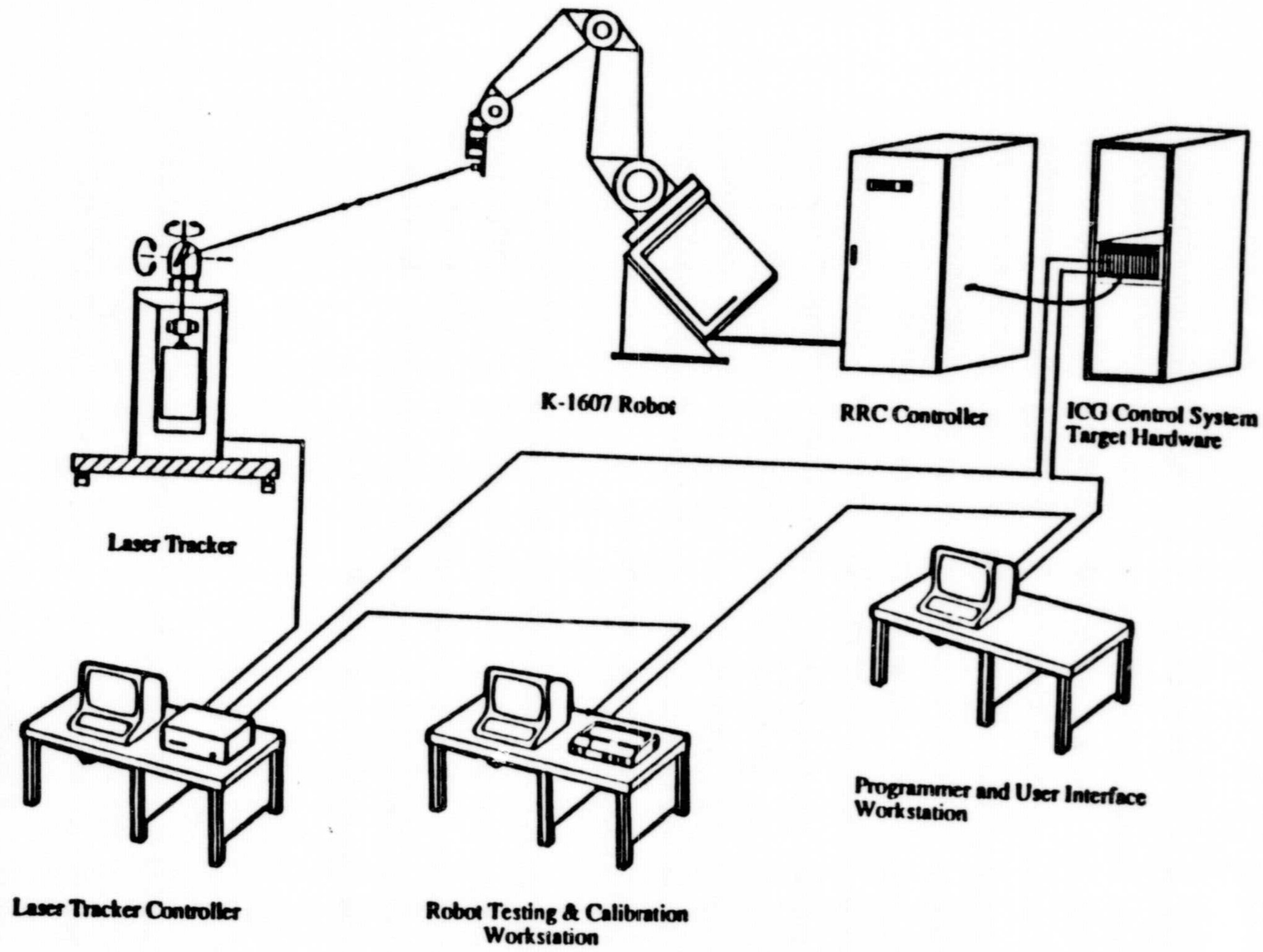

Figure 4.1 Schematic of the equipment set-up.

system and the RRC backplane on a 5 ms basis (ie, every other RRC cycle) [Fiala 89b]. Sun 3 workstations are used for software development and for user interaction with the system during runtime. Communication between the Sun(s) and the target boards for keyboard and file i/o takes place over 9600 baud serial lines.

The current implementation of the NASREM hierarchy consists of Primitive (trajectory generation) and Servo levels. Detailed information about the design of these levels may be found in [Wavering 88, Fiala 88]. These levels provide a number of different algorithms for trajectory generation and manipulator servoing. Two different trajectory generation algorithms are used for metrology test motions; one for joint space motions, and one for Cartesian straight line motions. For motions to goal poses specified in terms of desired joint positions, joint-interpolated quintic polynomial trajectories are used [Craig 86]. Joint space trajectory functions are evaluated every 5 ms. For Cartesian goal poses (represented as a 3 dimensional position vector and a quaternion rotation), quintic polynomial functions of the Cartesian variables are used. Cartesian trajectory functions are evaluated every 25 ms. The Cartesian trajectory points are transformed into joint space before commanding them to the Servo level. An inverse kinematics algorithm based on the augmented Jacobian [Seraji 89, Kreutz 89] is used to perform this transformation.

Although other algorithms are available, a high-gain individual joint PID servo was used for all of the metrology tests. This algorithm was used because of the high stiffness and disturbance rejection it provides. Gravity compensation torques are added to the error-based torques to counteract the effects of link masses in a 1-g environment. The following control equation is computed for each joint, each cycle of Servo execution:

$$\tau = K_p(\theta_d-\theta)-K_v\dot{\theta}+K_i\left(\int\theta_{err}\right)+\tau_{grav} \quad (4.1)$$

where τ = torque commanded to robot, K_p, K_v, K_i = position, velocity, and integral gains, θ_d = desired joint position, θ = actual position, $\dot{\theta}$ = actual joint velocity, $\int\theta_{err}$ = integral of position error, τ_{grav} = gravity compensation torque.

There is no deadband in the algorithm; that is, every error, no matter how small, is multiplied by the appropriate gain to determine a correcting torque. However, residual Coulombic friction outside the torque loop (bearing and seal friction) prevents very small torques from causing arm motion. Except where otherwise noted, the following gains were used for all metrology tests:

$K_p = diag[30000\ 30000\ 16000\ 12500\ 1700\ 2000\ 500]$ N-m/rad

$K_v = diag[800\ 800\ 350\ 250\ 70\ 80\ 50]$ N-m-s/rad

$K_i = diag[1000\ 1000\ 500\ 500\ 170\ 200\ 50]$ N-m/rad-s

These gains were determined experimentally. The around-the-loop time for this algorithm, including communication time, is 10 ms (although commands and feedback are updated every 5 ms).

The system has a simple user interface which allows motion commands to be specified from the keyboard or from a data file. The command information for the metrology test motions includes the following:

Command parameter	Comments on use for metrology tests
Trajectory algorithm	joint_quintic or Cartesian_quintic
Goal pose	desired joint positions or end plate Cartesian position and orientation with respect to base coordinates
Redundancy resolution	Cartesian_quintic only; specifies to use the augmented Jacobian-based inverse kinematics along with the desired elbow plane angle
Traversal time	desired duration of motion

For each motion, the user can also indicate whether or not position information is to be recorded when the motion is complete. If the final position is to be recorded, the user interface process delays for 1 s, reads the joint and Cartesian feedback buffers, stores this information, signals the laser tracker system to record data for the point, and delays for 2 s before continuing to the next command.

The position of the origin of the robot arm mechanical interface coordinate system, located on the end-of-arm mounting plate, was monitored with a laser tracker metrology system [K. Lau 85, API 90]. This system can direct a laser beam to a retroreflector target and determine its three dimensional space spherical coordinates, using an interferometer and precision encoders. As the target is moving, the laser tracker servoes the mirror which reflects the laser beam to keep it pointing on the target all the time. As long as the beam stays within the acceptance angle of the target, and the speed and acceleration of the target do not exceed certain limits set by the laser tracker servo-drive system and controller, the target is continuously tracked. The controller of the laser tracker can be directed to continuously sample and save the position coordinates of the retroreflector target at a frequency of up to 450 Hz, or sample only when directed to do so. The sample command signal can come from the keyboard or from a direct connection to an external controller.

A hollow cornercube retroreflector target was used for all the tests. A special fixture was built in order to mount the target to the interface plate of the robot arm (end-of-arm plate). The fixture had a weight of 1.715 Kg (3.773 lb), an axial offset of approximately 25 mm (1 in) and a radial offset which was essentially 0 mm (0 in). A 90-degree angle bracket was also built and used for the dimensional calibration of the target mounting fixture. An aluminum calibration bar was used for the initialization of the laser tracking system. Two target mounting locations were machined on the bar and their distance was measured with a coordinate measurement machine. The bar was clamped in a fixed location close to where measurements would be made.

A newly-developed robot testing and calibration workstation was used to analyze the data . The workstation has several basic communication programs and two ports, which allow it to exchange commands and data with robot and the laser tracker controllers. Ordinarily the workstation is connected to the communication ports of the robot and laser tracker controllers and coordinates the test activities. This is usually done by commanding the robot to execute the command programs required at each stage of the test and then waiting until the robot controller acknowledges the completion of the execution of these commands. The workstation either collects continuously sampled position data from the laser tracker controller or commands it to sample and store such data. Once that is completed any necessary processing of the data is done and the next step of the test is initiated. The robot command programs usually reside in the robot controller, so that the workstation action only involves their activation, thus minimizing the possibility of unpredictable robot behavior due to bad communications.

In the present set-up, however, it was decided to have the robot control system initiate all data collection actions via a direct connection to the metrology instrument controller. Although this means that the software used to conduct the test and record points is very robot specific, it was felt that it would more accurately simulate the way the FTS control system will perform these tests in space. In addition, the time delay between the end of the robot arm motion and the measurement of the position of the target is somewhat reduced with this approach. As mentioned in the discussion of the robot control system, each time the laser tracker controller was signalled to store a point, the robot control system also stored joint position and target Cartesian position information computed using forward kinematics. This robot control system position data was sent to the robot testing and calibration workstation after test completion via a serial line connected between the Macintosh II and the Sun 3 workstations.

4.3 Test Procedures

In designing the FTS performance test procedures it was desired to follow those recommended by the ANSI/RIA (American National Standards Institute / Robotic Industries Association) R15.05 Performance Subcommittee [RIA 90], and/or the ISO (International Organization for Standardization) Industrial Automation Systems Technical Committee ISO/TC 184 [ISO 90]. Unfortunately this was not possible because of the constraints of the present FTS environment, particularly the requirement that the position and orientation (pose) of the end-effector is measured at only one or two specific locations in the robot workspace where sensor nests will be located. Thus, only basic ideas from the two standard tests were used. Both the RIA and the ISO static PTP (Point-to-Point) accuracy and repeatability tests require the robot to move to various measurement positions, which are specified for the workspace of each robot, and the achieved poses are measured by appropriate robot metrology instruments. Each committee has selected a different set of points. The standard path between those points is also different, and the orientation can be random or fixed depending on the type of the test.

In the present test study only one measurement position was used, instead of the several positions specified by [RIA and/or ISO 90], because of the sensor nest limitations mentioned previously. The coordinates of the sensor nest location used for the current tests, with respect to the baseframe of the FTS arm, were provided by the FTS contractor and are shown in Figure 4.2. Although there was no actual sensor nest, all measurements were taken with the manipulator in the vicinity of the location where a sensor nest would be if the RRC robot were mounted horizontally (instead of at 45 degrees) as the right arm of the FTS. This position will be referred to as the simulated sensor nest or S2 in the

Not to scale

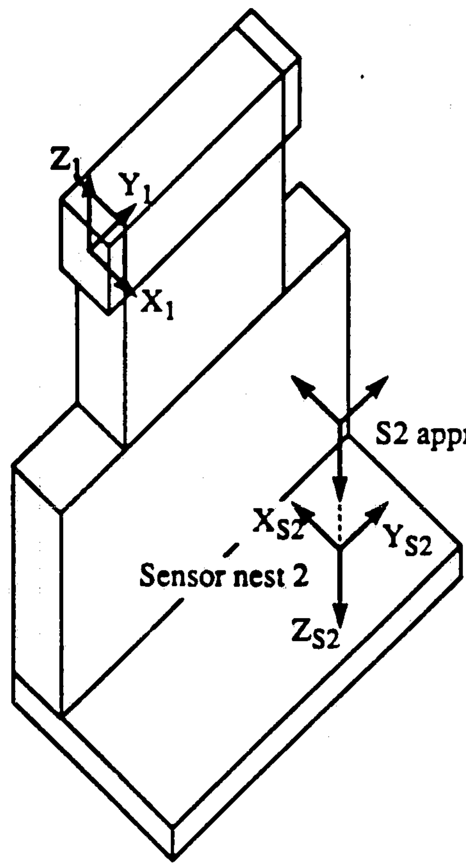

S2 location (with respect to $X_1Y_1Z_1$): (14.0, 28.0, -43.5, +180.0, 0.0, +180.0) (in, deg)

Figure 4.2. Location of sensor nest #2.

descriptions of the tests. Another position used for many of the tests is an approach point for the simulated sensor nest. At this point the robot arm interface plate has the same orientation as at S2, and is displaced about 0.46 m (18 in) along the -Z axis of the S2 coordinate frame. At the time these tests were performed, the design of the sensor nest dictated that such an approach point be used in moving into and out of the nest. The S2 approach position will be referred to as $S2_{app}$.

Although the RIA and ISO standard test positions were not used as measurement locations, they were used in many of the accuracy and repeatability tests as starting positions for motions that ended at the simulated sensor nest. These initial positions were used to assess how well the robot could move to a particular location from different areas of the workspace. The arm was commanded to move sequentially from each one of the vertices of the RIA standard path to the approach point, and from there to the measurement position. The RIA measurement positions were chosen instead of the ISO measurement positions as more representative of the positions where FTS will perform most of its work. The coordinates of the vertices of the RIA standard path were calculated based on a simple robot workspace size measurement test and the specifications provided by [RIA 90]. As with S2 and $S2_{app}$, these positions were transformed to account for the 45-degree mounting of the robot. Only eight of the standard test positions, out of twelve, fell within the workspace of the robot used and were used for the tests. The same end plate orientation was used at each of the standard positions.

A variation of this procedure was used for some tests, in which the robot was commanded to move directly from $S2_{app}$ to S2 and back for each of eight repetitions, without using the RIA positions as starting locations. This alternative was examined out of concern that the test which uses the standard test positions would take more time than is available.

The laser tracker was placed at a distance of approximately 2000 mm from the simulated sensor nest location. Figure 4.3 shows the relationship between the reference coordinate systems of the robot and the laser tracker. Although the Z axis of both coordinate systems is in the same direction, the X-Y plane of the laser tracker coordinate frame is about 450 mm above the robot base coordinate frame. Also shown is the relative X-Y location of the simulated sensor nest, S2. The Z position of the laser tracker target at S2 is about 620 mm below the X-Y plane of the robot base coordinate frame. During the tests the distance between the target, which was mounted on a fixture attached to the robot arm interface plate, and the laser tracker head varied from approximately 1500 mm to 3500 mm.

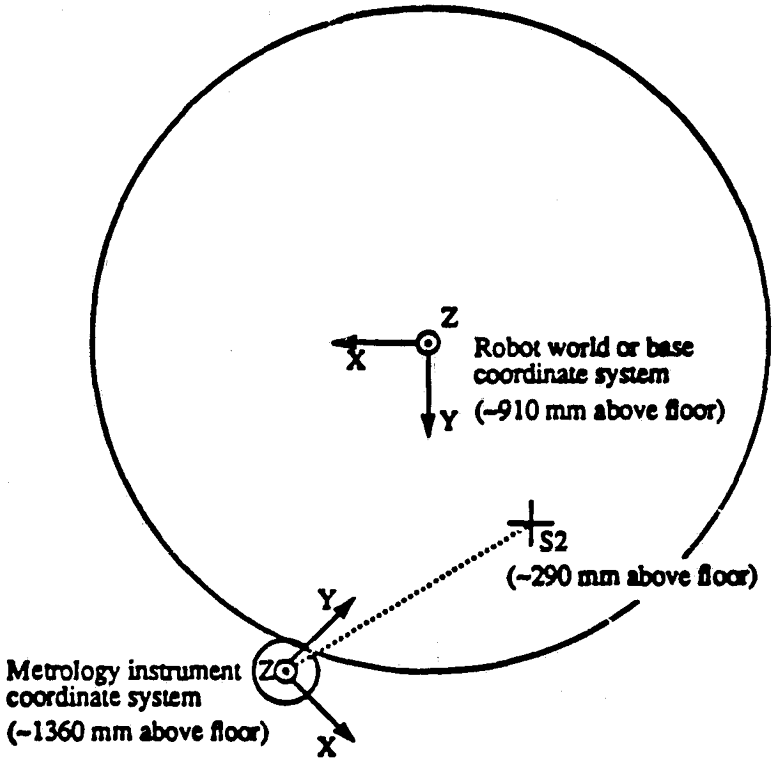

Figure 4.3 Relative locations of coordinate systems.

The laser tracker was initialized, before its use, with the help of the calibration bar. This was done in the following way. The laser beam was first locked on the target, then the target was moved from one of the bar target mounting locations to the other and the known distance was communicated to the laser tracker controller. Based on that information the controller calculated the radial distance to the two bar target mounting locations. The target could then be moved to its mount at the end of the arm for the performance test. As long as the laser beam was not broken or tracking was not lost the tracker would provide the three dimensional coordinates of the target at a maximum sampling frequency of 450 Hz. Throughout the tests the calibration bar was fixed and the laser tracker was not moved. To reinitialize, therefore, it was only necessary to provide the laser tracker controller with the previously-determined radial distance and check that the azimuth and elevation angles were the same as those measured during the first initialization.

The accuracy of the operation of the laser tracker was checked from time to time with the following tests:

1. Lock the beam on the target and record the azimuth and elevation angles. Without moving the target rotate the head of the laser tracker by 180 degrees (rotation about the azimuth axis) and the reflecting mirror by 180 degrees (rotation about the elevation axis) lock on the target and record the azimuth and elevation angles. The difference in the values of the angles before and after the rotation should be 180 degrees plus or minus an error.
2. Lock the beam on the target, switch to spherical coordinates and observe the fluctuations in the values of the radial distance, the azimuth and elevation angles. As long as there are no significant air flow velocity and temperature changes and the target remains fixed the fluctuations should be random and no systematic drift should be observed.
3. Initialize the laser tracker and then move the calibration bar to a new location. Move the target from one of the bar target mounting locations to the other and record the coordinates of the two locations. Calculate the distance between the two mounting locations and compare it to the previously measured distance, during its manufacturing, with high precision metrology instruments.
4. Initialize the laser tracker and record the coordinates of one of the two bar target mounting locations. Move the target away from that location and then return and put it back in the same location. Compare the coordinates measured before and after the move.

Due to small amplitude oscillations of most robot arms, even under steady state static conditions, the laser tracker is usually programmed to sample several times the position of the target and then average to obtain the coordinates for a single position observation. An experiment was performed and it was found that the robot used for the tests had no measurable amplitude oscillations, under steady state static conditions, at the simulated location of the sensor nest. It was then decided not to average the target position samples for all the tests reported here. This has the advantage of reducing the duration of the tests and of revealing the effects of any motion overshoots or undershoots.

The metrology tests described here were performed on April 10-May 14, 1990. The power to the laser was turned on and kept on for the entire duration of the tests. The robot was warmed up by running an exercise program for at least an hour prior to test execution. The only payload attached to the arm for all of the tests was the laser tracker target and its mounting bracket. The ambient temperature was 22-24 degrees C, and relative humidity was in the range of 45-55%.

Note: In the following sections, the coordinates X, Y, and Z referred to in the analysis of the data refer to laser tracker coordinates, unless otherwise noted.

4.3.1 Teach Mode Control Tests

The teach programming control mode is the predominant robot arm programming mode used today. It involves moving the robot arm to the desired locations, manually, through a teach pendant, or the keyboard. Once the robot arm is at a desired location the joint angles corresponding to that location are recorded. In the majority of the cases when the program is played back the robot arm is commanded to go back to the prerecorded joint angles, although sometimes it might be more convenient to use the calculated Cartesian coordinates, which correspond to those joint angles.

The main part of the FTS performance test will consist of teach mode control moves, in which the robot arm will be commanded to move from one or more initial positions to one or more previously-taught sensor nest locations. The objective of the tests was to measure the accuracy and repeatability errors of a robot arm when it is trying to reach the simulated FTS sensor nest location under teach mode control from the simulated initial positions. It was also desired to investigate the error variation as a function of the number of the test cycles, as well as the variation and drift of the achieved position.

The taught position used for the teach mode tests was S2. The eight RIA initial positions are used so that the robot moves through a large portion of the useful workspace during the test. The overall procedure of the tests is as follows:

Move to initial position
Move to $S2_{app}$
Move to S2
Record position data
Move to $S2_{app}$
Repeat above sequence for each different initial position

The completion of the above sequence for all initial positions constitutes performance of one test cycle. The duration of the $S2_{app}$-to-S2 motions was 15 seconds, resulting in an approximate *average* Cartesian velocity of 30 mm/s (1.2 in/s). This is quite slow, although it is probably representative of how fast the arm will move to the sensor nest position on DTF-1. Each repetition of this sequence takes about 6 min.

The Static Position (PTP motion) Accuracy, "is a statistical measure of the spatial deviation between commandec ɔd achieved robot positions", [RIA 90]. The testing and calibration workstation calculates and prints the accuracy errors as defined by both [RIA 90] and [ISO 90]. The formulas used are the following:

$$dPA = \frac{1}{N}\sum_{i=1}^{N} d_i \ . \quad (4.2)$$

$$d_i = \sqrt{(x_{ai}-x_c)^2+(y_{ai}-y_c)^2+(z_{ai}-z_c)^2} \ . \quad (4.3)$$

$$SPA = \sqrt{\frac{\sum_{i=1}^{N}(d_i-dPA)^2}{N-1}} \ . \quad (4.4)$$

$$\text{DeltaL} = \sqrt{(\bar{x}-x_c)^2+(\bar{y}-y_c)^2+(\bar{z}-z_c)^2} \quad . \quad (4.5)$$

$$\text{DeltaL}_x = \bar{x}-x_c \quad . \quad (4.6)$$

$$\text{DeltaL}_y = \bar{y}-y_c \quad . \quad (4.7)$$

$$\text{DeltaL}_z = \bar{z}-z_c \quad . \quad (4.8)$$

$$\bar{x} = \frac{1}{N}\sum_{i=1}^{N} x_{ai} \; ; \; \bar{y} = \frac{1}{N}\sum_{i=1}^{N} y_{ai} \; ; \; \bar{z} = \frac{1}{N}\sum_{i=1}^{N} z_{ai} \quad . \quad (4.9)$$

Where:

dPA, is the Positional Accuracy as defined by RIA, except that in this case only one measurement (commanded) position was used, the simulated sensor nest location.

N, is the number of measurement test cycles used.

d_i, is the magnitude of the accuracy error deviation at the ith measurement.

x_{ai}, y_{ai}, z_{ai}, are the coordinates of the ith measured (achieved) position.

x_c, y_c, z_c, are the coordinates of the commanded position, in this case the simulated sensor nest location.

SPA, is the standard deviation of dPA.

DeltaL, is the Unidirectional Positioning Accuracy as defined by ISO, except that in this case only one measurement (commanded) position was used, the simulated sensor nest location. It should be called unidirectional because the final approach to the commanded position is always from the same direction.

$\bar{x}$, $\bar{y}$, $\bar{z}$, are the coordinates of the mean of the N measured (achieved) positions.

The Positional Repeatability, "is the measure of deviations between achieved robot positions and the mean of those positions after ordering the robot to the same pose N times", [RIA 90]. The testing and calibration workstation calculates and prints the accuracy errors as defined by both [RIA 90] and [ISO 90]. The formulas used are the following:

$$\text{rREP} = \frac{1}{N}\sum_{i=1}^{N} m_i \quad . \quad (4.10)$$

$$m_i = \sqrt{(x_{ai}-\bar{x})^2+(y_{ai}-\bar{y})^2+(z_{ai}-\bar{z})^2} \quad . \quad (4.11)$$

$$SREP = \sqrt{\frac{\sum_{i=1}^{N}(m_i-rREP)^2}{N-1}} \quad . \quad (4.12)$$

$$r = rREP + 3\ SREP \quad . \quad (4.13)$$

Where:

rREP, is the Repeatability as defined by RIA, except that in this case only one measurement (commanded) position was used, the simulated sensor nest location.

m_i, is the magnitude of the deviation at the ith measurement from the mean of the N measured (achieved) positions.

SREP, is the standard deviation of rREP.

r, is the Unidirectional Repeatability as defined by ISO, except that in this case only one measurement (commanded) position was used, the simulated sensor nest location. It should be called unidirectional because the final approach to the commanded position is always from the same direction.

The orientation accuracy and repeatability errors of the interface plate of the robot arm could not be measured with the laser tracker available at the present time.

4.3.1.1.a Teach mode joint angles kinematics control

For this version of the accuracy and repeatability tests, joint interpolated motion was used to move to all positions. The RRC controller was used to obtain equivalent joint positions for S2, $S2_{app}$, and the initial positions. The test was repeated seven times, resulting in 56 recorded points. Before running the tests, the robot was moved to the nominal S2 position, and the robot joint angle positions and laser tracker readings for this position were recorded to use this as the taught point. The actual joint values which were recorded for this point were then used as command angles for S2 for executing the tests.

4.3.1.1.b Analysis and Conclusions

The laser tracker coordinates of the 56 measured positions were divided into 7 analysis groups. The first group contained the coordinates of the first 8 measured positions, which correspond to the first 8 cycles (8 vertices of the RIA standard path) of the test. The second group contained the coordinates of the first 16 measured positions. The third group contained the coordinates of the first 24 measured positions, etc., so each subsequent group contained the coordinates of the previous group plus the coordinates of the next 8 positions until all 56 were included. The data contained in each group were analyzed separately and the results of the analysis were used to determine the effect of the number of measured positions on the results.

Table 4.1 in the Appendix shows the results of the analysis of the last group of data which contains all 56 measured positions. First, the laser tracker measured coordinates of the commanded, previously taught, position are printed. The dimension of the coordinates are in mm as are all the dimensions in all the tables and plots reported here. Then the coordinates of the laser tracker-measured achieved positions are printed. Finally the ISO and RIA defined accuracies and repeatabilities are calculated and printed.

Figure 4.4 is a three dimensional plot of the measured achieved positions (triangular marks), their mean position (cross mark), and the commanded position (square mark). The coordinate frame in that figure is that of the laser tracker after it was translated to the centroid of those positions.

Figure 4.5 is a plot of the same positions as they are projected on a plane defined by the X and Z coordinate axes. As can be seen the cluster of points forms a "galactic cloud" with an orientation which is approximately orthogonal to the orientation of the axis of the first joint of the robot arm. Because of that, it is suspected, although it has not been verified, that positioning errors from the first joint drive are mostly responsible for the measured repeatability errors. To reach the simulated sensor nest position the arm has to extend itself significantly thus making it sensitive to angular errors from the first joint drive. The points also seem to be oriented in neat rows and columns. This is because their distances are very small and they have been positioned at the resolution-limited positions of the laser tracker instrument.

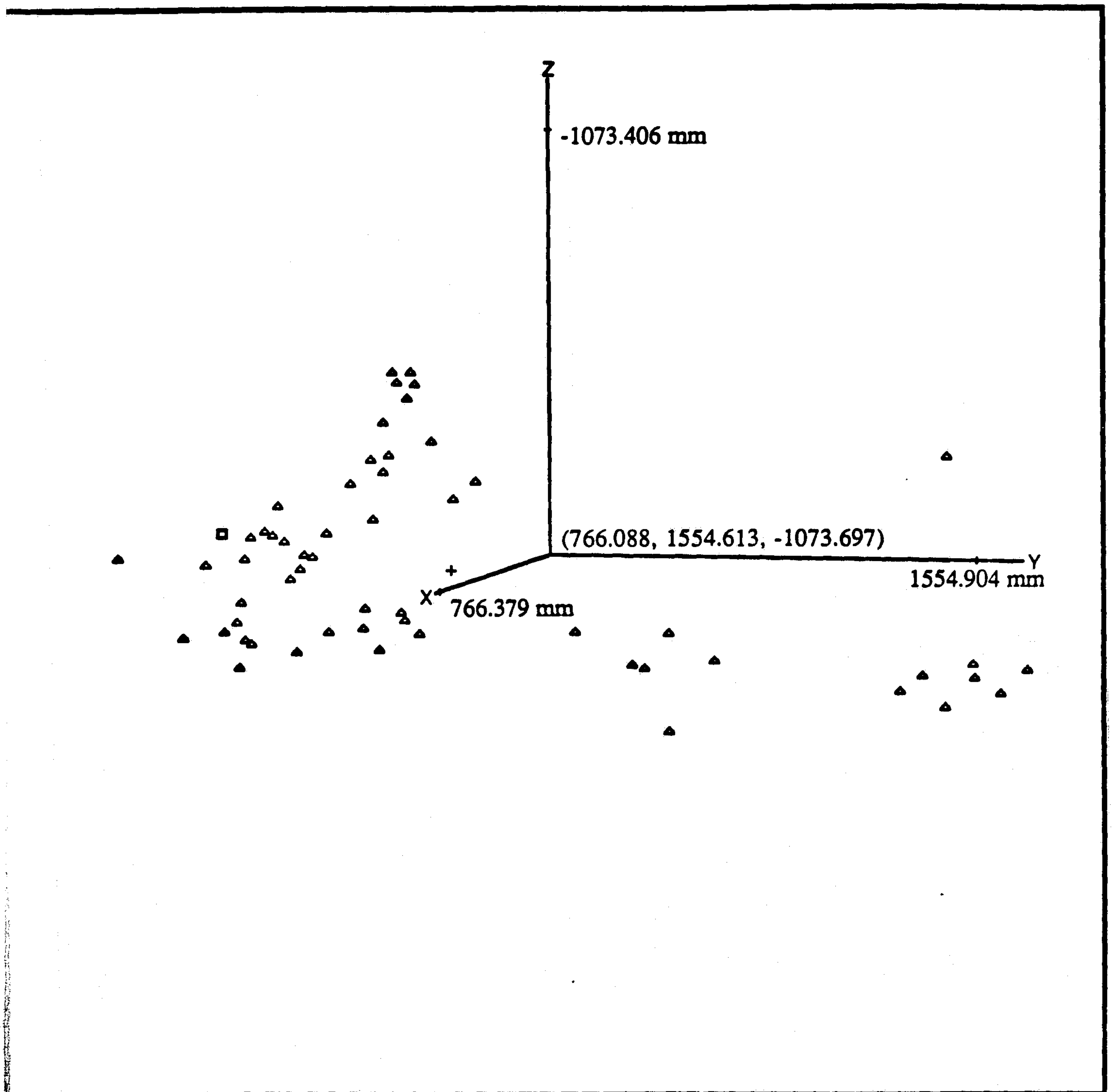

Plot of the PTP Test Achieved Positions
Each triangle is located at an achieved position
The square marks the commanded position
The cross marks the mean of the achieved positions

Figure 4.4 Teach mode joint angles kinematics control positions plot.

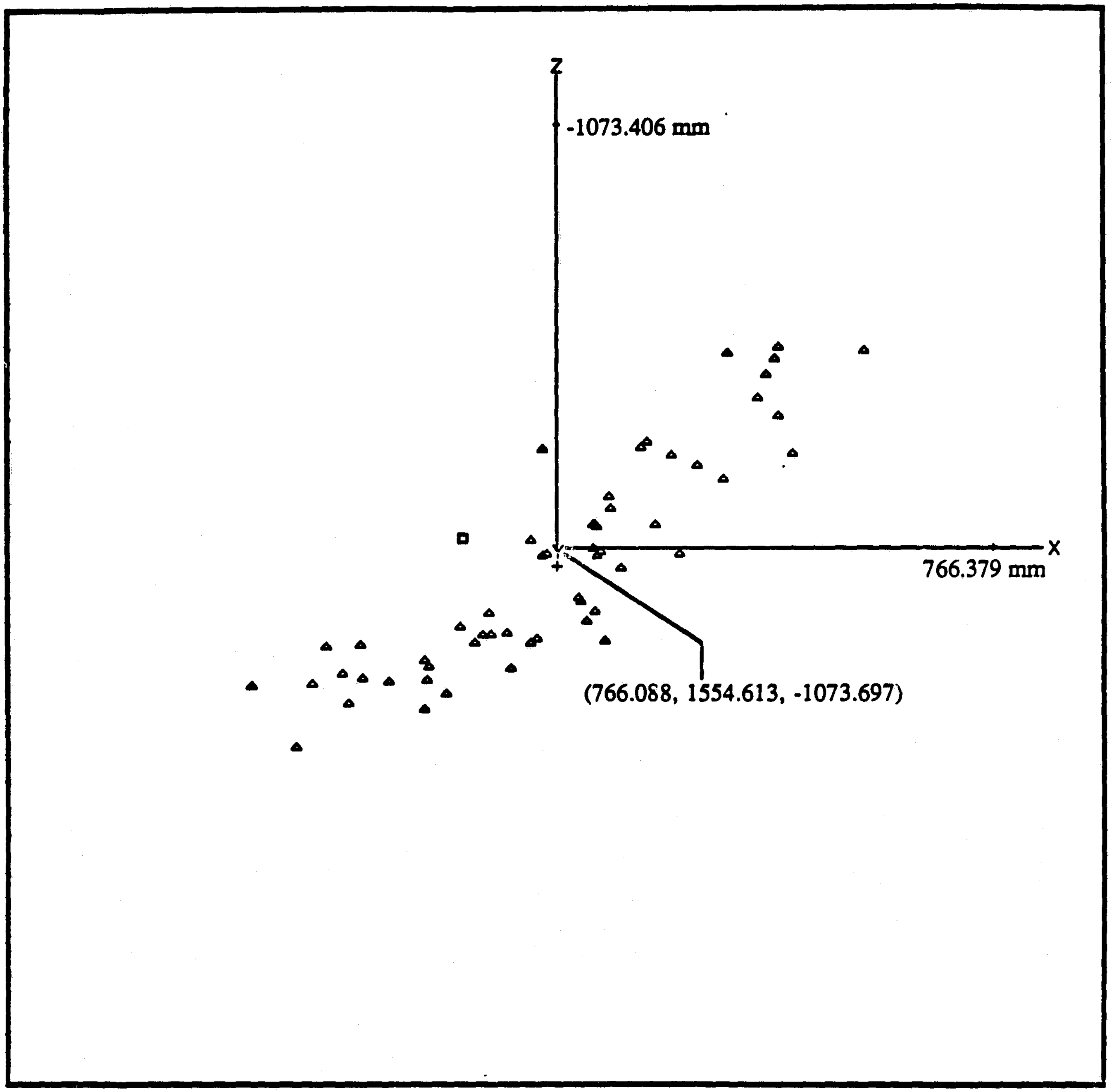

Plot of the PTP Test Achieved Positions
Each triangle is located at an achieved position
The square marks the commanded position
The cross marks the mean of the achieved positions

Figure 4.5 Teach mode joint angles kinematics control positions plot.

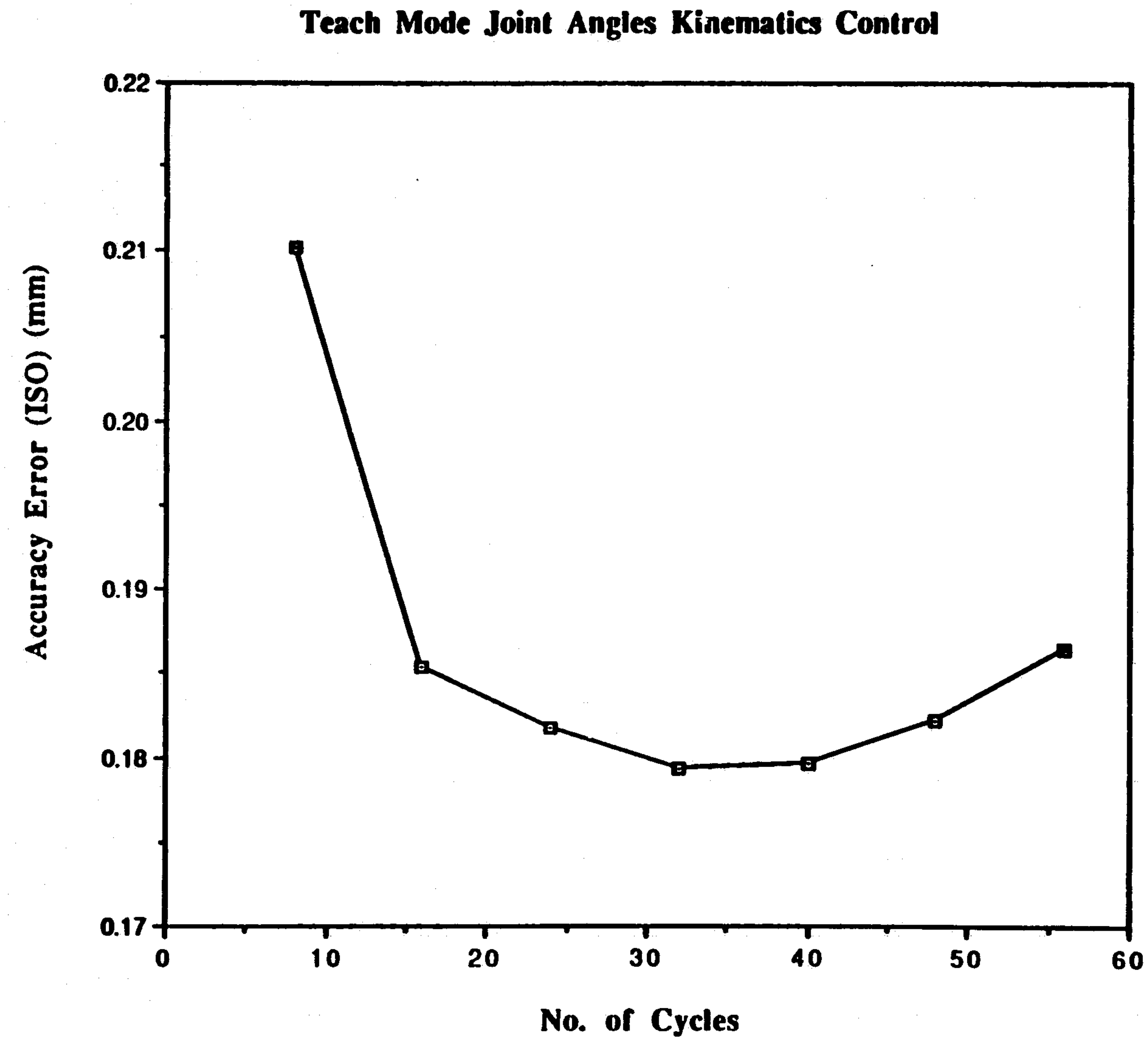

Figure 4.6 Position accuracy error plot.

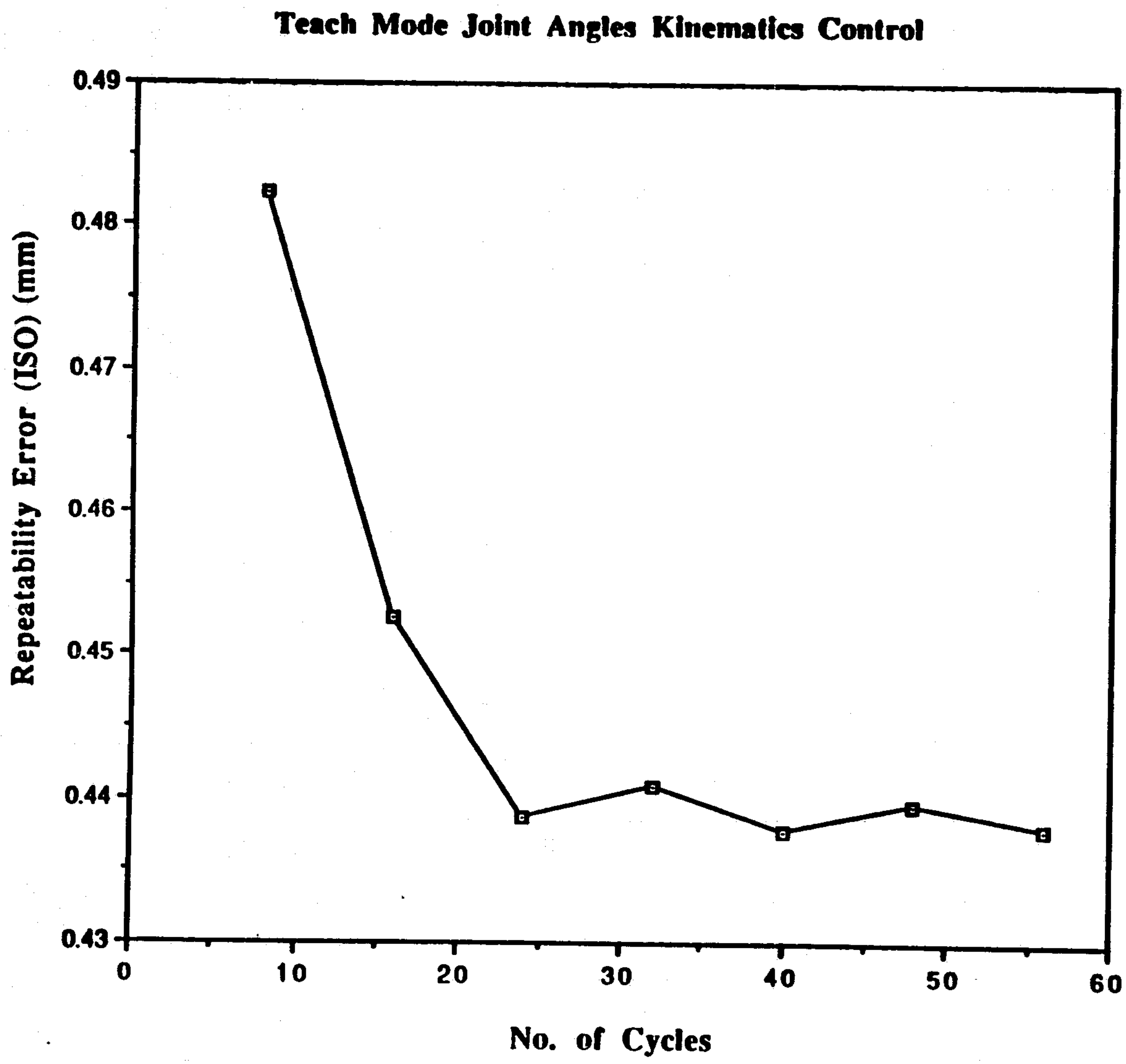

Figure 4.7 Position repeatability error plot.

Figure 4.6 is a plot of the ISO defined accuracy error versus the number of cycles contained in each analysis group. Figure 4.7 is a plot of the ISO defined repeatability error versus the number of cycles contained in each analysis group. As can be seen from these plots the errors seem to follow an exponential decay curve reaching an asymptote after 24 to 32 cycles. The small rise in the accuracy error after 40 cycles is not considered significant although it needs to be investigated.

To better understand the nature of this exponential decay of the accuracy and repeatability errors the X, Y, and Z axes, laser tracker coordinates of the 56 measured positions were plotted as a function of the number of cycles and are shown in Figures 4.8, 4.9, 4.10 respectively. These plots show a periodicity with a fundamental frequency of 8 cycles and a few smaller amplitude higher frequency oscillations. There is an obvious drift during the first 8 cycles, which corresponds to the first group of analysis data, and a less pronounced drift during the next 8 cycles. After the first 16 cycles the coordinates seem to follow a relatively stable periodic oscillation with a peak-to-peak amplitude of approximately 0.3 mm for the X-axis coordinates, 0.5 mm for the Y-axis coordinates, and 0.23 mm for the Z-axis coordinates. The 8 cycles periodicity is expected as a result of using the 8 vertices of the RIA standard path as different initial positions. The drift during the first 8 to 16 cycles probably comes from thermal drift (the robot arm was exercised for a reasonable amount of time and cycles before each test), and dynamic motion transients which include friction. The errors measured during the first 8 to 16 cycles are probably representative of those which occur during all intermittent robot operations.

The variation in the measured achieved position was previously characterized by the repeatability error. From Fig. 4.5 it appears that the asymptotic value of the ISO defined repeatability error is approximately 0.44 mm, which is larger than the peak-to-peak amplitude of the X and Z-axes steady state oscillation, but not of the one along the Y- axis. This indicates that if a robot behaves like the one used for these tests the peak-to-peak amplitude of its steady state oscillation would be a more appropriate measure of the variation of its achieved position rather than the repeatability error. The ISO repeatability error measured after the first 8 cycles (0.482 mm) is closer to predicting the peak-to-peak amplitude of the achieved position oscillation. In the case of the RIA defined repeatability (given by eq. 4.10) the value of 3 $\times$ standard deviation should be added to the repeatability error in order to come close to the true achieved position variation.

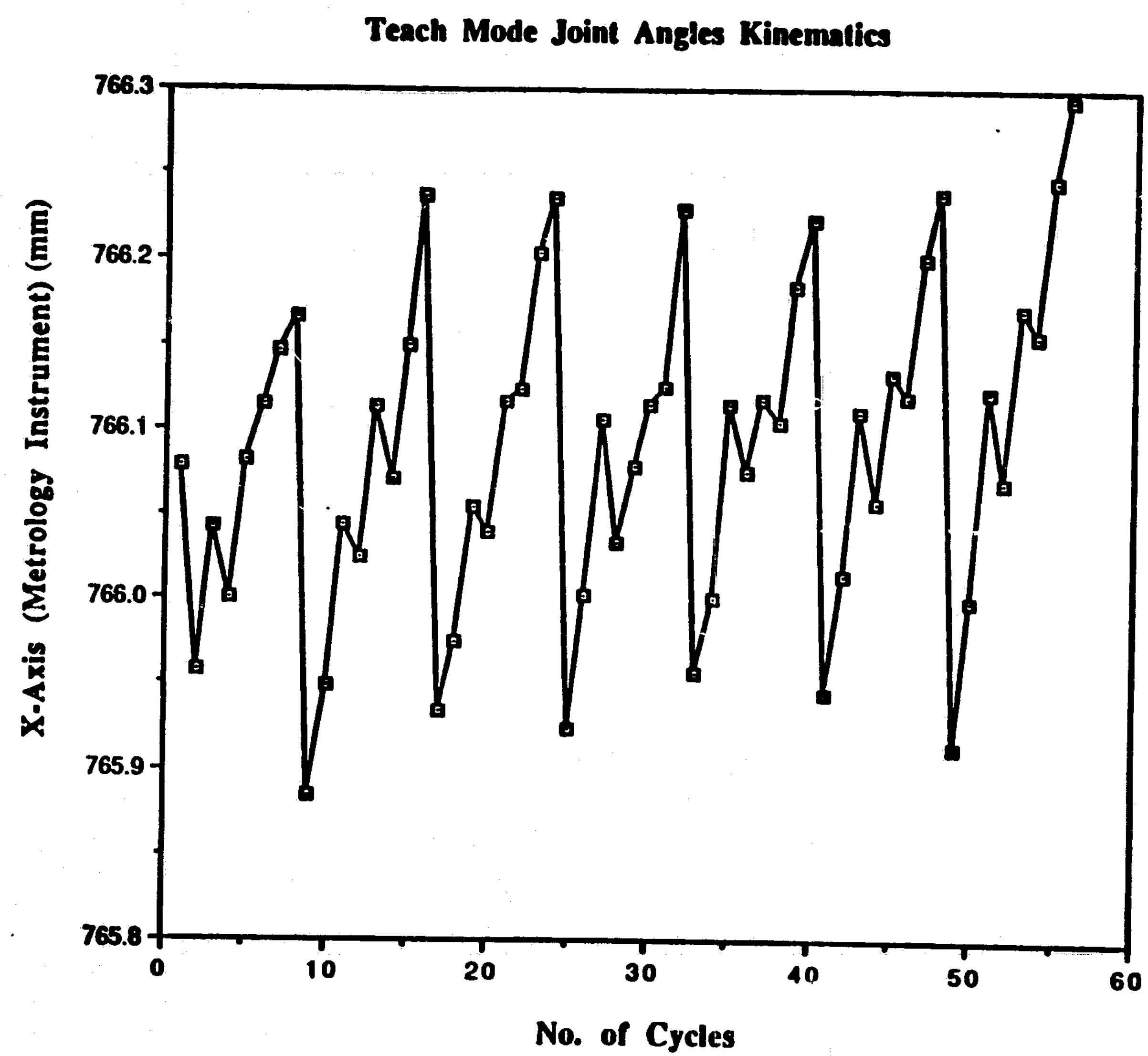

Figure 4.8 Measured position coordinate plot.

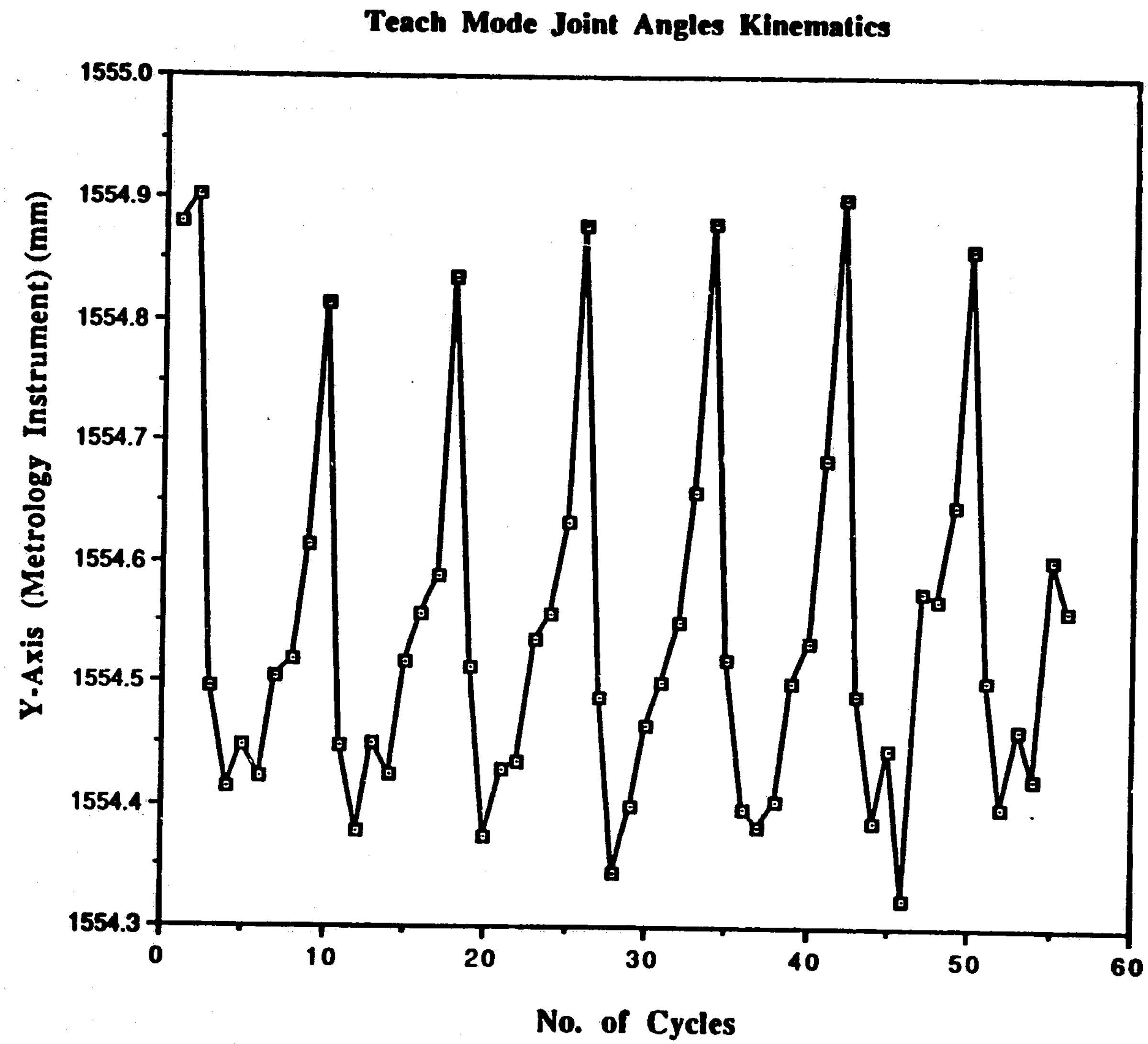

Figure 4.9 Measured position coordinate plot.

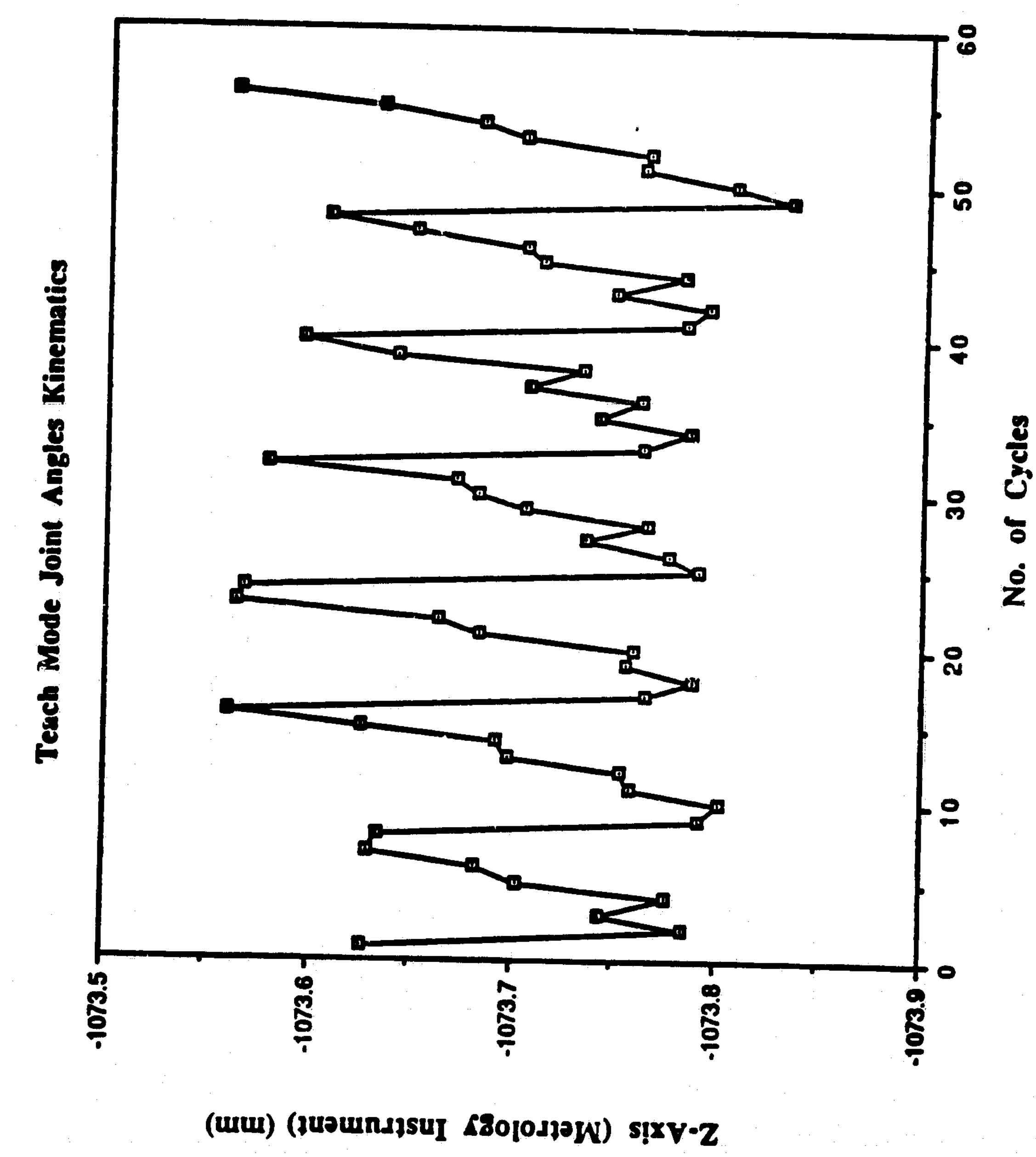

Figure 4.10 Measured position coordinate plot.

As can be seen from Figures 4.8, 4.9, 4.10 the measured achieved position is not really very random. For the same initial position of the RIA standard path approximately the same measured achieved position is obtained with a small amount of random displacement superimposed. Is that the result of the robot position control algorithm used, which does not stop servoing for as long as there is a joint angle position error? This of course raises the question, what would happen if only one initial position was used, would the random component dominate the achieved position? Another test which will be reported later will try to answer that question.

4.3.1.2.a Teach mode inverse kinematics control

This test is identical to the previous one, with the exception that S2 was recorded as a Cartesian position, and the Cartesian quintic polynomial trajectory algorithm was used to move between $S2_{app}$ and S2 resulting in an approximately straight line motion. This motion would be necessary if the design of the sensor nest is such that a straight approach is required. The Cartesian quintic polynomial trajectory algorithm gives a better approximation of that type of trajectory than the joint interpolation algorithm. The inverse kinematics algorithm was therefore used for each trajectory point in these motions. The duration of the motions was the same as in the previous test, and joint interpolated motion was used to move between the initial positions and $S2_{app}$.

4.3.1.2.b Analysis and Conclusions

The laser tracker coordinates of the 56 measured positions were again divided into 7 analysis groups. The data contained in each group were analyzed separately and the results of the analysis were used to determine the effect of the number of measured positions on the results.

Table 4.2 in the Appendix shows the results of the analysis of the last group of data which contains all 56 measured positions. Figure 4.11 is a three dimensional plot of the measured achieved positions (triangular marks), their mean position (cross mark), and the commanded position (square mark). The coordinate frame in that figure is that of the laser tracker after it was translated to the centroid of those positions.

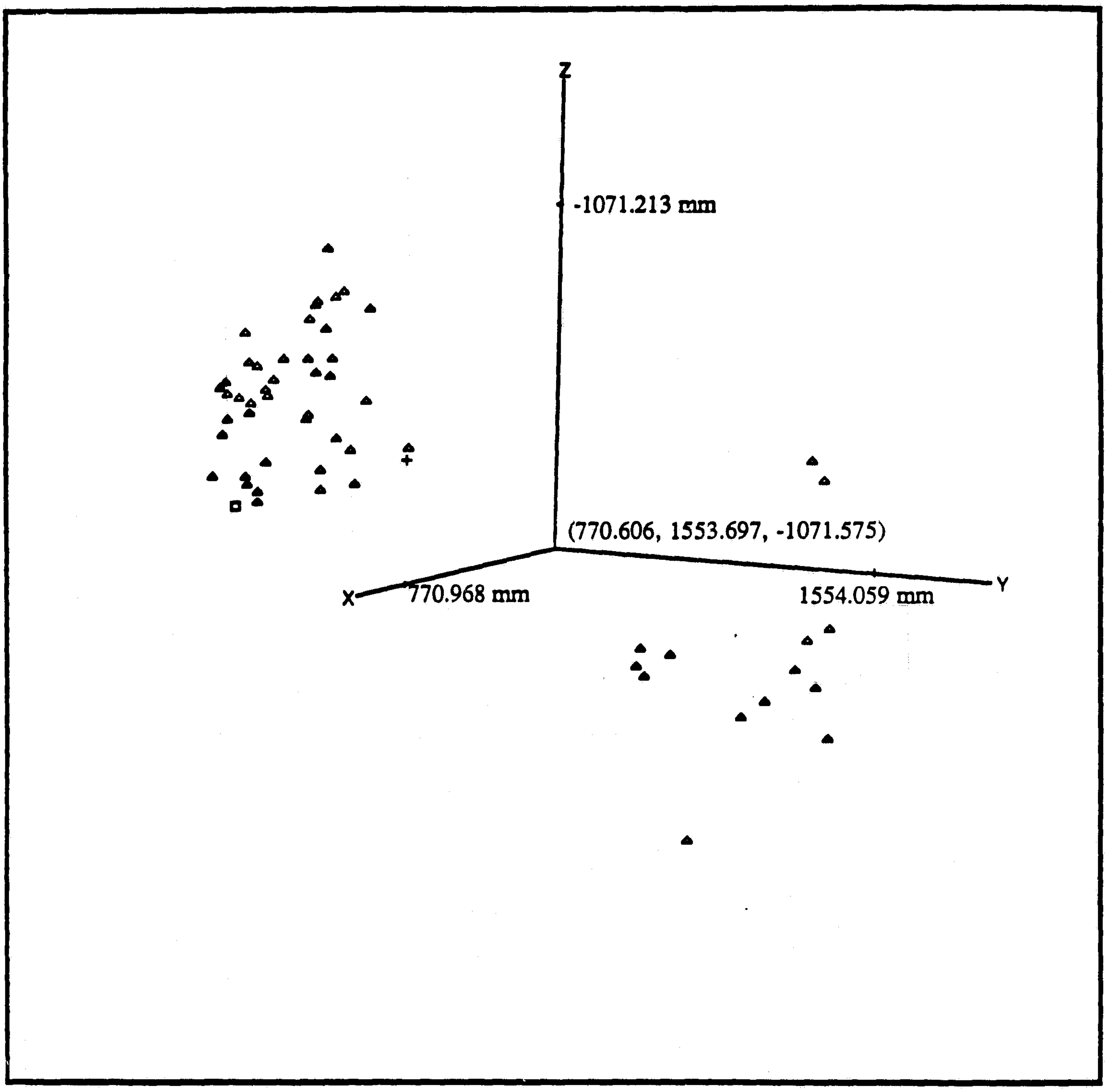

Plot of the PTP Test Achieved Positions
Each triangle is located at an achieved position
The square marks the commanded position
The cross marks the mean of the achieved positions

Figure 4.11 Teach mode inverse kinematics control positions plot.

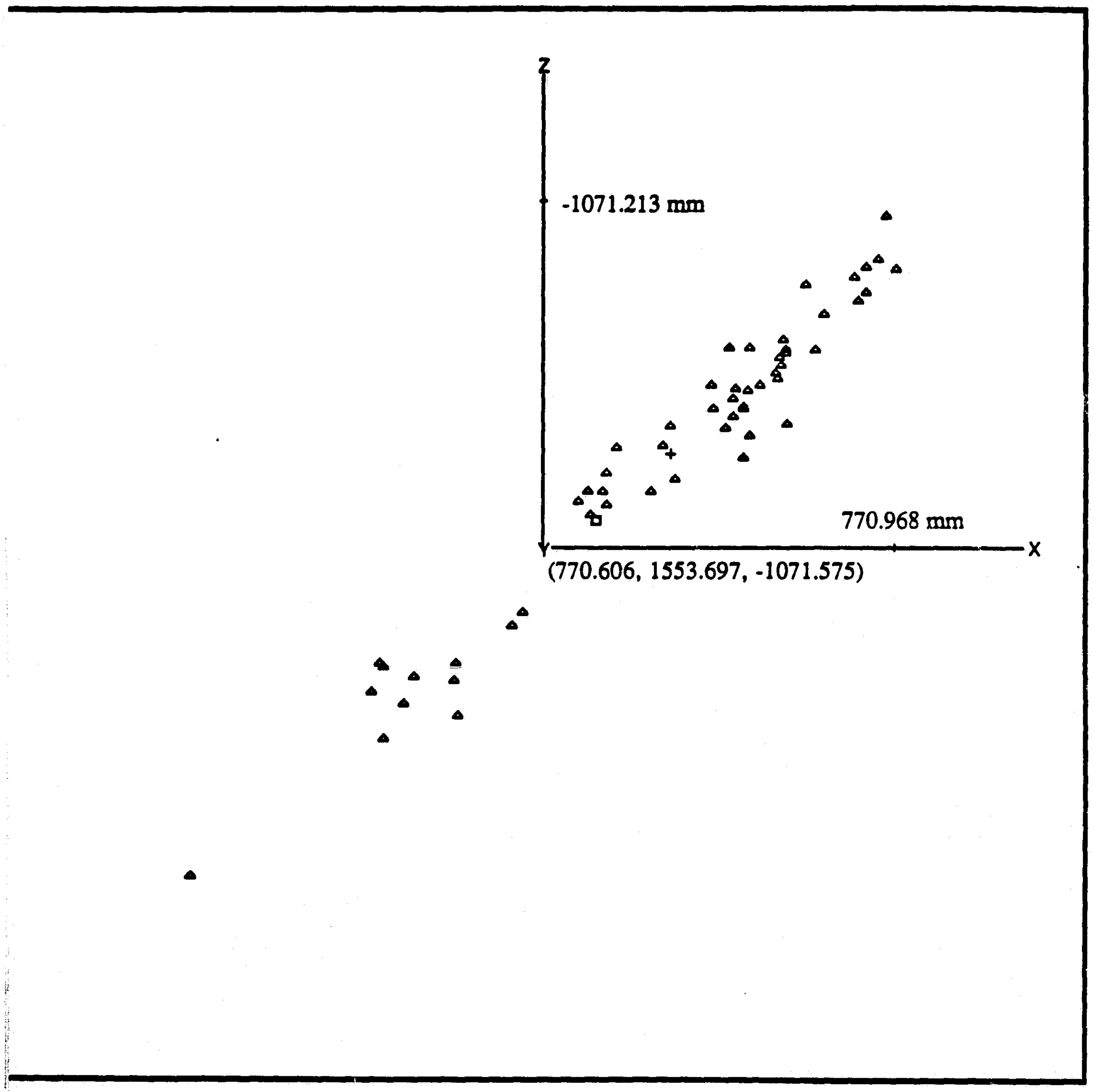

Plot of the PTP Test Achieved Positions
Each triangle is located at an achieved position
The square marks the commanded position
The cross marks the mean of the achieved positions

Figure 4.12   Teach mode inverse kinematics control positions plot.

Figure 4.12 is a plot of the same positions as they are projected on a plane defined by the X and Z coordinate axes. As can be seen, the cluster of points again forms a galactic cloud with an orientation which is approximately orthogonal to the orientation of the axis of the first joint of the robot arm.

Figure 4.13 is a plot of the ISO defined accuracy error versus the number of cycles contained in each analysis group. Figure 4.14 is a plot of the ISO defined repeatability error versus the number of cycles contained in each analysis group. As can be seen from these plots the errors seem to decrease reaching an asymptote after 24 to 32 cycles.

To better understand the nature of this decrease of the accuracy and repeatability errors the X, Y, and Z axes, laser tracker coordinates of the 56 measured positions were plotted as a function of the number of cycles and are shown in Figures 4.15, 4.16, 4.17 respectively. These plots show again a periodicity with a fundamental frequency of 8 cycles and a few smaller amplitude higher frequency oscillations. There is an obvious drift during the first 8 cycles, which correspond to the first group of analysis data, and a less pronounced drift during the next 8 cycles. After the first 16 cycles the coordinates seem to follow a relatively stable periodic oscillation with a peak-to-peak amplitude of approximately 0.5 mm for the X-axis coordinates, 0.55 mm for the Y-axis coordinates, and 0.45 mm for the Z-axis coordinates. The 8 cycles periodicity is expected as a result of using the 8 vertices of the RIA standard path as different initial positions. The drift during the first 8 to 16 cycles probably comes from thermal drift (the robot arm was exercised for a reasonable amount of time and cycles before each test), and dynamic motion transients which include friction. The errors measured during the first 8 to 16 cycles are probably representative of those which occur during all intermittent robot operations.

The variation in the measured achieved position was previously characterized by the repeatability error. From Fig. 4.14 it appears that the asymptotic value of the ISO defined repeatability error is approximately 0.67 mm, which is larger than the peak-to-peak amplitude of the X, Y and Z-axes steady state oscillation. The ISO repeatability error measured after the first 8 cycles (0.86 mm) is large and reflects the large amplitude of the drift of the achieved position in the Z and X-axes directions. In the case of the RIA defined repeatability (given by eq. 4.10) the value of $3 \times$ standard deviation should again be added to the repeatability error in order to come close to the true achieved position variation.

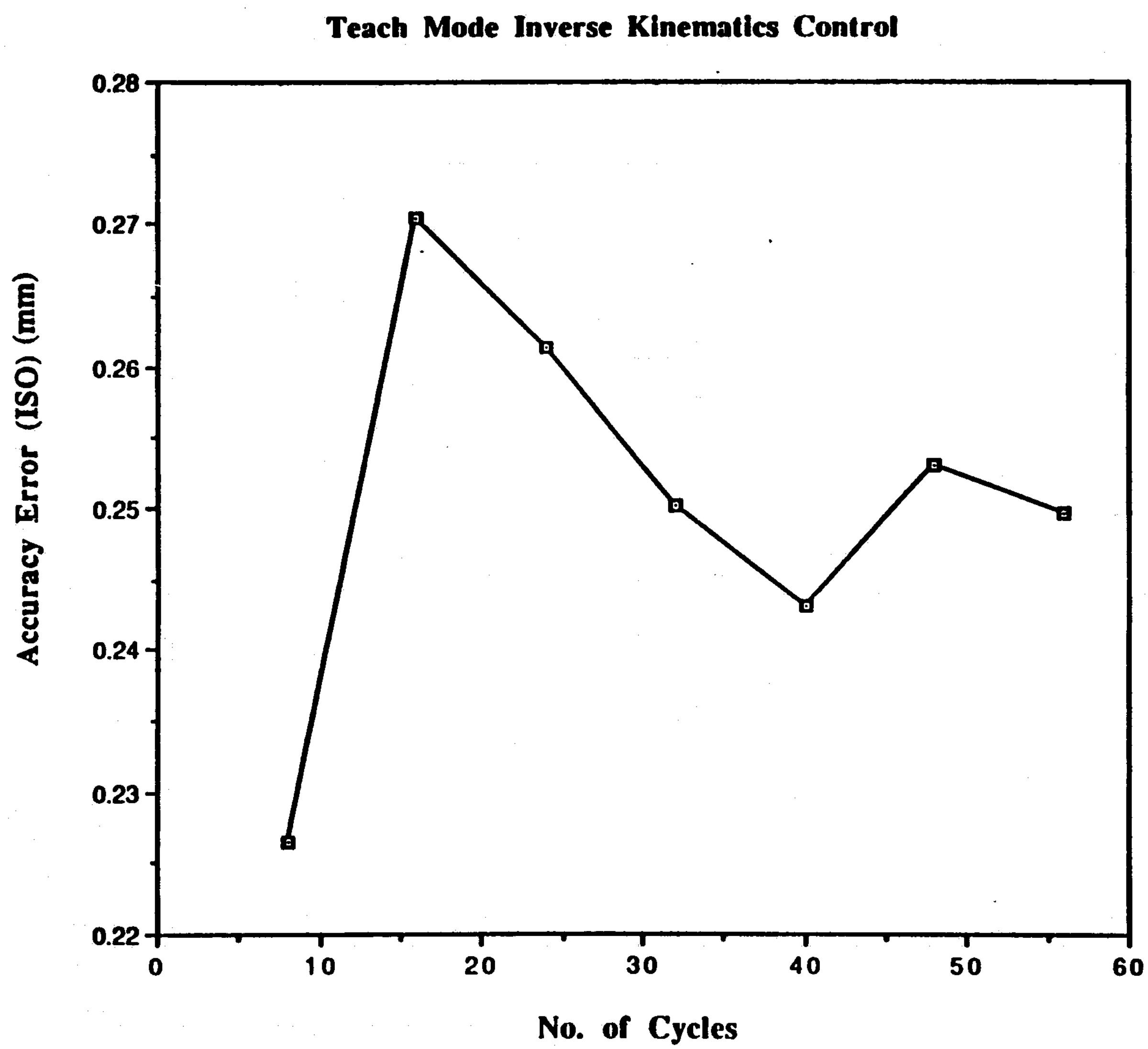

Figure 4.13 Position accuracy error plot.

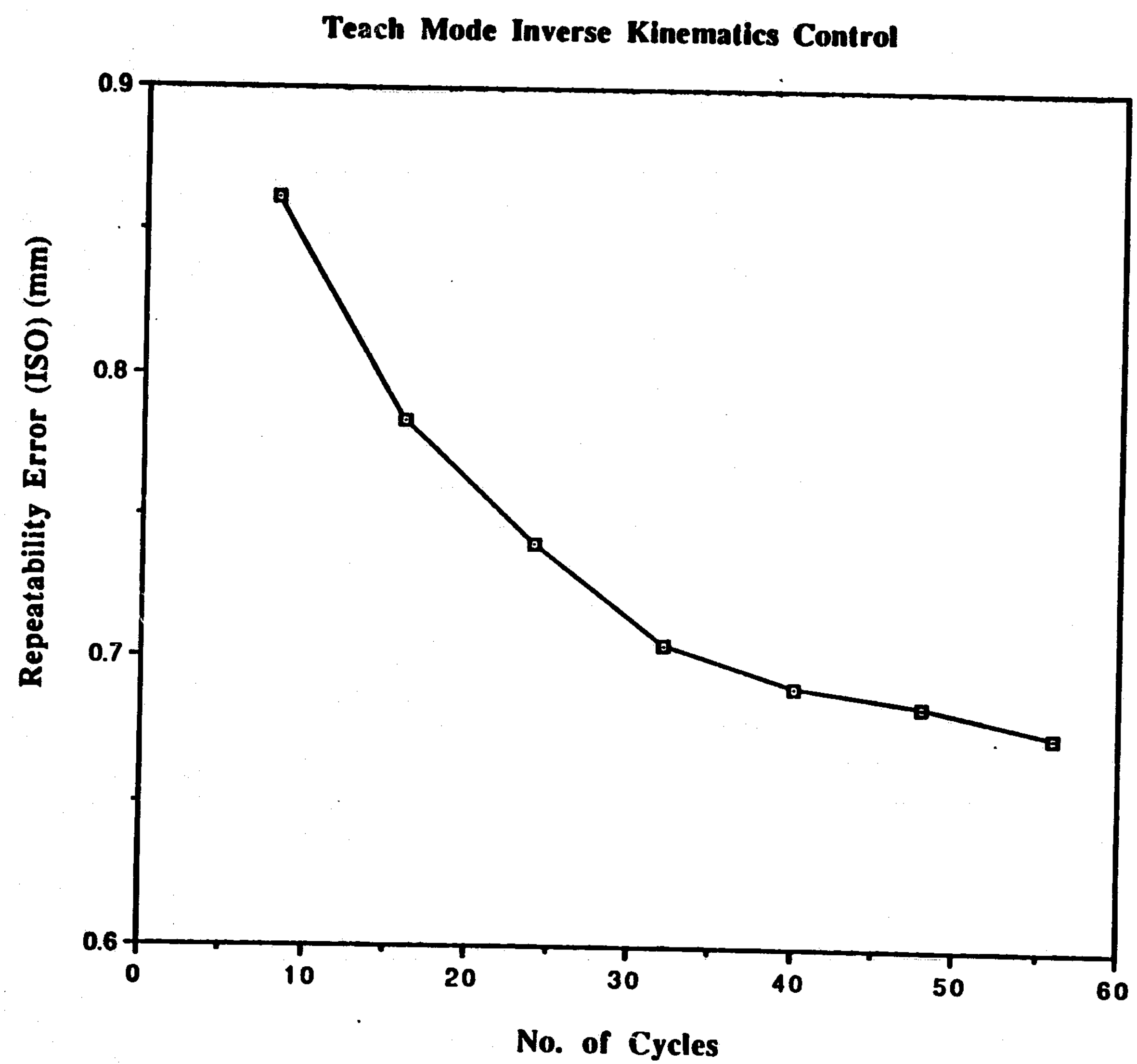

Figure 4.14 Position repeatability error plot.

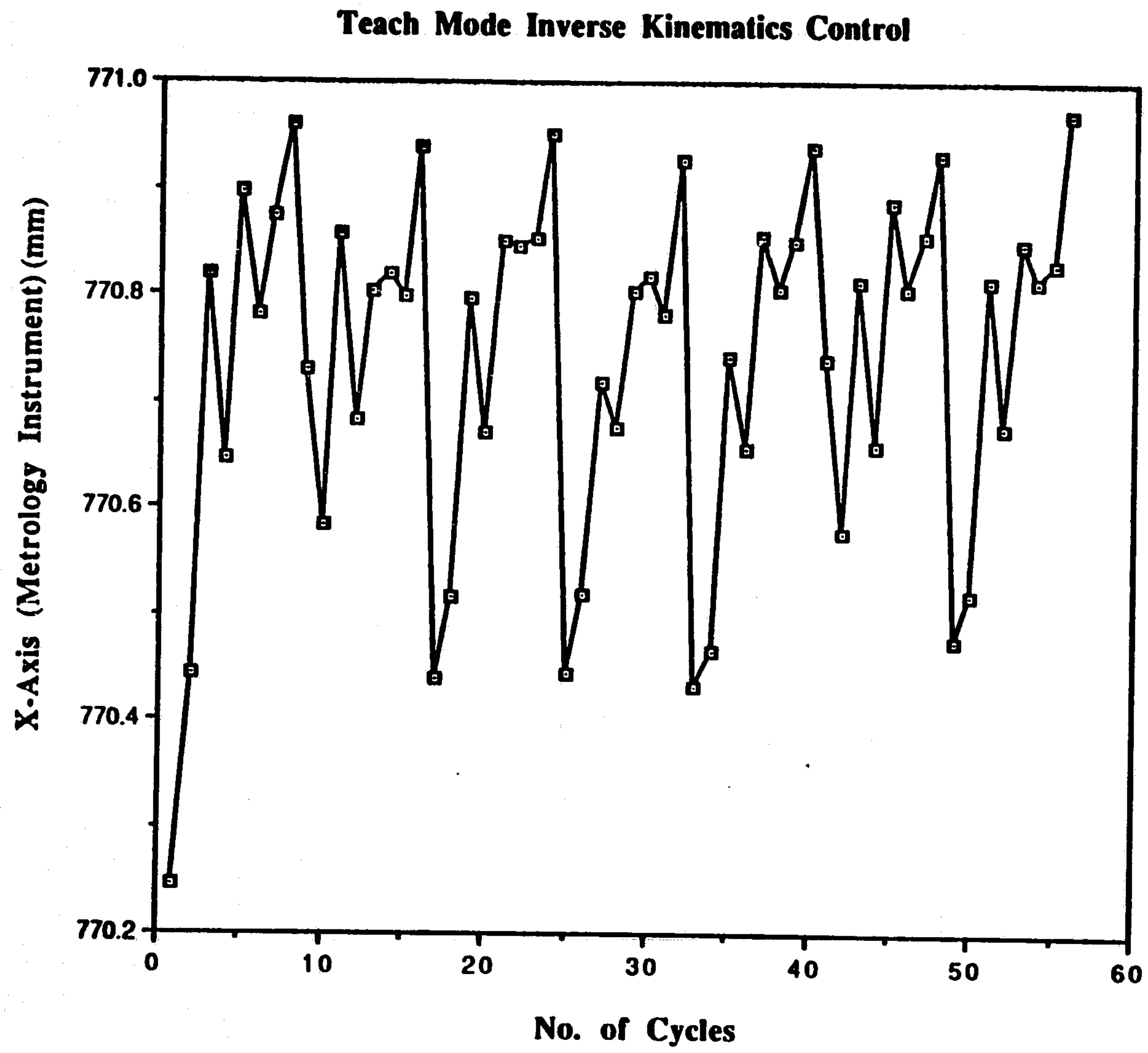

Figure 4.15 Measured position coordinate plot.

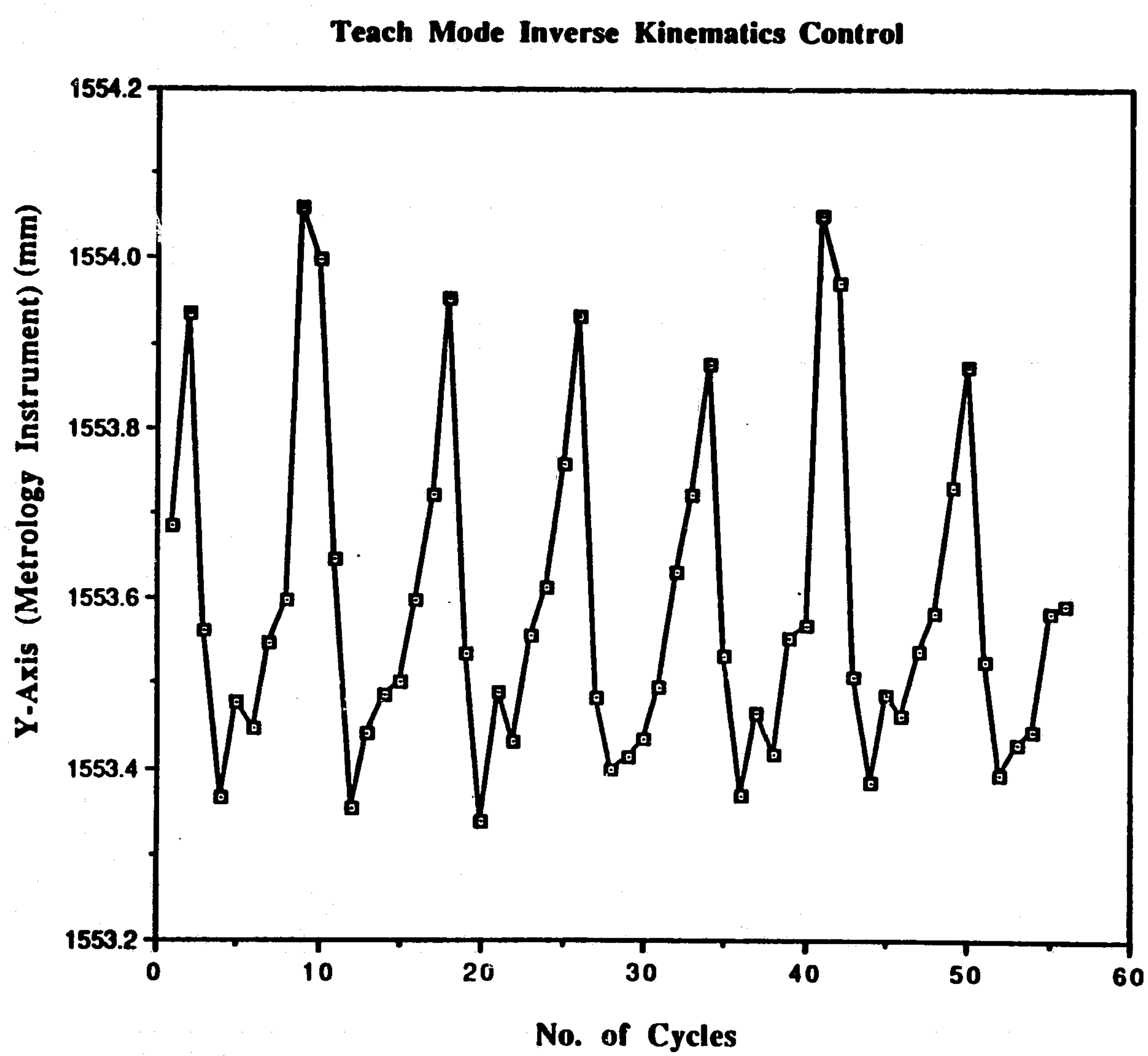

Figure 4.16 Measured position coordinate plot.

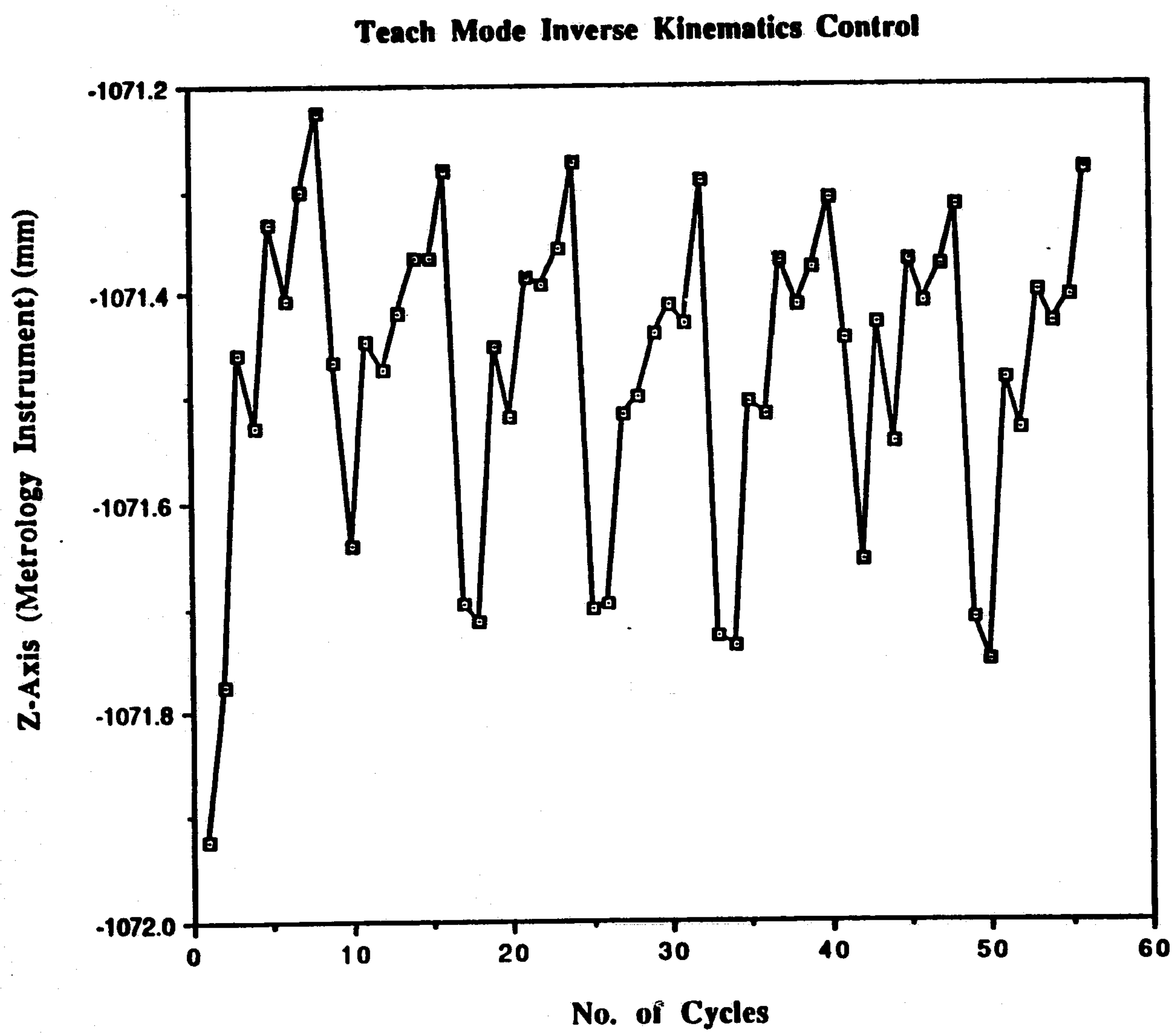

Figure 4.17 Measured position coordinate plot.

As can be seen from Figures 4.15, 4.16, 4.17 the measured achieved position is again not really very random. For the same initial position of the RIA standard path approximately the same measured achieved position is obtained with a small amount of random displacement superimposed.

Comparing the errors measured with joint interpolated motion with those obtained for Cartesian interpolated motion, it can be seen that in the second case they are larger for both accuracy and repeatability, and the peak-to-peak amplitudes of the coordinate oscillations. This makes sense since in the case of Cartesian interpolated motion the errors due to the inverse kinematics algorithms are also included.

4.3.2 Coordinates Transformation Test

The coordinates transformation is a mathematical relationship which relates the baseframe of the robot arm with the coordinate frame of the robot metrology instrument, for this work the laser tracker instrument. It allows the transformation of any metrology instrument measured coordinates to robot baseframe coordinates or the reverse, thus allowing all position and orientation information to be referred to a common frame of reference. The purpose of including the coordinates transformation determination was to support the off-line programming test and the forward kinematics error analysis, another possible use is the non-destructive evaluation for the detection of any possible deformation of the FTS robotic arm and sensor nest, and their common foundation.

4.3.2.a Test

The purpose of this test is to determine the relative transformation between the base coordinate systems of the robot and the laser tracker. To make this determination, a number of points must be recorded in both robot and laser tracker coordinates. The procedure for this test is:

Move to S2
Record position data
Move to S2 + 3 mm in the world X direction
Record position data

Move to S2
Record position data
Move to S2 + 3 mm in the world Y direction
Record position data
Move to S2
Record position data
Move to S2 + 3 mm in world Z direction
Record position data
Move to S2
Record position data

The duration of each of the small motions was 3 s. The time required for the entire sequence is about 0.5 min. The position of the target was recorded by both the robot control system and by the laser tracker at the end of each motion. The sequence of motions was repeated twice, for a total of 14 data points.

4.3.2.b Analysis and Conclusions

The transformation is presented here as a translation vector and as a rotation matrix. If the translation vector is used to translate the robot base coordinate frame, its origin will coincide with the origin of the laser tracker coordinate frame. The rotation matrix consists of the directional cosines of the laser tracker coordinate frame axes unit vectors, with respect to the robot baseframe coordinate axes. If x_t, y_t, z_t, are the coordinates of the target with respect to the laser tracker coordinate frame and x_r, y_r, z_r, are the coordinates of the same target position with respect to the robot base coordinate frame then

$$\begin{bmatrix} x_r \\ y_r \\ z_r \end{bmatrix} = \begin{bmatrix} u_{xx} & u_{yx} & u_{zx} \\ u_{xy} & u_{yy} & u_{zy} \\ u_{xz} & u_{yz} & u_{zz} \end{bmatrix} \begin{bmatrix} x_t \\ y_t \\ z_t \end{bmatrix} + \begin{bmatrix} x_0 \\ y_0 \\ z_0 \end{bmatrix} . \quad (4.14)$$

where x_0, y_0, z_0, are the coordinates of the translation vector, and

$$\begin{bmatrix} u_{xx} & u_{yx} & u_{zx} \\ u_{xy} & u_{yy} & u_{zy} \\ u_{xz} & u_{yz} & u_{zz} \end{bmatrix}$$

is the rotation matrix.

To determine the coordinates transformation the robot arm was moved to several positions inside the simulated sensor nest allowable workspace and the coordinates of the target were measured by the laser tracker and the robot controller. The best translation vector and rotation matrix to fit these data was determined by a double least squares optimization algorithm.

Table 4.3 in the Appendix gives the results of the coordinates transformation analysis for 14 target positions. First the coordinates of the target as measured by the laser tracker controller are given, then the coordinates of the same target positions as measured by the robot controller are given. Next, the coordinates of the target as measured by the laser tracker controller after they have been converted to robot control system coordinates using equation 4.14 are given. These coordinates should be very close to the robot control system measured coordinates printed above them; otherwise the transformation is not successful. Finally, the calculated transformation translation vector and rotation matrix are given. Figure 4.18 is a plot of the robot control system-measured target positions and the laser tracker controller-measured positions after they have been converted to robot control system coordinates. Ideally the corresponding points from those two sets should coincide with each other. In practice there will always be small differences due to numerical errors, errors in the kinematic models and motions of the robot and laser tracker controllers, and curve fitting errors of the transformation optimization algorithm.

Table 4.4 in the Appendix gives the results of the coordinates transformation analysis for the first 7 target positions out of the group of 14 used in the previous analysis and Figure 4.19 is the plot of those points. To evaluate the effectiveness of the transformation the differences between the robot controller-measured target positions and the laser tracker controller-measured coordinates of the same positions after they have been converted to robot controller coordinates was calculated and the root mean square error was evaluated. In the case of the group of the 14 data positions that was found to be 0.0544 mm, while in the case of the group of the 7 data positions it was found to be 0.0585 mm. Thus there is a slight improvement in the accuracy of the transformation when more data points are used. The difference is very small, though, which can be seen by examining the converted coordinates from the two tables.

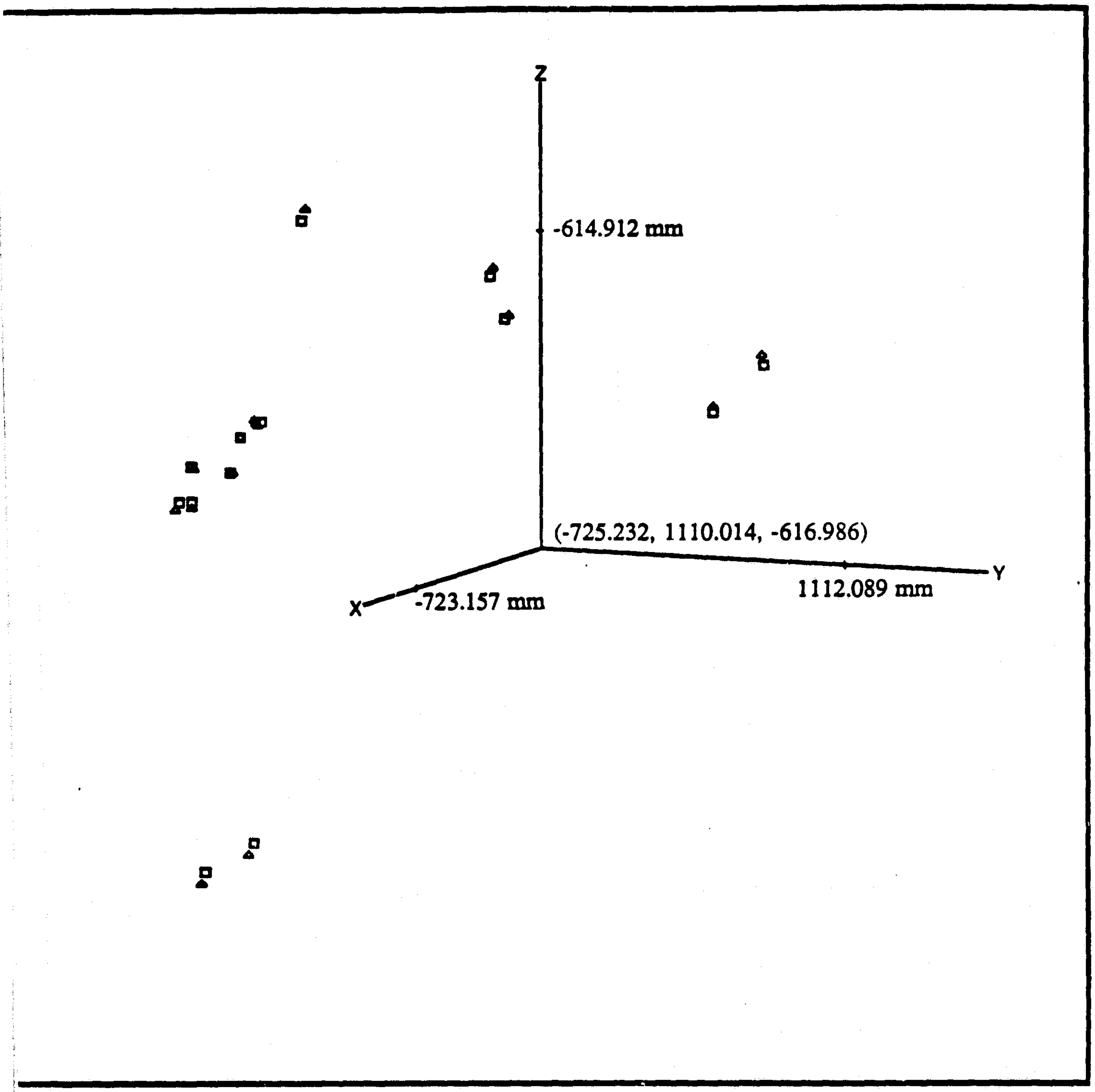

Each triangle is located at a robot controller measured position
The square marks the robot metrology instrument measured positions which were converted to robot controller coordinates

Figure 4.18 Coordinates transformation analysis plot.

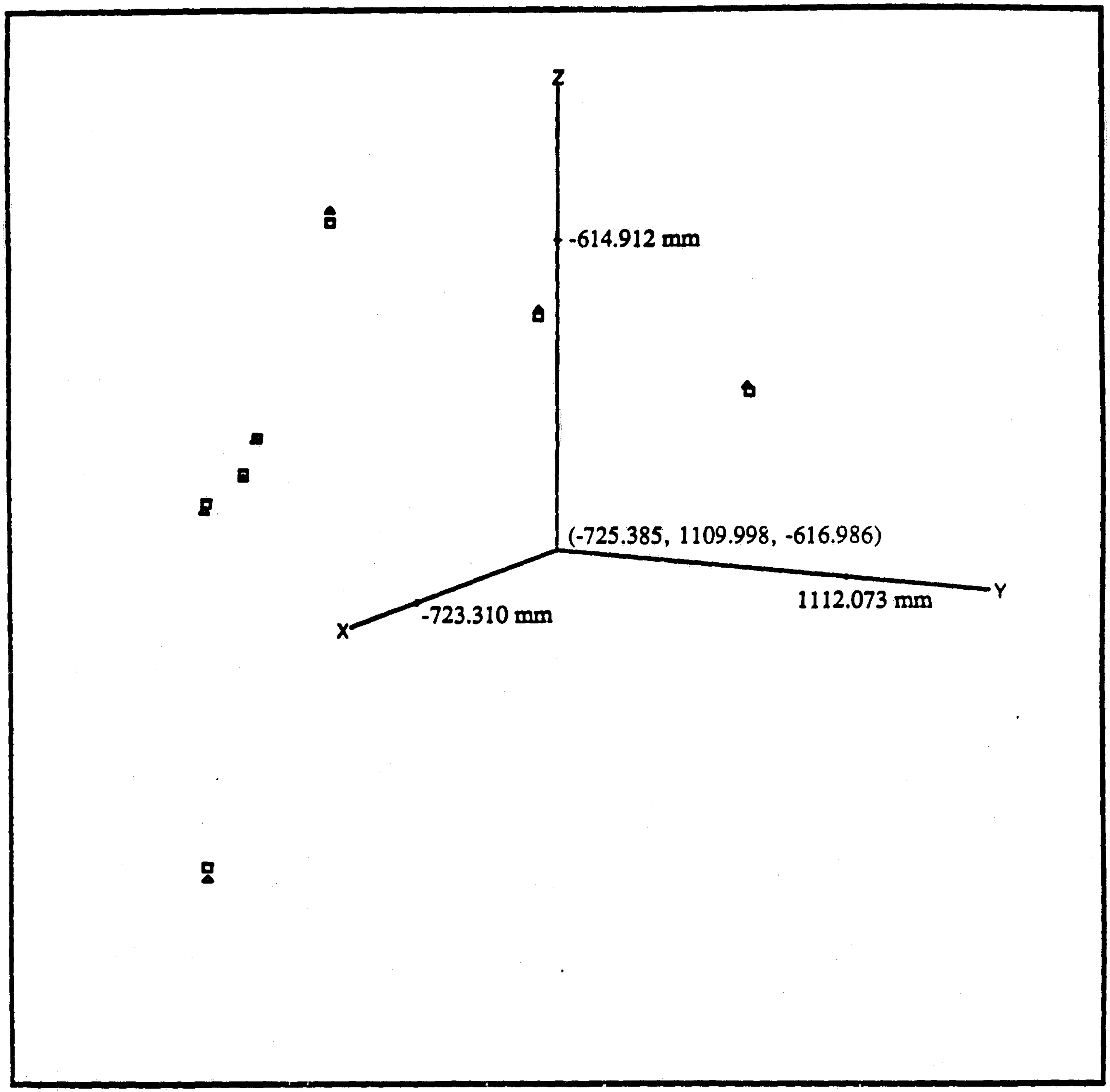

Each triangle is located at a robot controller measured position
The square marks the robot metrology instrument measured positions which were converted to robot controller coordinates

Figure 4.19 Coordinates transformation analysis plot.

To use the coordinates transformation test for non-destructive evaluation to detect any possible deformation of the FTS robotic arm and sensor nest, or their common foundation, the transformation vector would be compared with previous results to identify pronounced differences (a few millimeters or more). For this type of application a more thorough study of the effect of the number of data positions to errors in the calculation of the translation vector and rotation matrix should be performed.

4.3.3 Off-Line Programming Tests

In the off-line programming mode of operation, the robot position commands are generated by a computer and no teaching is involved during the generation of the commands. This of course requires the computer to have an accurate knowledge of the current robot arm model and its environment. This would be a preferable mode of operation for the FTS arm when it is working in the automatic mode, since it would be very difficult to teach it all the functions it is supposed to perform in space. Furthermore, since the dimensions of the arm and its surrounding objects might change due to heating, vibration or other reasons, teach control programming might not be very practical.

The objectives of the tests performed were to measure the accuracy and repeatability errors of a robot arm when it is trying to reach the simulated FTS sensor nest location under off-line programming control. It was also desired to investigate the variation in the values of those errors as a function of the number of the test cycles and also the variation and drift of the achieved position. The simulated FTS sensor nest location was specified with respect to the laser tracker coordinate frame and then its coordinates were converted to robot controller Cartesian coordinates, which then became the new commanded position coordinates. The laser tracker coordinate frame coordinates were converted using the coordinates transformation determined by the group of the 14 data positions mentioned previously. In order to move to that commanded position the robot controller had to use the inverse kinematics algorithm to determine the corresponding joint angles.

Two different types of off-line programming tests were performed. In the first case the path of the arm was similar to that described in the "Teach Mode Control Tests" section and included the 8 positions of the RIA standard path. In the second case those positions were dropped and all motions initiated from the approach point and followed a straight line path motion to the commanded position. The reason this second path was used was to reduce the duration of the test, since this simple back and forth motion takes less time than the motion to the standard path positions. If the test results from these two cases are comparable then the second path would be preferable.

The testing and calibration workstation calculates and prints the accuracy and repeatability errors as defined by both [RIA 90] and [ISO 90]. The formulas used are those given by equations 4.2 to 4.13.

4.3.3.1.a Standard initial positions off-line programming

The procedure for this test is very similar to the teach mode accuracy and repeatability test. The only difference is in how the goal position at S2 is determined. For the off-line programming test, instead of moving the robot to S2 and using the recorded data as the goal position, the goal position is determined by transforming the position recorded by the laser tracker into robot coordinates. Since this position is a Cartesian position, the Cartesian trajectory algorithm and inverse kinematics algorithm are used to move between $S2_{spp}$ and S2. The time required for this test is the same as for the teach mode tests (about 6 min per 8-position test).

4.3.3.1.b Analysis and Conclusions

The laser tracker coordinates of the 56 measured positions were again divided into 7 analysis groups. The data contained in each group were analyzed separately and the results of the analysis were used to determine the effect of the number of measured positions on the results.

Table 4.5 in the Appendix shows the results of the analysis of the last group of data which contains all 56 measured positions. Figure 4.20 is a three dimensional plot of the measured achieved positions (triangular marks), their mean position (cross mark), and the commanded position (square mark). The coordinate frame in that figure is that of the laser tracker after it was translated to the centroid of those positions.

Figure 4.21 is a plot of the same positions as they are projected on a plane defined by the X and Z coordinate axes. As with previous tests, the cluster of points forms a galactic cloud

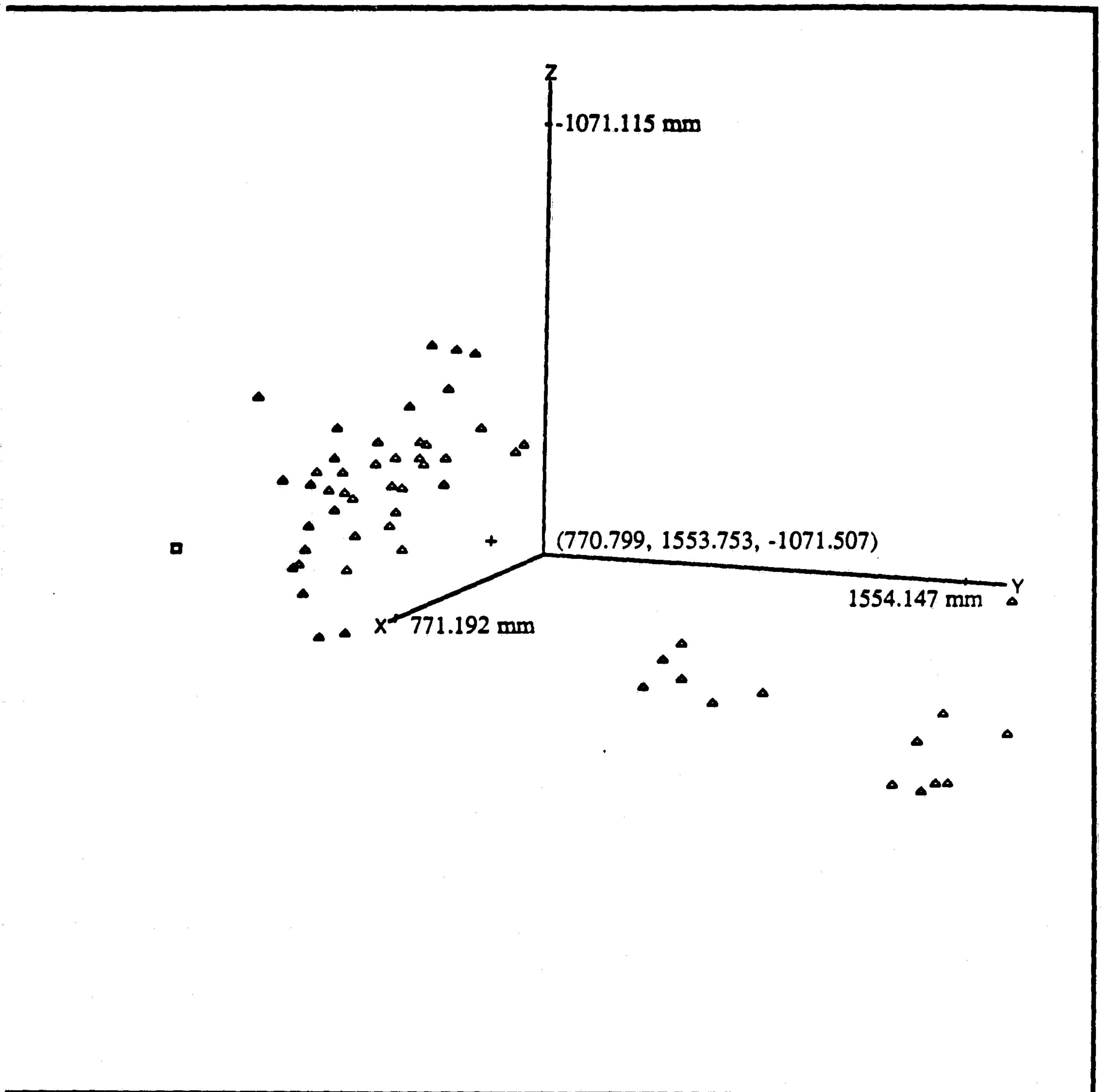

Plot of the PTP Test Achieved Positions

Each triangle is located at an achieved position

The square marks the commanded position

The cross marks the mean of the achieved positions

Figure 4.20 Standard initial positions off-line programming positions plot

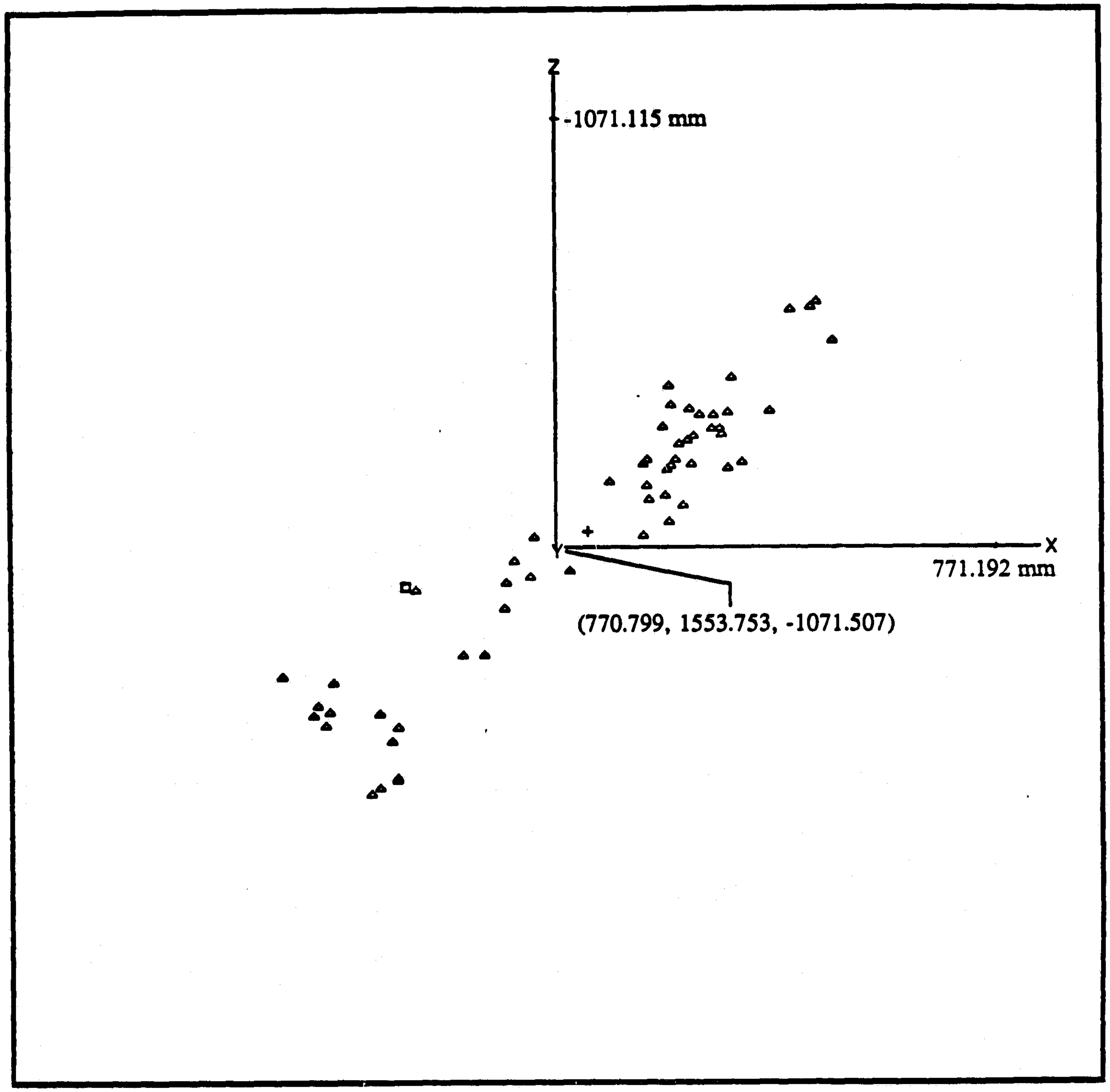

Plot of the PTP Test Achieved Positions
Each triangle is located at an achieved position
The square marks the commanded position
The cross marks the mean of the achieved positions

Figure 4.21 Standard initial positions off-line programming positions plot.

with an orientation which is approximately orthogonal to the orientation of the axis of the first joint of the robot arm.

Figure 4.22 is a plot of the ISO defined accuracy error versus the number of cycles contained in each analysis group. Figure 4.23 is a plot of the ISO defined repeatability error versus the number of cycles contained in each analysis group. As can be seen from these plots the errors seem to decrease exponentially reaching an asymptote after 24 to 32 cycles.

To better understand the nature of this decrease of the accuracy and repeatability errors the X, Y, and Z axes, laser tracker coordinates of the 56 measured positions were plotted as a function of the number of cycles and are shown in Figures 4.24, 4.25, 4.26 respectively. These plots show again a periodicity with a fundamental frequency of 8 cycles and a few smaller amplitude higher frequency oscillations. There is an obvious drift during the first 8 cycles, which correspond to the first group of analysis data. After the first 8 cycles the coordinates seem to follow a relatively stable periodic oscillation with a peak-to-peak amplitude of approximately 0.45 mm for the X-axis coordinates, 0.55 mm for the Y-axis coordinates, and 0.43 mm for the Z-axis coordinates. The 8 cycles periodicity is again expected, because of the different starting positions. The drift during the first 8 cycles probably comes from thermal drift (the robot arm was exercised for a reasonable amount of time and cycles before each test), and dynamic motion transients which include friction. Again, the errors during the first 8 to 16 cycles are probably characteristic of those which may be expected during intermittent operation.

The variation in the measured achieved position was previously characterized by the repeatability error. From Fig. 4.21 it appears that the asymptotic value of the ISO defined repeatability error is approximately 0.56 mm, which is larger than the peak-to-peak amplitude of the X, Y and Z-axes steady state oscillation. The ISO repeatability error measured after the first 8 cycles (0.664 mm) is large and reflects the large amplitude of the drift of the achieved position in the Y-axis direction. In the case of the RIA defined repeatability (given by eq. 4.10) the value of $3 \times$ standard deviation should be added to the repeatability error in order to come close to the true achieved position variation.

As can be seen from Figures 4.24, 4.25, 4.26 the measured achieved position is not really very random. For the same initial position of the RIA standard path approximately the same measured achieved position is obtained with a small amount of random displacement

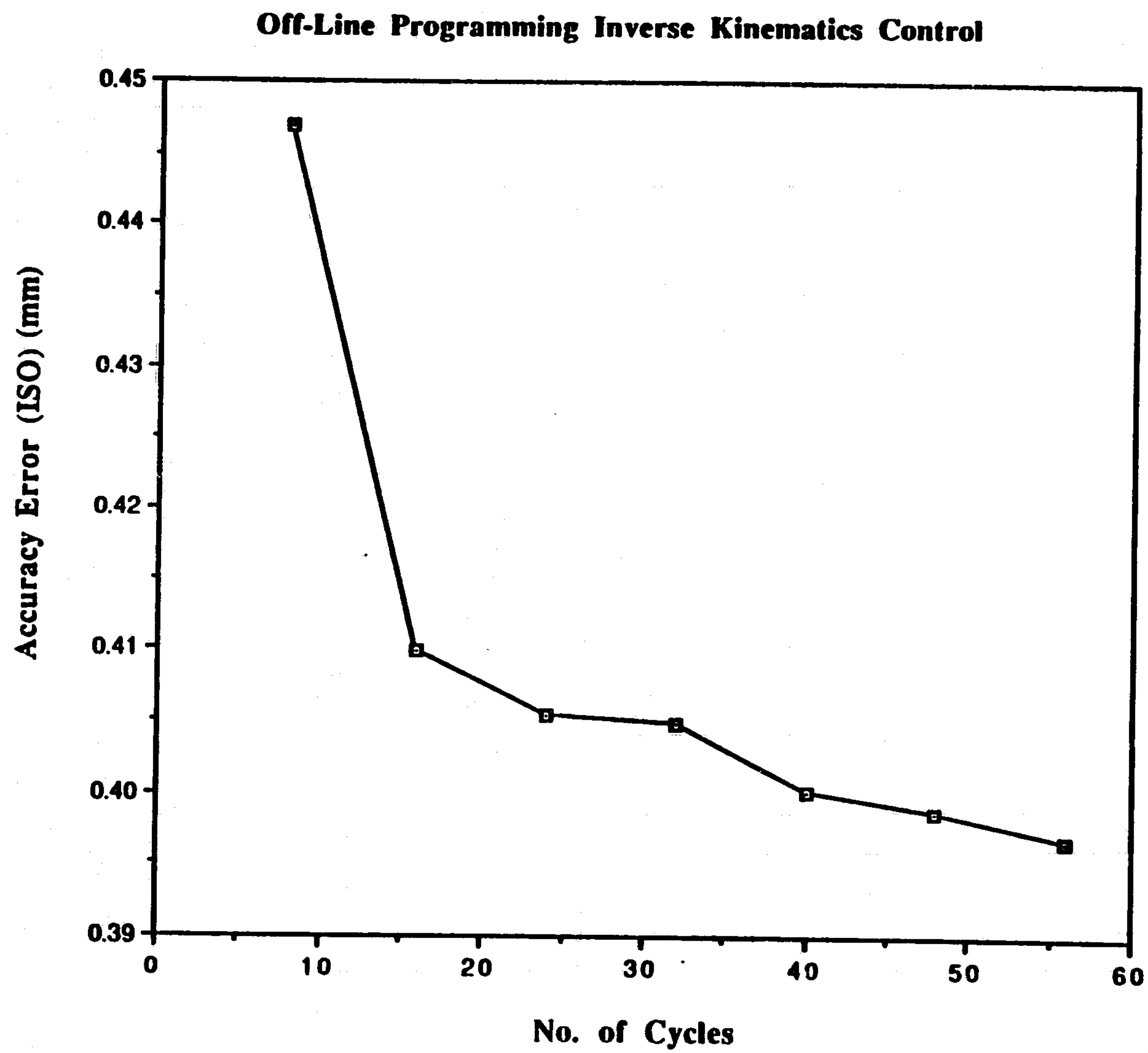

Figure 4.22 Position accuracy error plot.

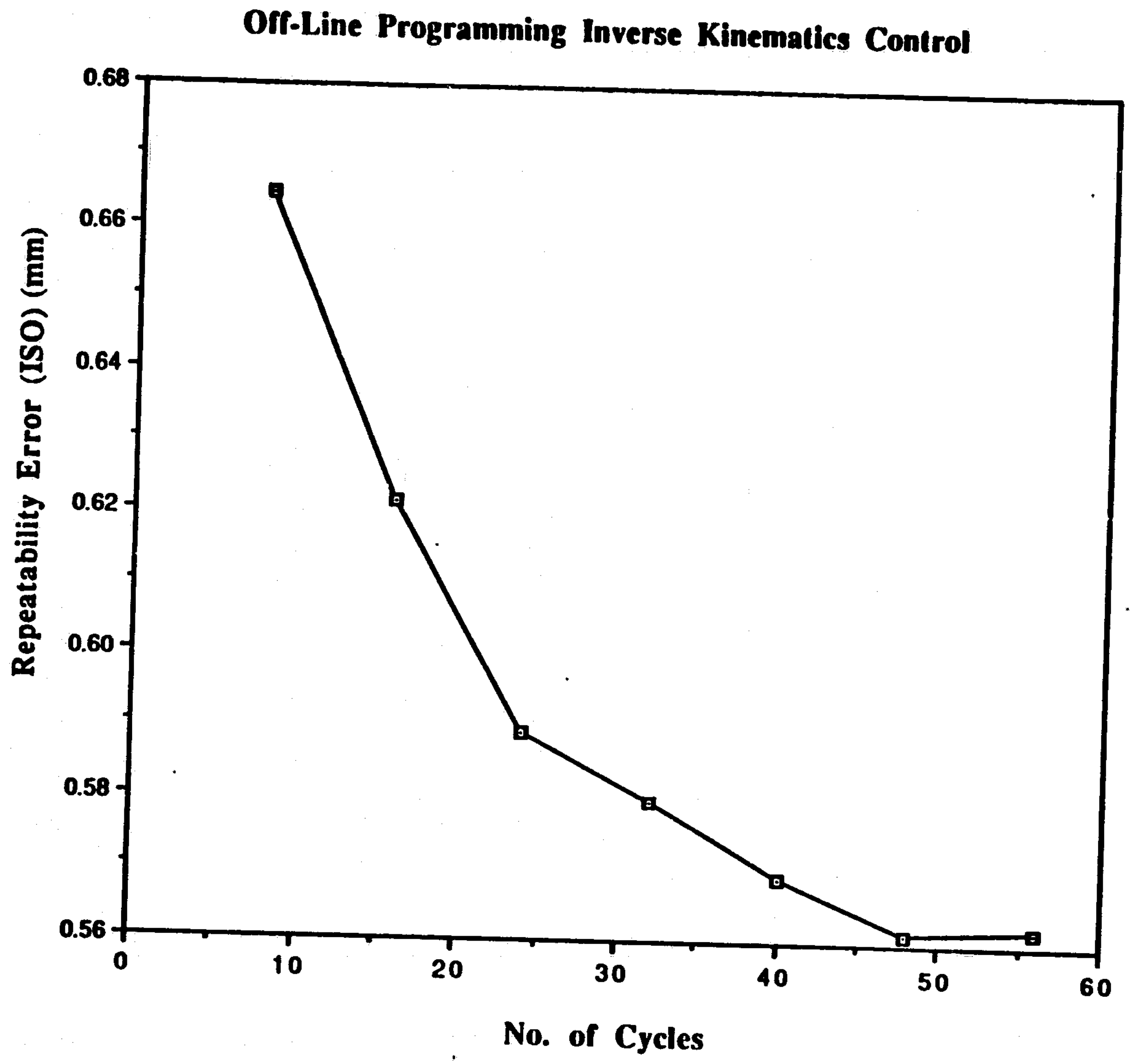

Figure 4.23 Position repeatability error plot.

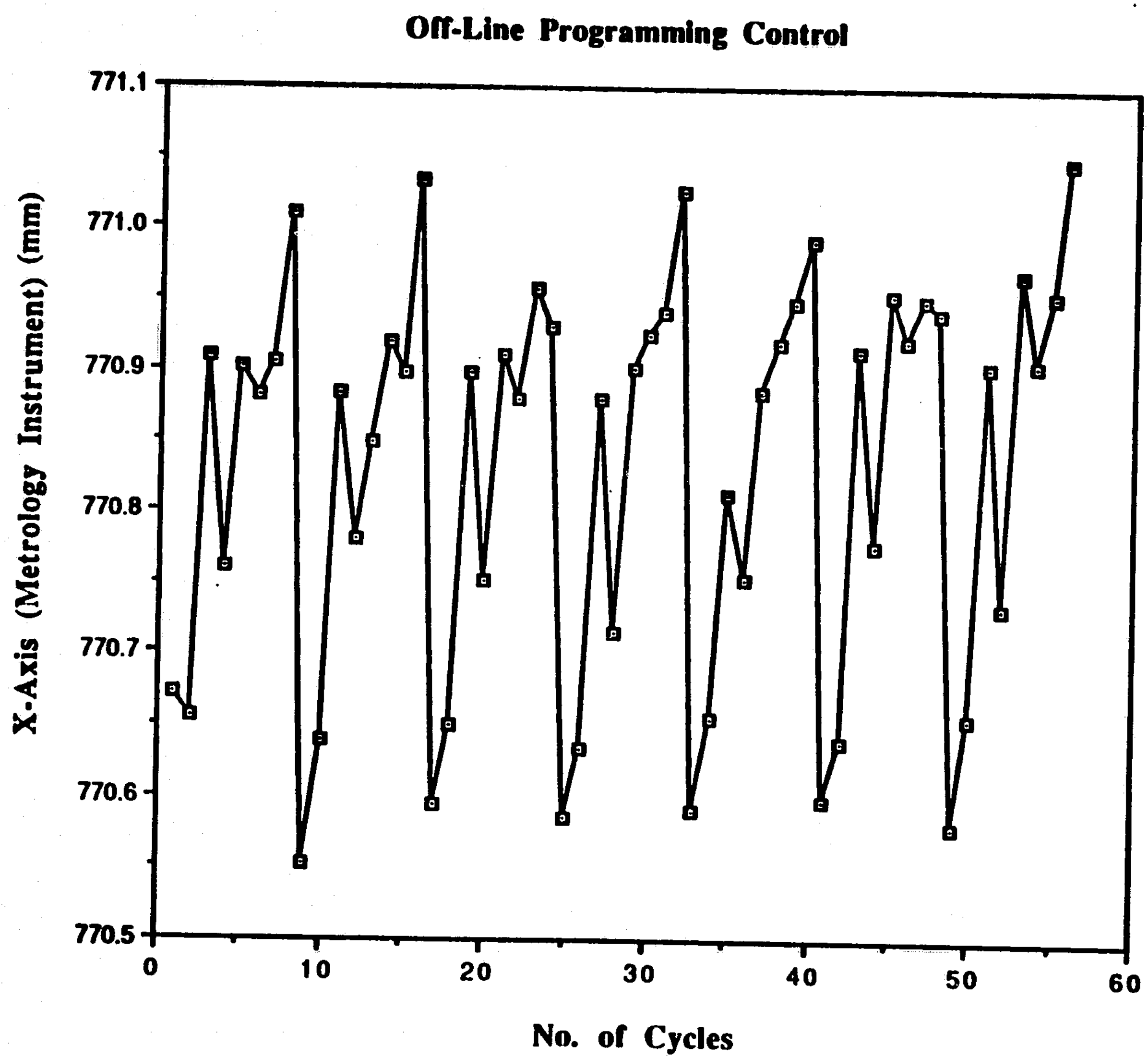

Figure 4.24 Measured position coordinate plot.

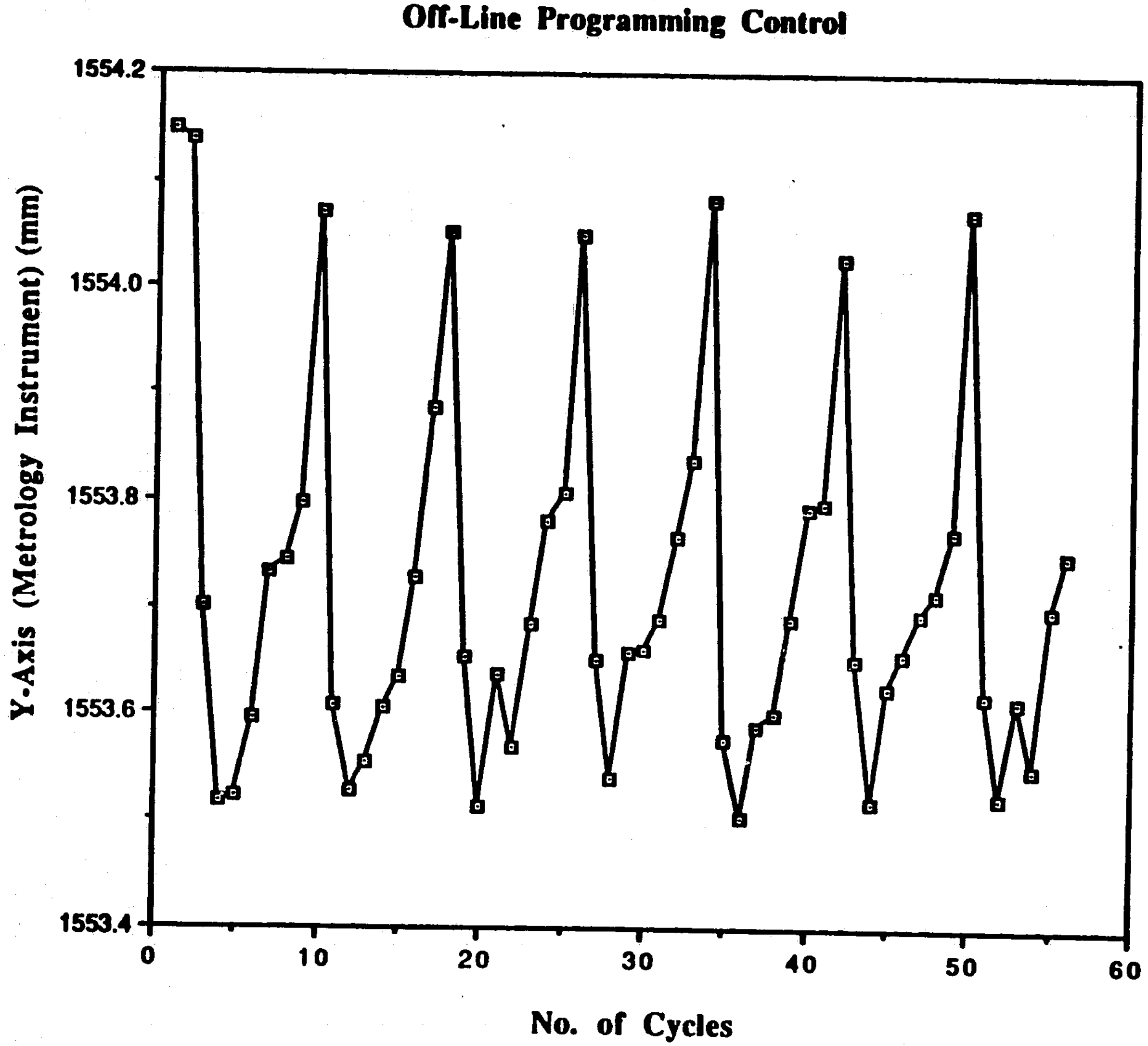

Figure 4.25 Measured position coordinate plot.

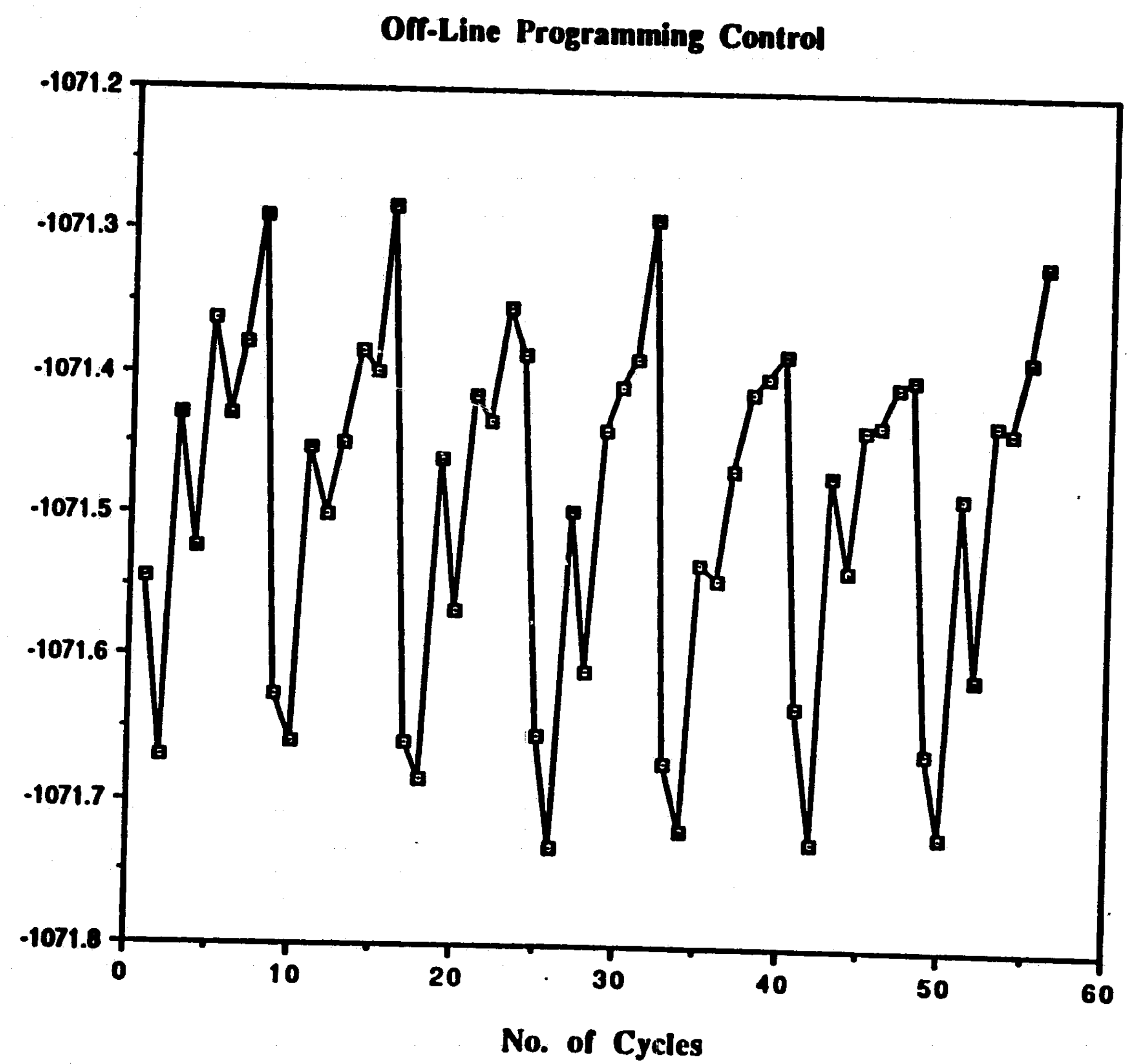

Figure 4.26 Measured position coordinate plot.

superimposed. Is that the result of the robot position control algorithm used, which does not stop servoing for as long as there is a joint angle position error? This of course raises the question, what would happen if only one initial position was used, would the random component dominate the achieved position? The test which will be reported in the next section will try to answer that question.

Comparing the errors, which are measured when the teach mode joint angles kinematics control is used and when off-line programming control is used, it can be seen that in the second case they are larger for both accuracy and repeatability, and the peak-to-peak amplitudes of the coordinates oscillations. This makes sense since in that case the errors due to the inverse kinematics algorithms are also included.

4.3.3.2.a Limited motion off-line programming

The off-line programming tests were repeated, eliminating the motions to and from the different initial positions. By comparing the results of this test with those of the previous test the effect of moving from different initial positions can be determined. For each repetition of this test, the robot moved between $S2_{app}$ and S2 eight times, using Cartesian-interpolated motion. Again, the position data was recorded each time the robot reached S2 and the test was repeated seven times, resulting in 56 data points. The motion time between $S2_{app}$ and S2 was the same as that used for the previous tests. Each repetition of the sequence of eight points took just over 3 min for this test.

4.3.3.2.b Analysis and Conclusions

The laser tracker coordinates of the 56 measured positions were again divided into 7 analysis groups. The data contained in each group were analyzed separately and the results of the analysis were used to determine the effect of the number of measured positions on the results.

Table 4.6 in the Appendix shows the results of the analysis of the last group of data which contains all 56 measured positions. Figure 4.27 is a three dimensional plot of the measured achieved positions (triangular marks), their mean position (cross mark), and the

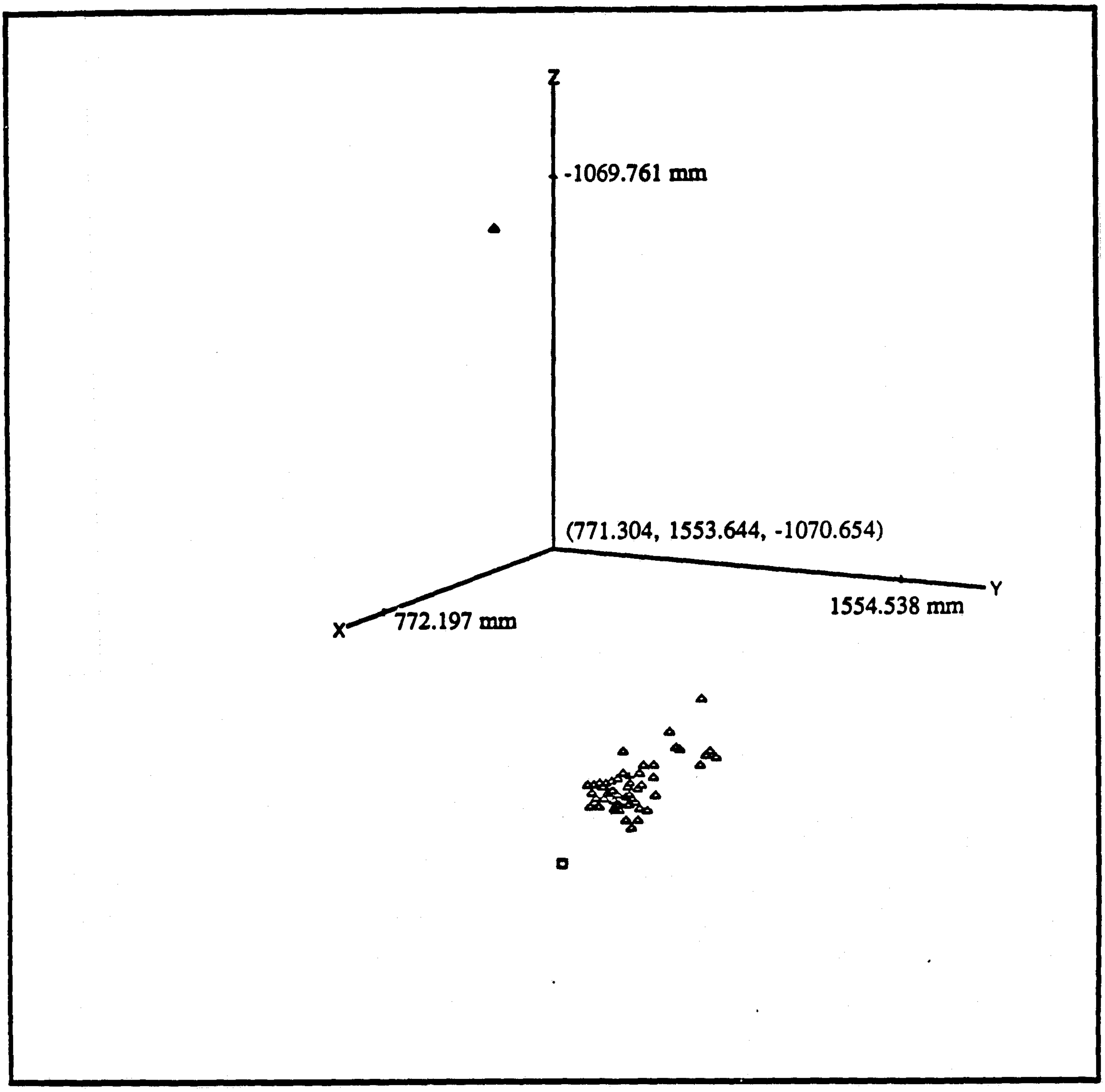

Plot of the PTP Test Achieved Positions
Each triangle is located at an achieved position
The square marks the commanded position
The cross marks the mean of the achieved positions

Figure 4.27 Limited motion off-line programming positions plot.

commanded position (square mark). The coordinate frame in that figure is that of the laser tracker after it was translated to the centroid of those positions.

Figure 4.28 is a plot of the same positions as they are projected on a plane defined by the X and Z coordinate axes. As can be seen the cluster of points forms again a galactic cloud with an orientation which is approximately orthogonal to the orientation of the axis of the first joint of the robot arm. In this case, though, the first two points in that plot can be seen to be located away from the rest, which cluster together in a tight group. The coordinates of those points correspond to the first two cycles of the test and the corresponding achieved positions. From Table 4.6 it can be seen that the first achieved position is approximately 1.0 mm away from the rest along both the Z and X axes. It is higher than the rest along the Z-axis direction, and forward along the X-axis direction.

Figure 4.29 is a plot of the ISO defined accuracy error versus the number of cycles contained in each analysis group. Figure 4.30 is a plot of the ISO defined repeatability error versus the number of cycles contained in each analysis group. As can be seen from these plots the errors seem to decrease exponentially reaching an asymptote after 40 to 56 cycles. The values of these errors start from rather high values as compared to those from the previous section (Figures 4.22, 4.23), probably because of the difference in the coordinates of the achieved positions of the first two cycles as compared to the rest. The level of the asymptotes is higher too.

To better understand the nature of this decrease of the accuracy and repeatability errors the X, Y, and Z axes, laser tracker coordinates of the 56 measured positions were plotted as a function of the number of cycles and are shown in Figures 4.31, 4.32, 4.33 respectively. These plots show again a periodicity with a fundamental frequency of 8 cycles and a few smaller amplitude higher frequency oscillations. There is a significant drift during the first 8 cycles, which corresponds to the first group of analysis data. After the first 8 cycles the coordinates seem to follow a relatively stable periodic oscillation. This significant drift at the beginning of the test is due mainly to the achieved positions during the first two cycles which are far away (especially the first one) from the rest. The periodic oscillations of the achieved positions are unexpected in this case, since all moves initiate from the same position (the approach position).

The off-line programming limited motion test was repeated four more times under various operating conditions to determine the source of the periodic oscillations and whether the commanded position (square mark). The coordinate frame in that figure is that of the laser tracker after it was translated to the centroid of those positions.

Figure 4.28 is a plot of the same positions as they are projected on a plane defined by the X and Z coordinate axes. As can be seen the cluster of points forms again a galactic cloud with an orientation which is approximately orthogonal to the orientation of the axis of the first joint of the robot arm. In this case, though, the first two points in that plot can be seen to be located away from the rest, which cluster together in a tight group. The coordinates of those points correspond to the first two cycles of the test and the corresponding achieved positions. From Table 4.6 it can be seen that the first achieved position is approximately 1.0 mm away from the rest along both the Z and X axes. It is higher than the rest along the Z-axis direction, and forward along the X-axis direction.

Figure 4.29 is a plot of the ISO defined accuracy error versus the number of cycles contained in each analysis group. Figure 4.30 is a plot of the ISO defined repeatability error versus the number of cycles contained in each analysis group. As can be seen from these plots the errors seem to decrease exponentially reaching an asymptote after 40 to 56 cycles. The values of these errors start from rather high values as compared to those from the previous section (Figures 4.22, 4.23), probably because of the difference in the coordinates of the achieved positions of the first two cycles as compared to the rest. The level of the asymptotes is higher too.

To better understand the nature of this decrease of the accuracy and repeatability errors the X, Y, and Z axes, laser tracker coordinates of the 56 measured positions were plotted as a function of the number of cycles and are shown in Figures 4.31, 4.32, 4.33 respectively. These plots show again a periodicity with a fundamental frequency of 8 cycles and a few smaller amplitude higher frequency oscillations. There is a significant drift during the first 8 cycles, which corresponds to the first group of analysis data. After the first 8 cycles the coordinates seem to follow a relatively stable periodic oscillation. This significant drift at the beginning of the test is due mainly to the achieved positions during the first two cycles which are far away (especially the first one) from the rest. The periodic oscillations of the achieved positions are unexpected in this case, since all moves initiate from the same position (the approach position).

The off-line programming limited motion test was repeated four more times under various operating conditions to determine the source of the periodic oscillations and whether the

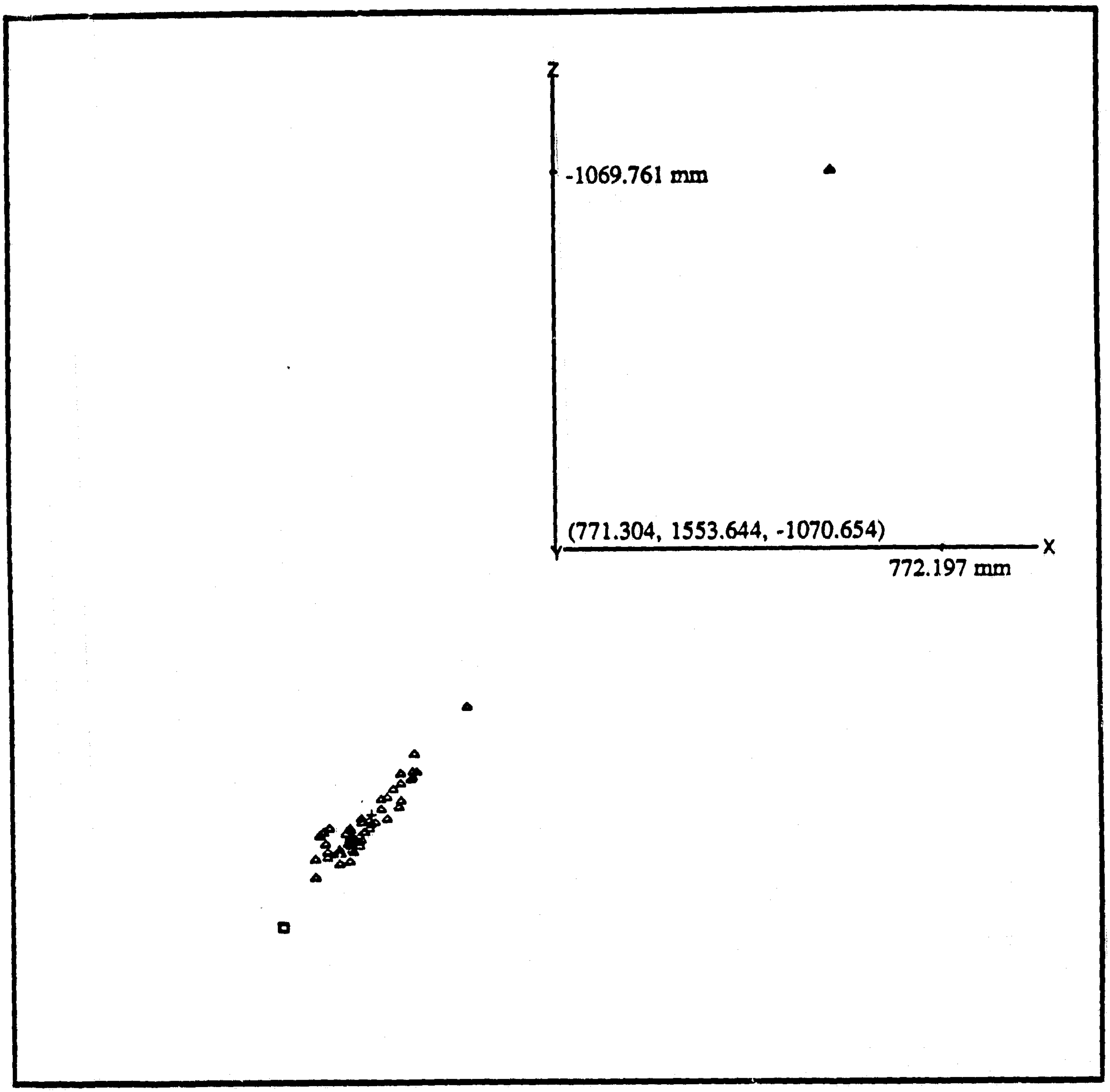

Plot of the PTP Test Achieved Positions
Each triangle is located at an achieved position
The square marks the commanded position
The cross marks the mean of the achieved positions

Figure 4.28 Limited motion off-line programming positions plot.

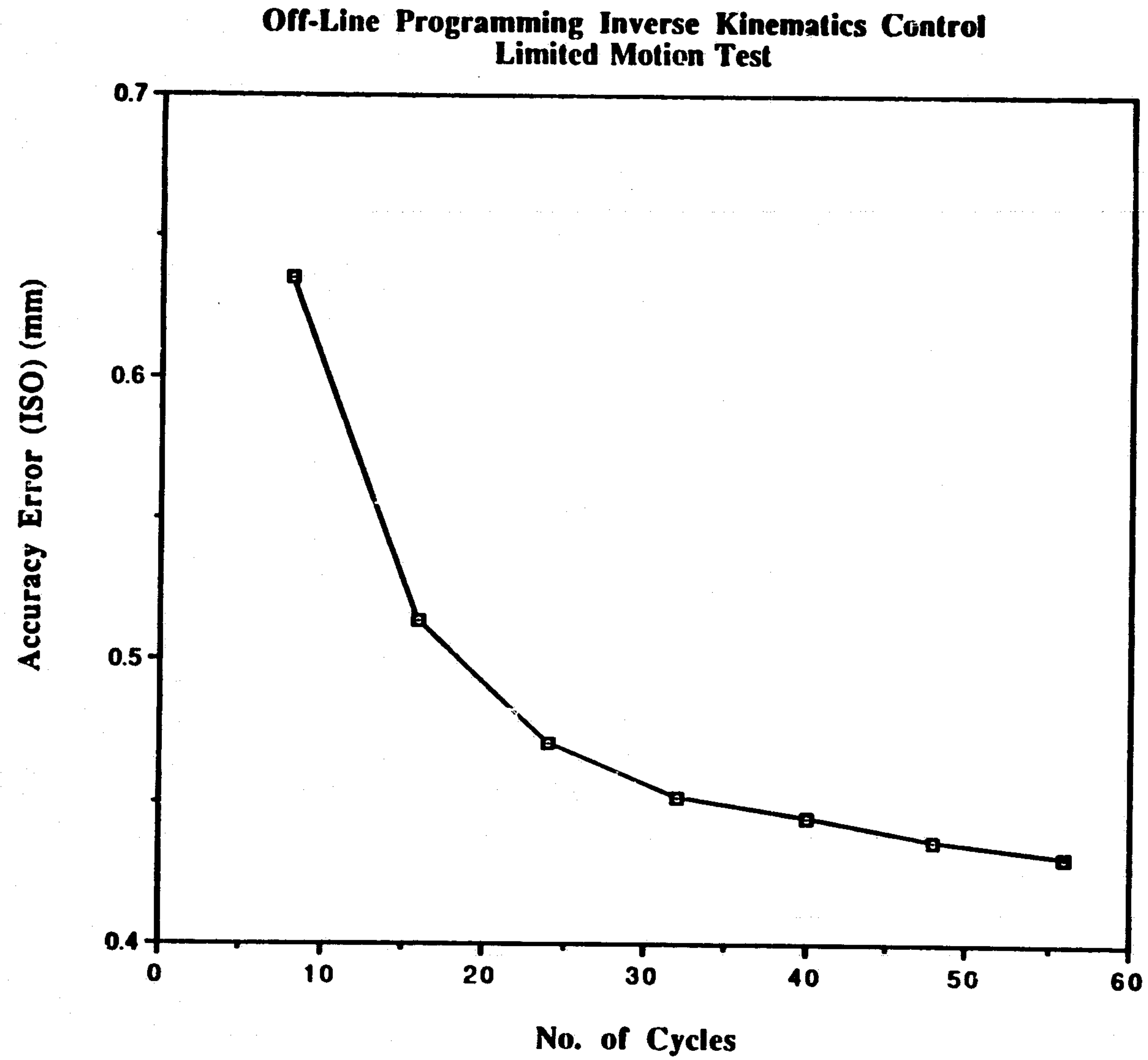

Figure 4.29 Position accuracy error plot.

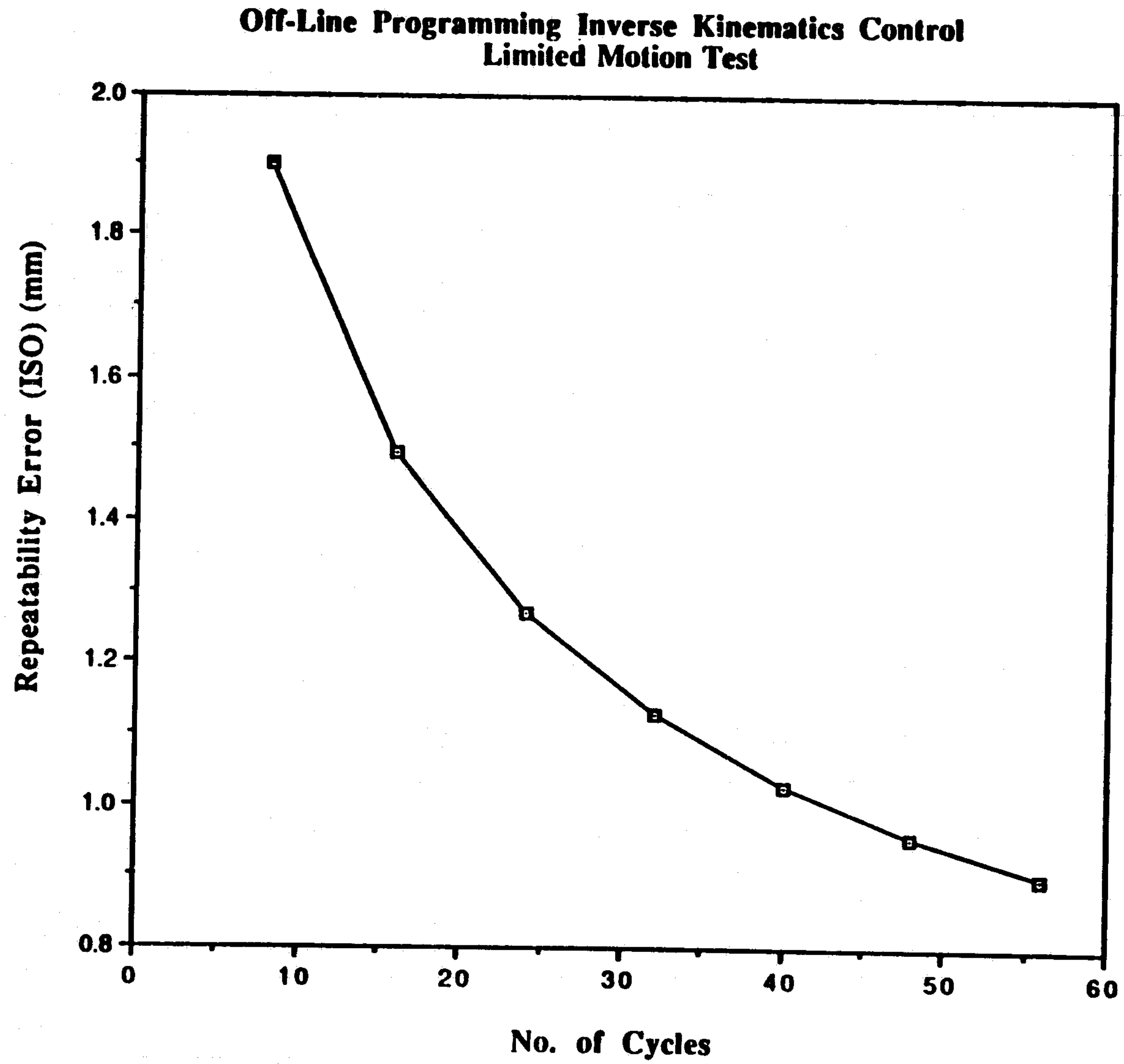

Figure 4.30 Position repeatability error plot.

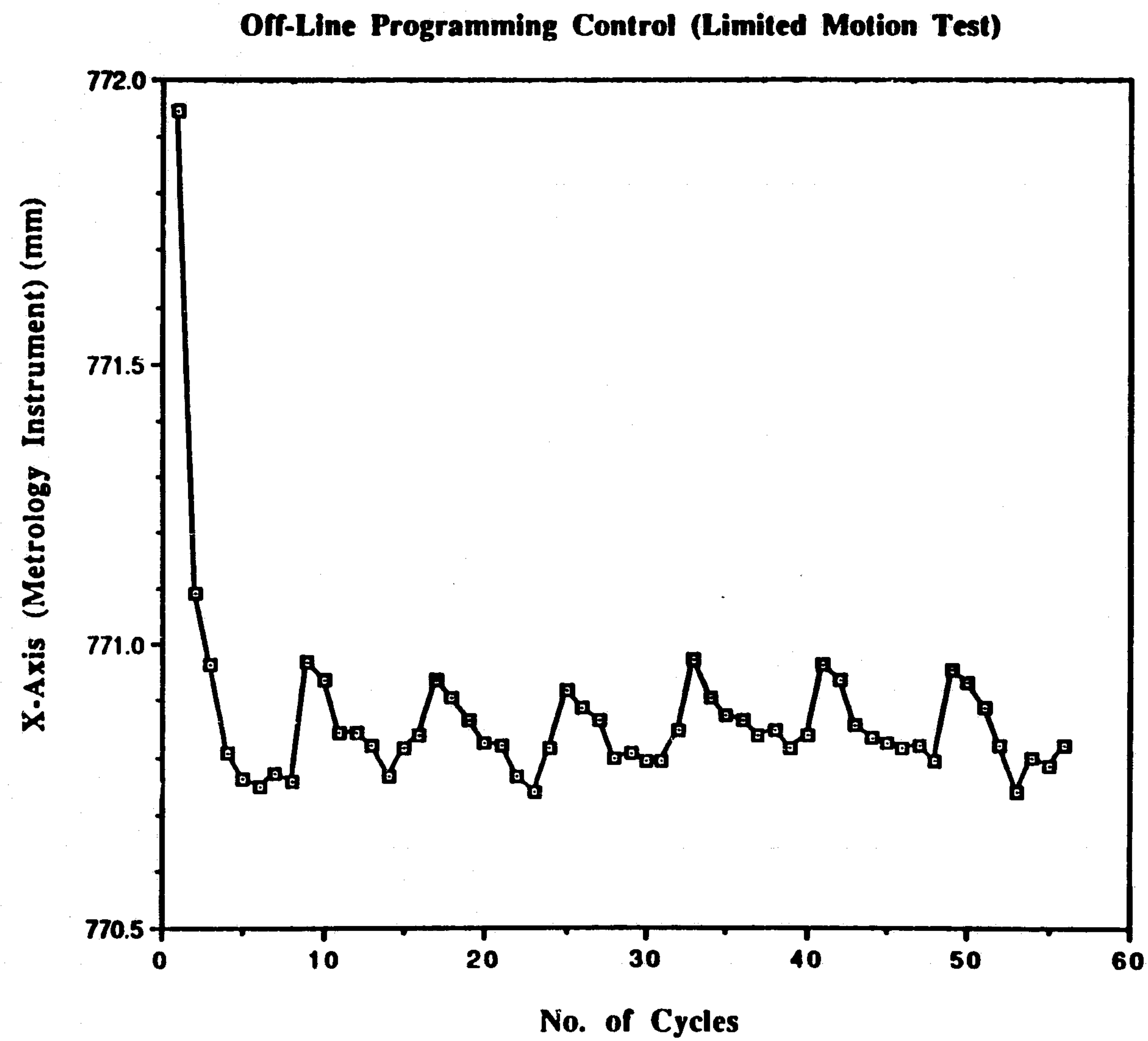

Figure 4.31 Measured position coordinate plot.

Off-Line Programming Control (Limited Motion Test)

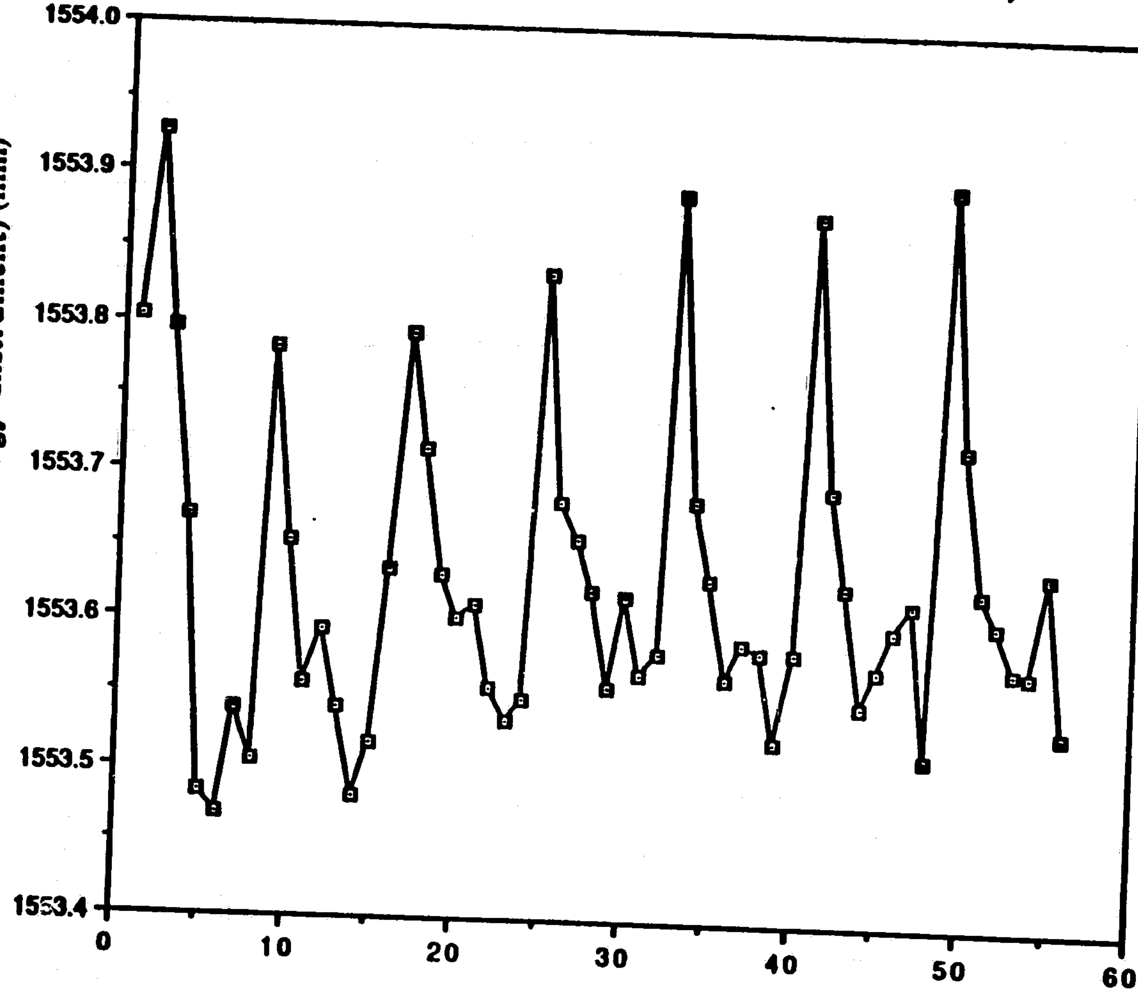

Figure 4.32 Measured position coordinate plot.

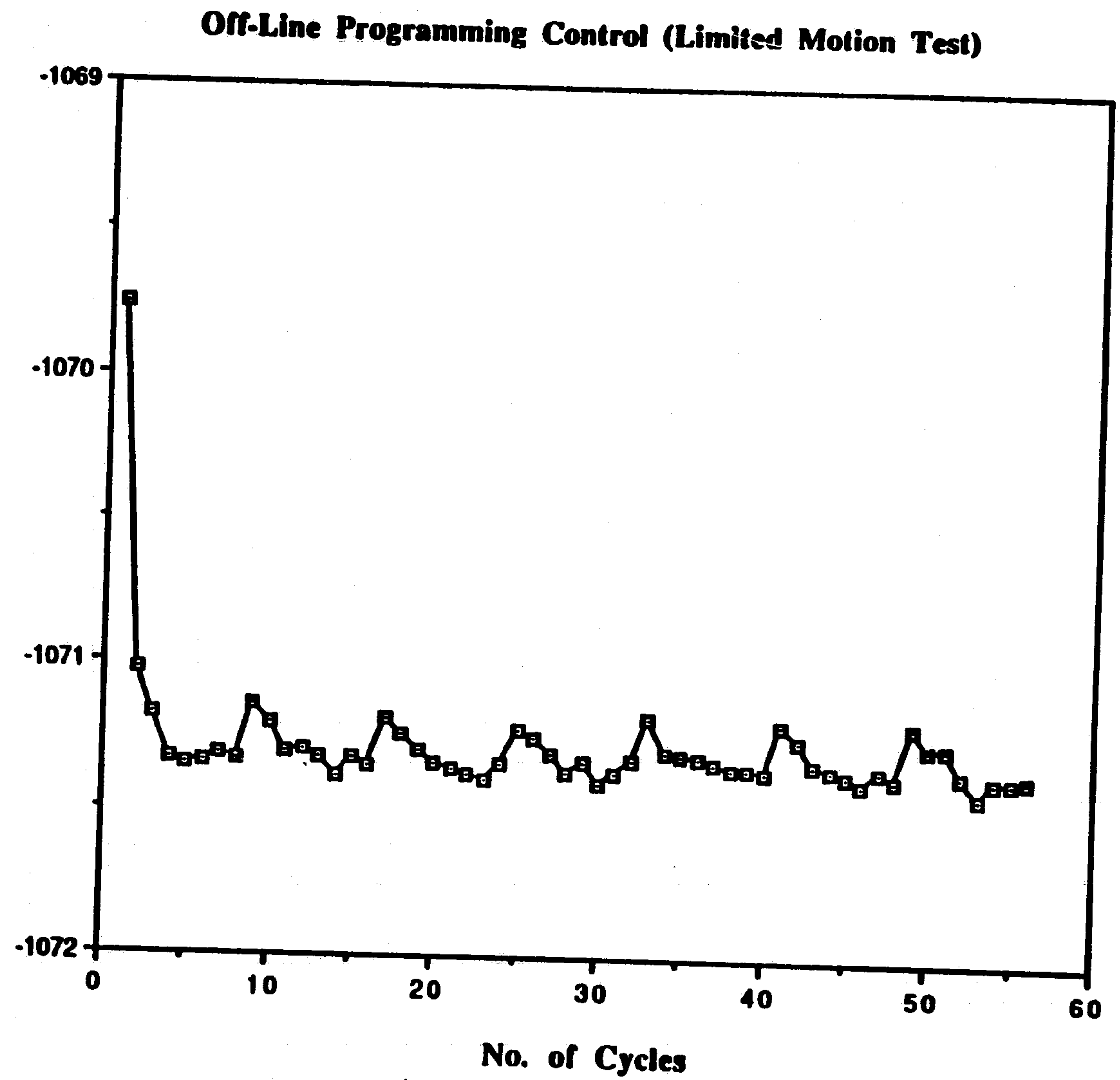

Figure 4.33 Measured position coordinate plot.

large position error during the first few cycles is accidental or not. In each test 120 cycles of motion were recorded. In the first case (test #2), the test conditions were the same as those used in the previous tests. In the second case (test #3), a time delay between every 8 cycles, of approximately 10 seconds was eliminated, because it was thought that it might be responsible for the periodic oscillations. In the third case (test #4), in addition to the time delay between every 8 cycles being eliminated, the integral gain of the joint servo control was reduced to zero. In the fourth case (test #5), an additional delay of less than 100 mseconds, for resetting the command file every 8 cycles was also eliminated.

As can be seen from these plots, as soon as the integral controller gain was set to zero both the periodic oscillations and the large position error during the first few cycles disappears, while a position drift has now been added. Figures 4.34, 4.35, 4.36, show the laser tracker X, Y, Z, coordinates for the #4 test (no large time delay, no integral control). Ignoring the drift, the measured achieved positions seem to be distributed rather randomly.

Comparing the results of the off-line programming test for motions from the standard RIA path positions (see Figures 4.22, 4.23) with those for limited motions (see Figures 4.29, 4.30), it can be seen that the errors measured for the limited motion case are larger for both accuracy and repeatability. The peak-to-peak amplitudes of the coordinates oscillations probably cannot be compared because of the large position error during the first few cycles of the limited motion off-line programming control case. From the test data discussed so far it appears that the limited motion off-line programming test cannot be used as a substitute of the standard RIA path positions off-line programming test, because the behavior of the robot arm seems to be quite different for these two cases. The effect of the integral gain, time delays and travel distance on performance has to be studied more carefully. Preliminary results from tests with shorter travel distances and no integral control show a significant drift over the duration of the tests.

4.3.4 Robot Position Resolution Tests

The objectives of the resolution tests were to observe and measure the ability of a robot arm to move its end-effector by small increments in specific directions and the effect of the number of measured increments on the results. Since, to the best of our knowledge, no established robot position resolution tests exist, a simple test and metric were established for the work reported here. Three orthogonal directions of motion, parallel to the robot arm

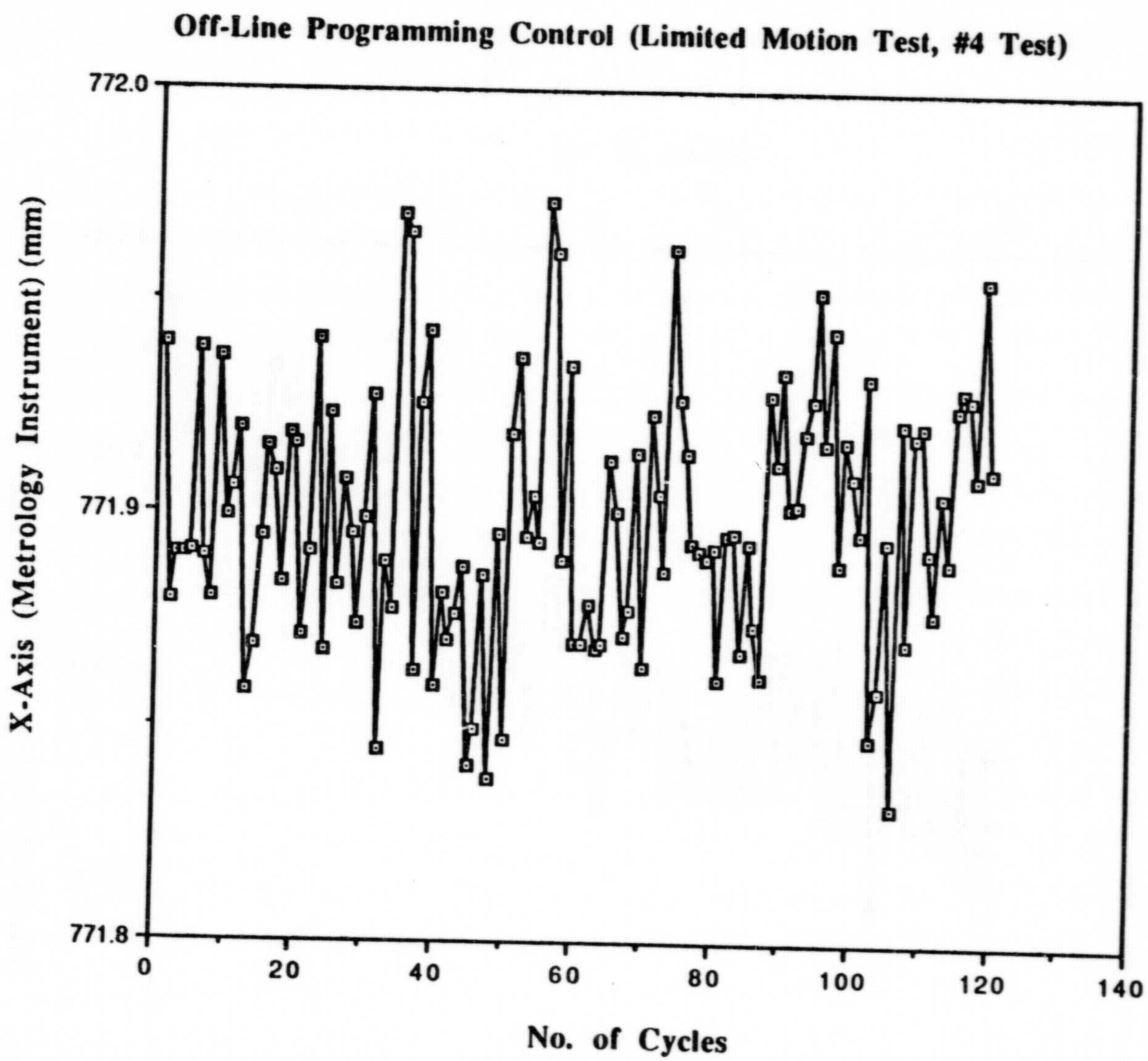

Figure 4.34 Measured position coordinate plot.

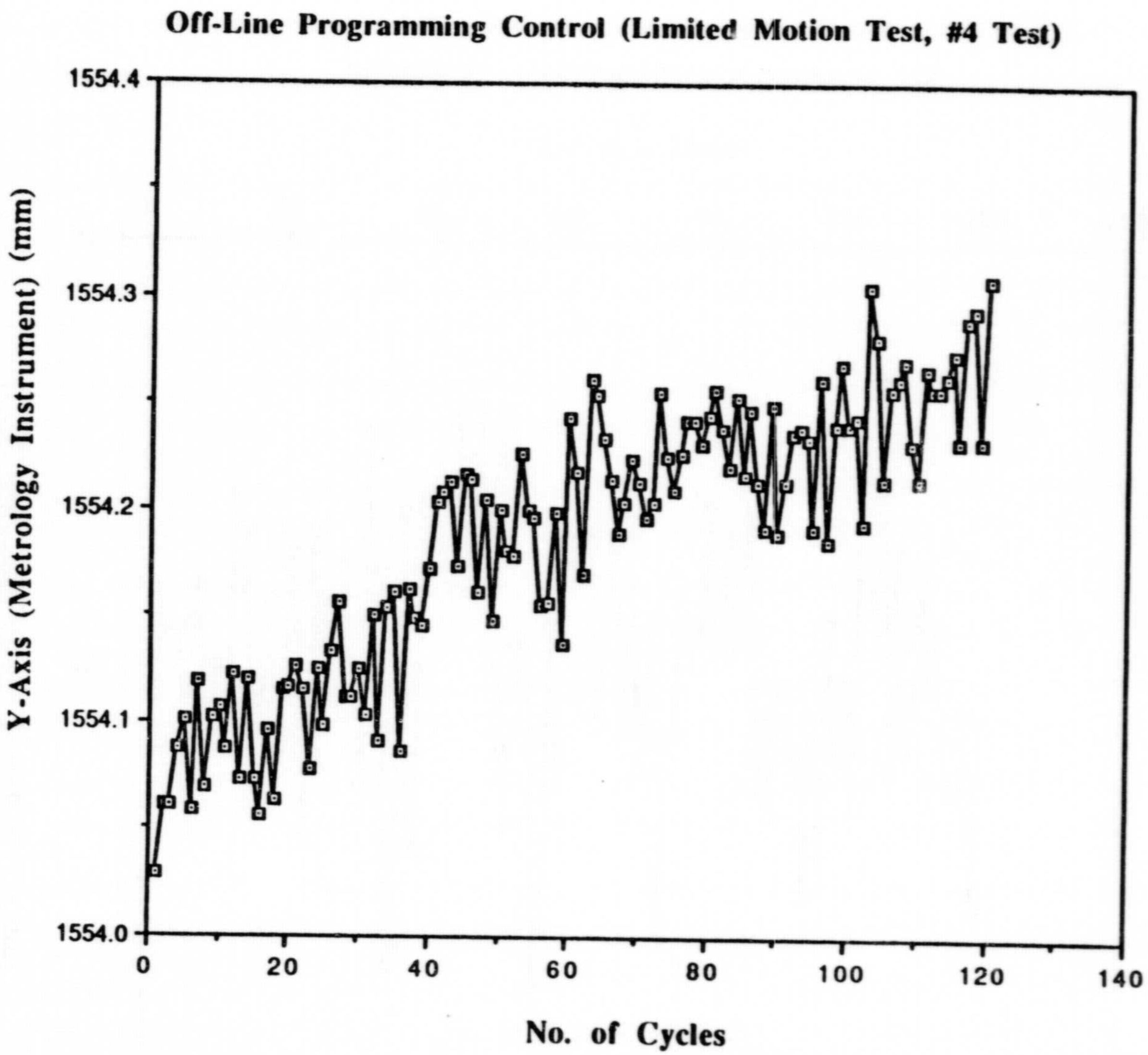

Figure 4.35 Measured position coordinate plot.

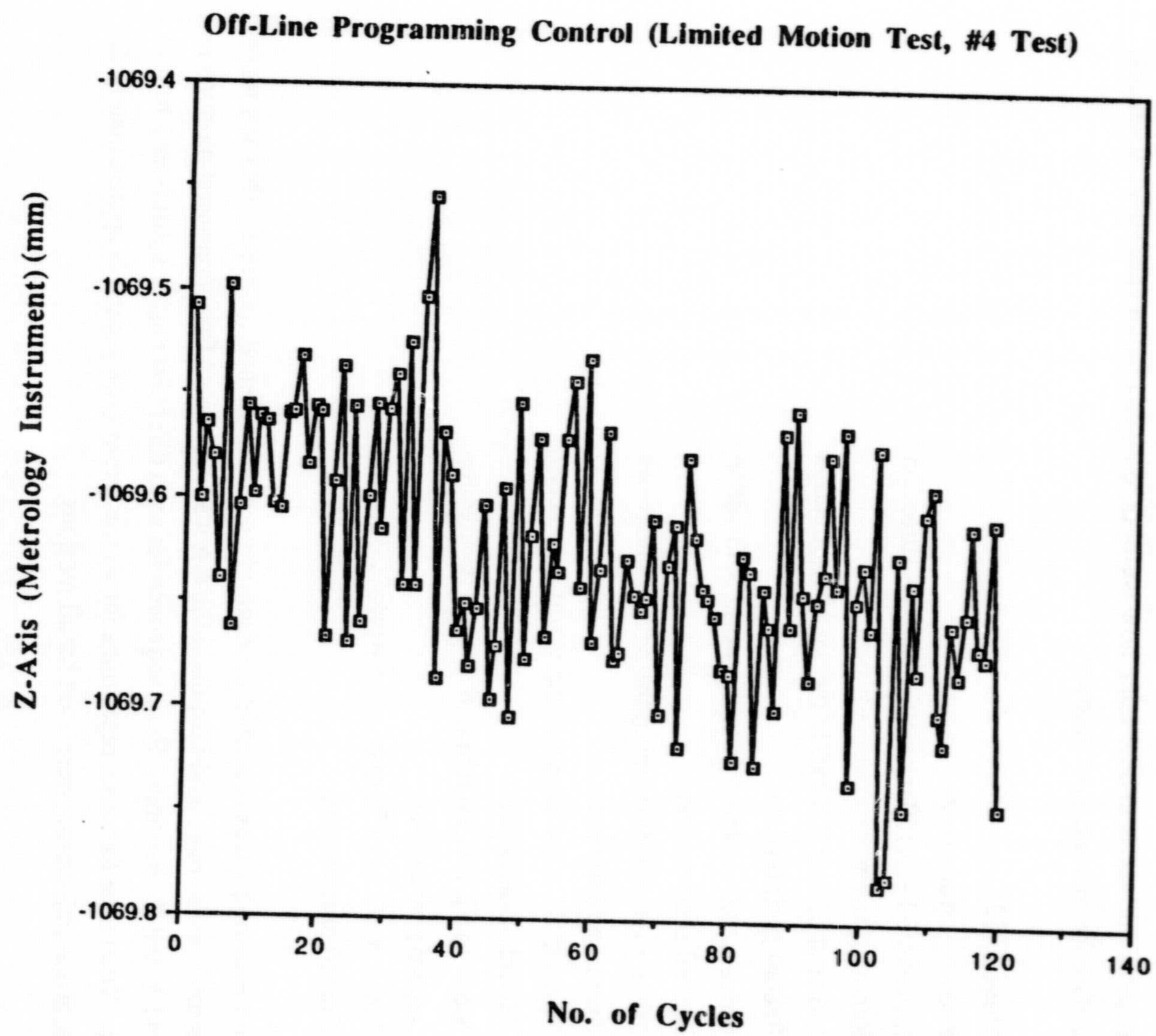

Figure 4.36 Measured position coordinate plot.

baseframe coordinate axes, with the simulated sensor nest location as the nominal position, were selected for the resolution test incremental moves. Increments of various lengths were tested. Due to the small size of the allowable workspace a forward and backward incremental motion had to be used.

4.3.4.a Tests

The purpose of this test is to determine how well the robot can move very small distances. The procedure for this test is as follows:

Move to S2
Record position data
Move to S2 + 0.150 mm in the world X direction
Record position data
Move to S2 + 0.300 mm in the world X direction
Record position data
Move to S2 + 0.450 mm in the world X direction
Record position data
Move to S2 + 0.600 mm in the world X direction
Record position data
Move to S2 + 0.450 mm in the world X direction
Record position data
Move to S2 + 0.300 mm in the world X direction
Record position data
Move to S2 + 0.150 mm in the world X direction
Record position data

A motion time of 5 s was specified for each of these incremental motions. This sequence was repeated seven times, and then the same test was performed for incremental motions in the world Y and Z directions. Each sequence for each direction requires just over 1 min to perform. Total time for seven repetitions for all directions (168 points) is approximately 23 min. Cartesian trajectories were used for all motions.

4.3.4.b Analysis and Conclusions

The laser tracker coordinates of the 56 measured positions in each orthogonal direction of movement were again divided into 7 analysis groups. The data contained in each group were analyzed separately and the results of the analysis were used to determine the effect of the number of measured positions on the results.

The mean and the standard deviation of the magnitudes of the increments in each direction and for each analysis group were calculated. Table 4.7 in the Appendix shows the results of the analysis of the last group of data which contains all 56 measured positions in each orthogonal direction of movement, for commanded incremental moves of 0.15 mm.

Figure 4.37 is a three dimensional plot of the measured achieved positions (cross marks for the X-direction moves, square marks for the Y-direction moves and triangle marks for the Z-direction moves). The coordinate frame in that figure is that of the laser tracker after it was translated to the centroid of those positions. As can be seen from that figure the incremental moves in each direction are not of equal length or direction.

Figures 4.38, 4.39, 4.40 are plots of the mean values of the measured magnitudes of the increments in the three directions of motion, versus the number of cycles contained in each analysis group. As can be seen from these plots, the mean values seem to decrease and approach an asymptote after 24 to 32 cycles for the data coming from the X and Z-axes directions of movement, but not for the Y-axis direction of movement.

The 0.15 mm incremental motion tests gave very questionable results, raising doubts whether this robot arm and controller can move in increments that small in specific directions. To check whether the situation improves with larger size increments the test was repeated with increments of 0.5 mm length. Table 4.8 in the Appendix shows the results of the analysis of the last group of data which contains all 56 measured positions in each orthogonal direction of movement, for commanded incremental moves of 0.5 mm. Figure 4.41 is a three dimensional plot of the measured achieved positions.

Comparing the plots from Figures 4.37 and 4.41 it can be seen that no significant improvement in the regularity of the magnitude and straightness of the incremental moves has been achieved. This of course raises the question of whether the mean value of the magnitudes of the increments is a sufficient measure for characterizing robot arm

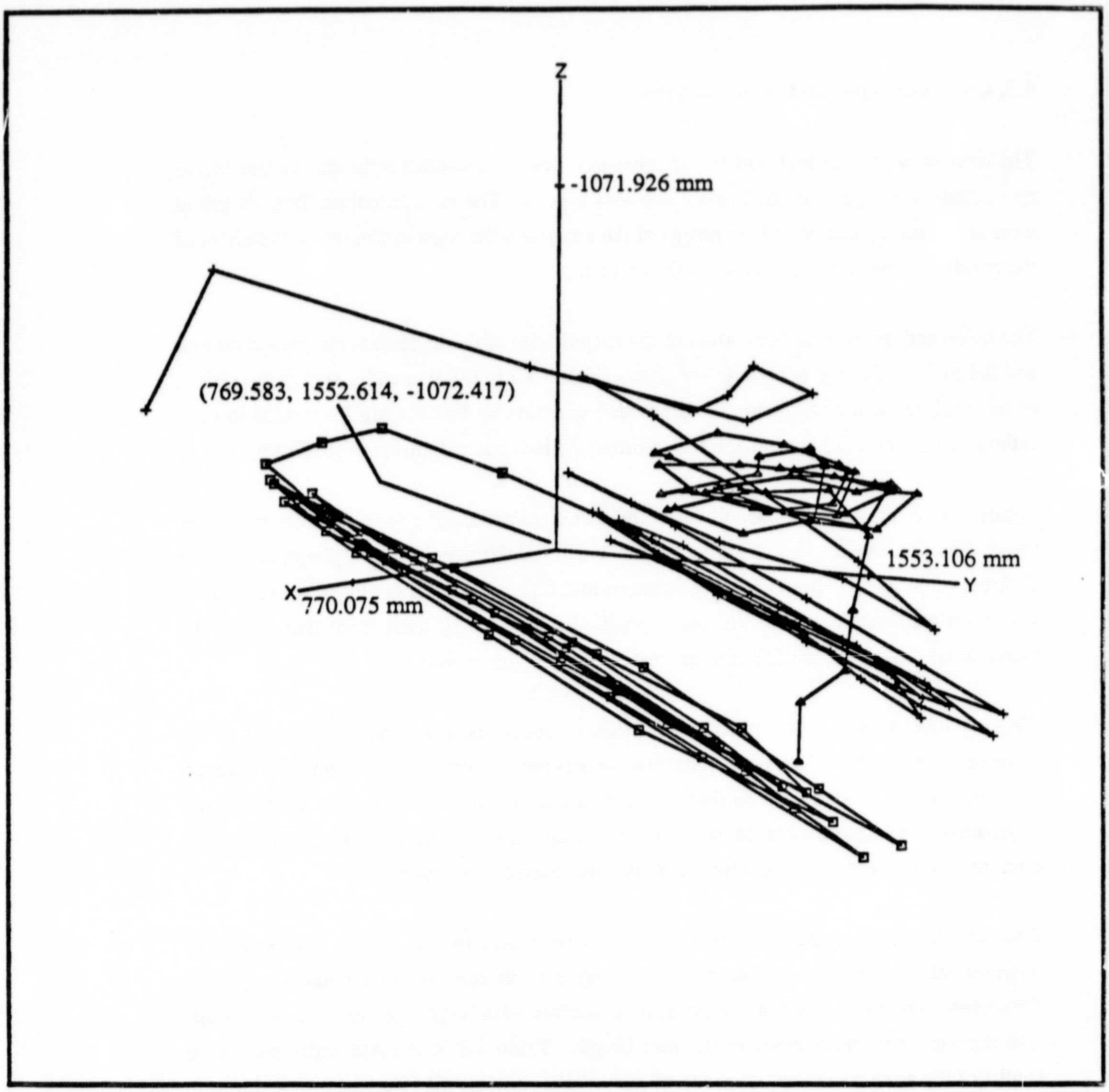

The cross marks the X-direction move
The square marks the Y-direction move
The triangle marks the Z-direction move

Figure 4.37 Robot resolution test positions.

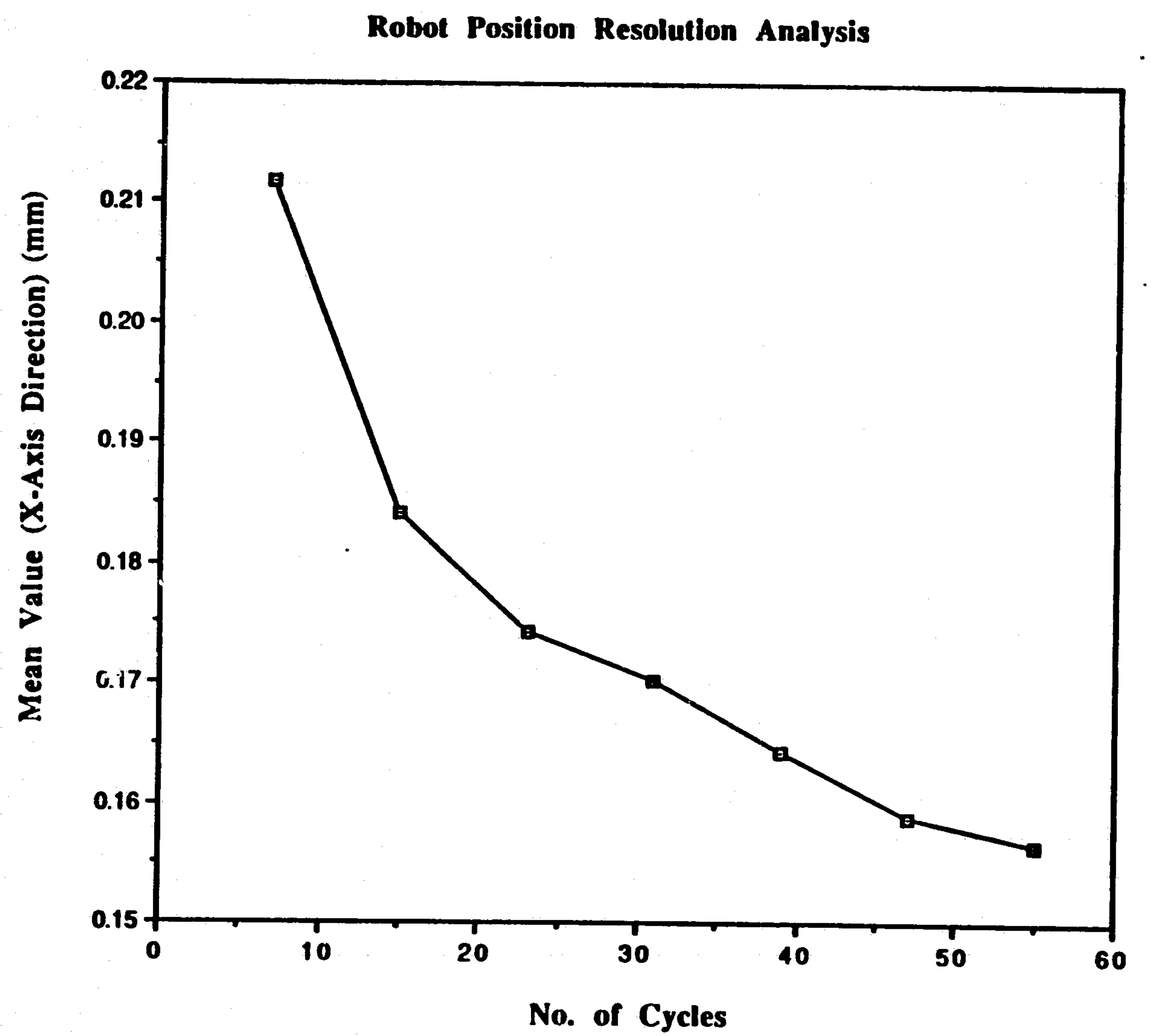

Figure 4.38 Plot of the measured magnitudes of the increments.

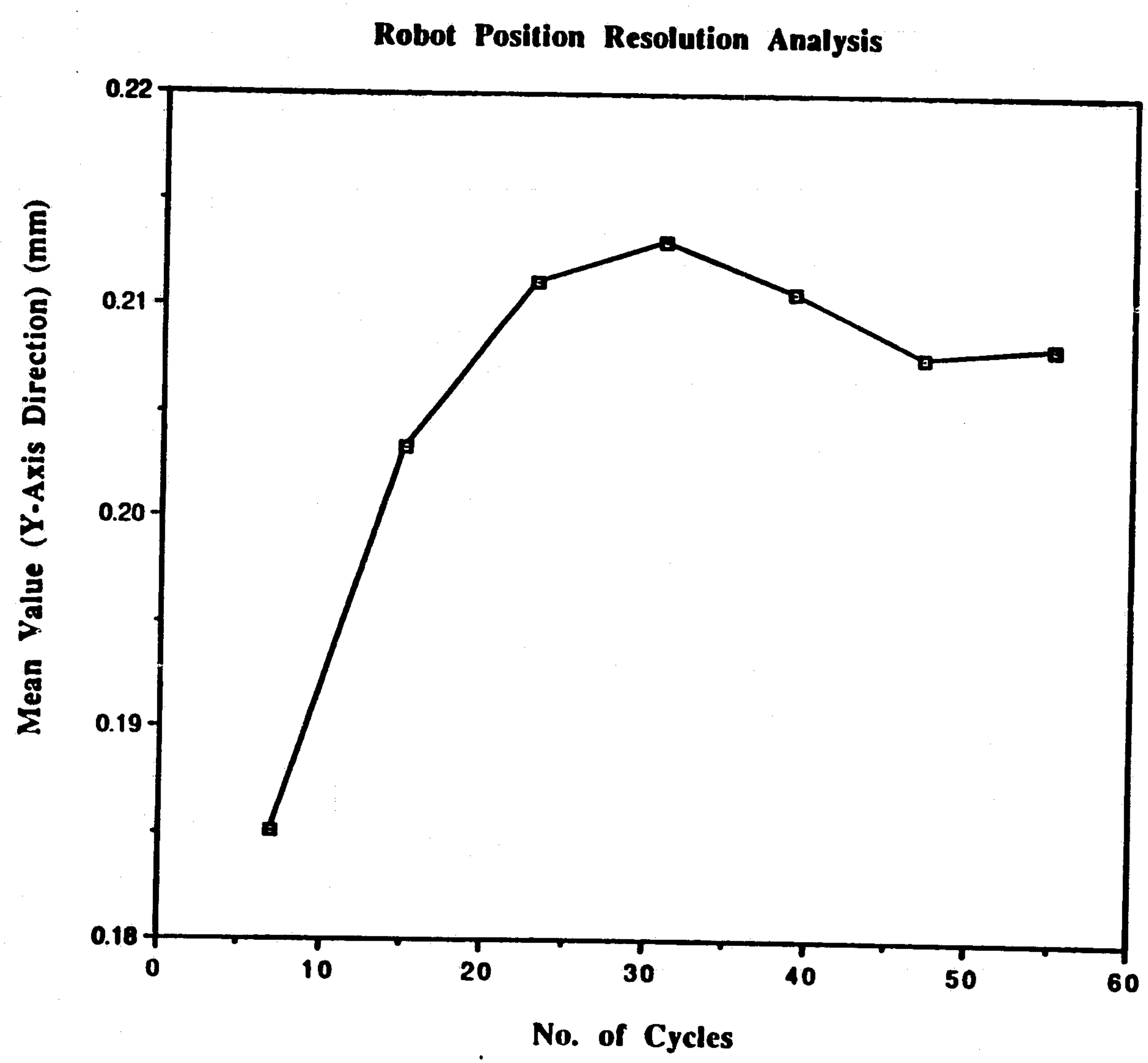

Figure 4.39 Plot of the measured magnitudes of the increments.

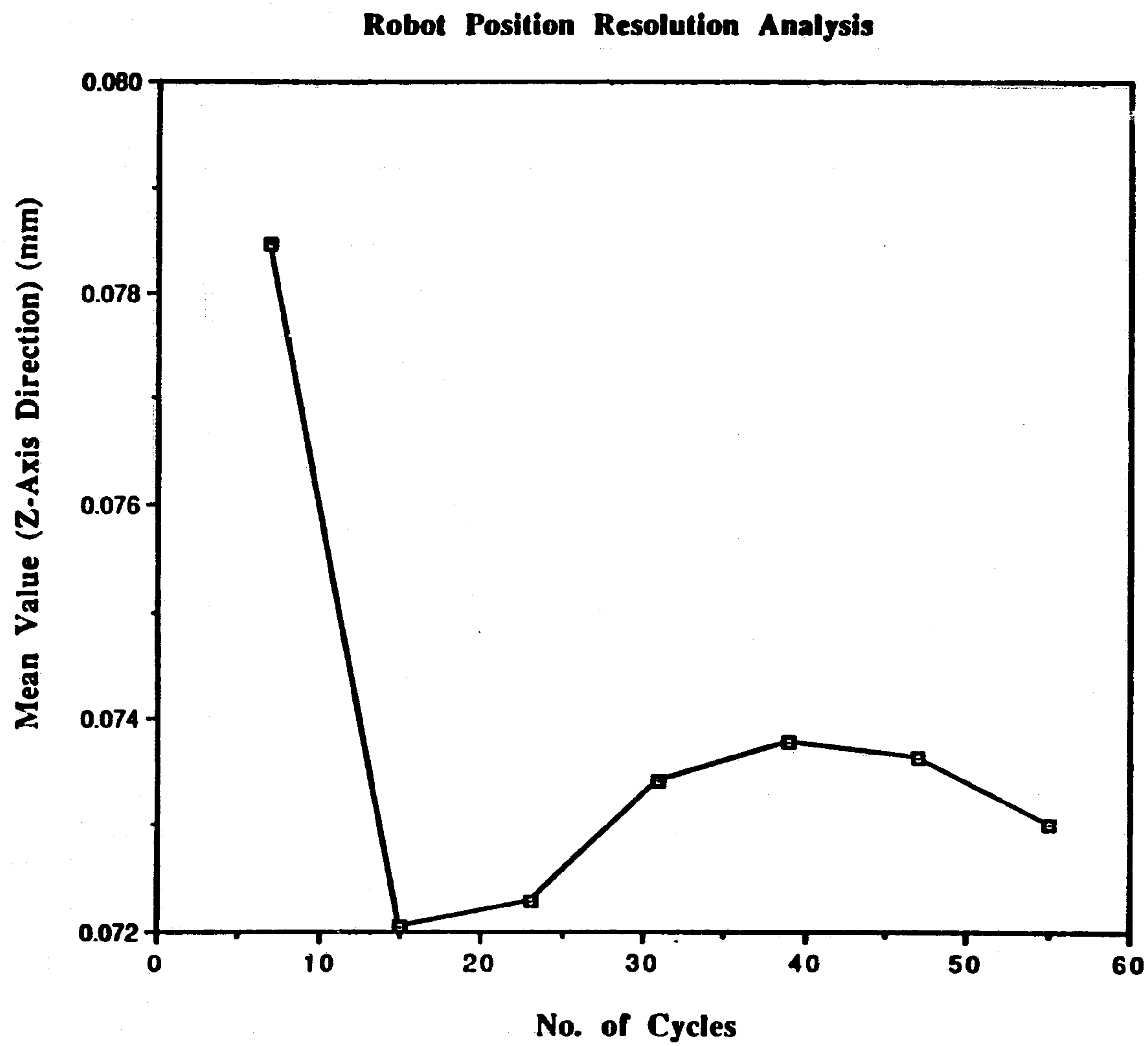

Figure 4.40 Plot of the measured magnitudes of the increments.

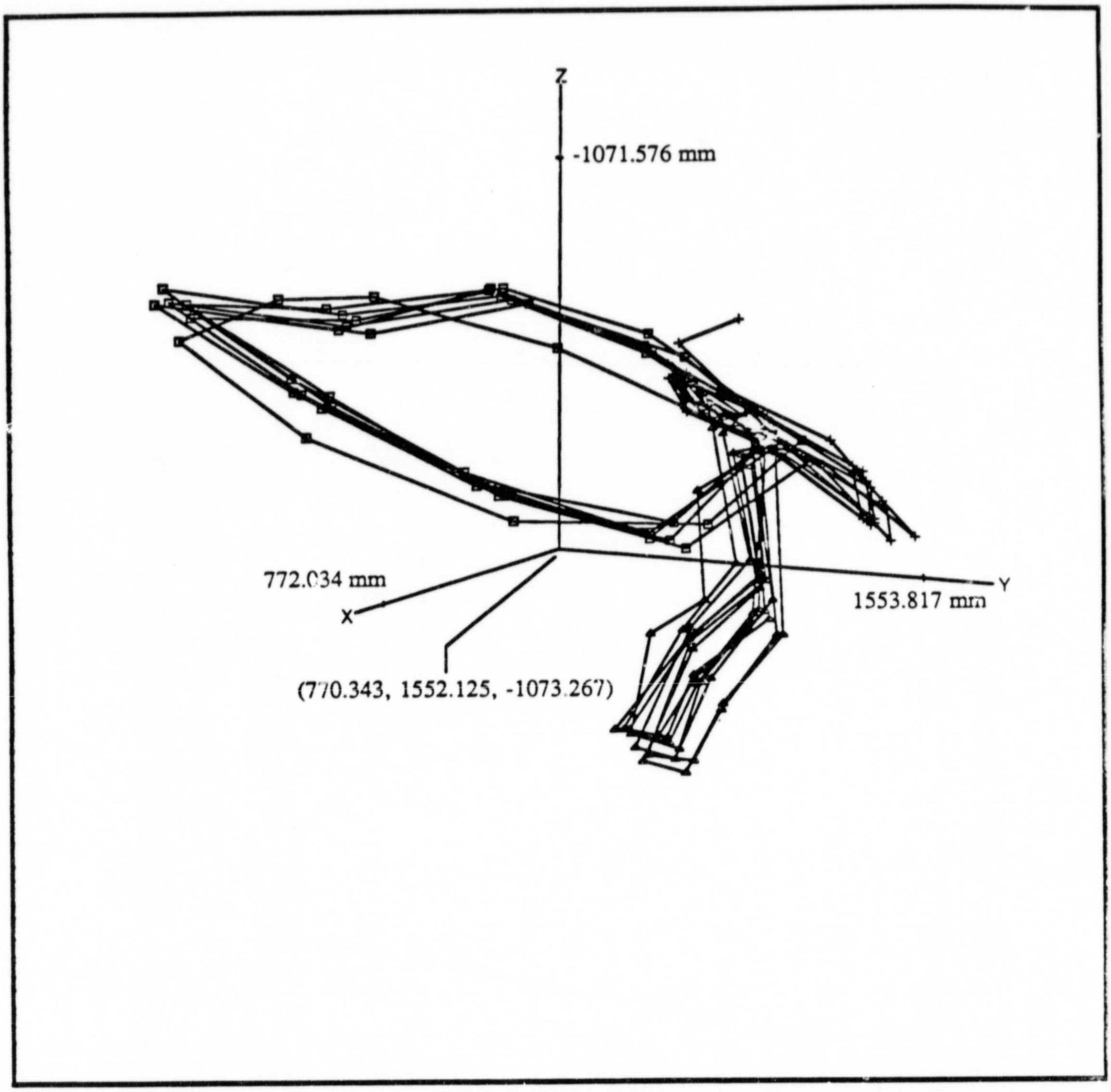

The cross marks the X-direction move
The square marks the Y-direction move
The triangle marks the Z-direction move

Figure 4.41 Robot resolution test positions.

resolution. Perhaps if the mean value of the orientation error, with respect to the commanded direction of move is included, a more complete description of the measured achieved move will be provided. Another more compact way of characterizing robot arm resolution would be to provide the mean value of the projection of the measured achieved motion along the direction of commanded move.

In general, very small motions along orthogonal baseframe coordinate axes will be difficult for a serial revolute arm to perform. This is because in most cases the motion of the arm joints contribute in a complex way to Cartesian motion of the end effector, and joint-related disturbances, such as stiction, become significant. Due to the smallness of the motion the torque commands are initially not sufficient to overcome stiction. If an integral control term is used, it will sense the error and build up the torque until motion initiates, then the arm will probably overshoot the commanded position and the whole process will be repeated again. Some possibilities for improving the incremental positioning resolution include modifying the servo gains, and adding dither or other friction compensation torques to the control. A more detailed study of this small torque-small displacement interaction would have to be performed on the robot arm being tested to better understand the resolution error problem.

4.4 Forward Kinematics Error Analysis

Under joint interpolated teach mode control the robot control system servo algorithm, combined with the torque loop control, motor amplifiers, joint drives, and joint position and torque sensors, causes the robot to move the joints to prerecorded angles. Therefore the teach mode control performance tests may reveal defects of any of the above components. Under off-line programming the robot control system must also use the inverse kinematics algorithms to determine the joint angles which correspond to the commanded Cartesian coordinates. These angles then become the commands which are sent to the servo level. Therefore the off-line programming performance tests may reveal defects of the inverse kinematics algorithms as well as the servo algorithm, the mechanical part of the robot arm, and other servo components. The objective of the analysis described in this section was to test the performance of the forward kinematics model and algorithms. Forward kinematics algorithms are used by many new sophisticated robot controllers for compliance control, precision move control, calibration, etc.

No new tests had to be performed for the forward kinematics analysis work; any test data which included target position information measured by the laser tracker and the robot controller could be used for the purposes of this analysis. The idea behind this analysis is to use the coordinates transformation to convert the laser tracker measured coordinates to robot controller coordinates, then compare these converted coordinates to the robot controller calculated coordinates for the same target positions. The differences in the two sets of coordinates are due to errors in the forward kinematics algorithms of the robot controller and the laser tracker controller, since they are the ones used by the controllers to convert from joint positions to target Cartesian coordinates. Equations 4.2 to 4.13 are then used to calculate the accuracy and repeatability errors, where in this case the coordinates of the achieved positions are the coordinates of the calculated errors and the coordinates of the commanded position are all zeroes, which are the desired values of the errors.

One of the major sources of robot kinematic modelling errors is the joint position initialization error. When the robot power is turned on its controller has to find the precise location of its joints. Every time it does that a small bias error is added to the joint position estimate. The combination of these errors results in a small translation and rotation of the robot baseframe every time the power is turned off and on. The forward kinematics error analysis can be used to estimate the contribution of this initialization error to the position accuracy and repeatability errors. If the position data used to estimate the coordinates transformation and the forward kinematics errors are collected before the robot power is turned off, there will be no contribution from the joint position initialization offset error. This is true because the coordinates transformation includes the translation and rotation of the robot baseframe due to that error. If, on the other hand, the target positions are collected after the power is turned off and on, any difference in the joint position initialization will contribute to the measured performance errors.

To determine an estimate of the initialization error, two sets of data were analyzed. The first was collected at about the same time the coordinates transformation data were collected (with no reinitialization), while the second was collected the next day after the robot arm power was turned off and on a couple of times. Of course, every effort was made to keep all the other conditions of the experiment approximately the same, like the room temperature, the amount of robot arm exercise, etc. The analysis of these two sets of data are presented in the following sections.

4.4.1 Continuous operation error analysis and Conclusions

The test data used for this analysis are those of the teach mode inverse kinematics test listed in Table 4.2. At the end of that test and before the robot arm power was turned off data from 14 positions were collected in order to determine the mathematical transformation between the coordinate frame of the laser tracker and the robot baseframe. It is this transformation listed in Table 4.3 that was used to convert the data used for this analysis.

The laser tracker coordinates of the 56 measured positions were again divided into 7 analysis groups. The data contained in each group were analyzed separately and the results of the analysis were used to determine the effect of the number of measured positions on the results.

Table 4.9 in the Appendix shows the results of the analysis of the last group of data which contains all 56 measured positions. Figure 4.42 is a three dimensional plot of the calculated forward kinematics errors (triangular marks), and their mean (cross mark).

Figure 4.43 is a plot of the ISO defined accuracy error versus the number of cycles contained in each analysis group. Figure 4.44 is a plot of the ISO defined repeatability error versus the number of cycles contained in each analysis group. As can be seen from these plots the values of both of these errors are small compared to the errors measured from all the previous tests. The variation in their values as a function of the number of cycles is very small too.

4.4.2 Interrupted operation error analysis and Conclusions

The test data used for this analysis are those of the teach mode joint angles kinematics test listed in Table 4.1. The same transformation used to convert the data of the continuous operation forward kinematics error analysis was used for these data too. This is the transformation listed in Table 4.3.

The laser tracker coordinates of the 56 measured positions were again divided into 7 analysis groups. The data contained in each group were analyzed separately and the results of the analysis were used to determine the effect of the number of measured positions on the results.

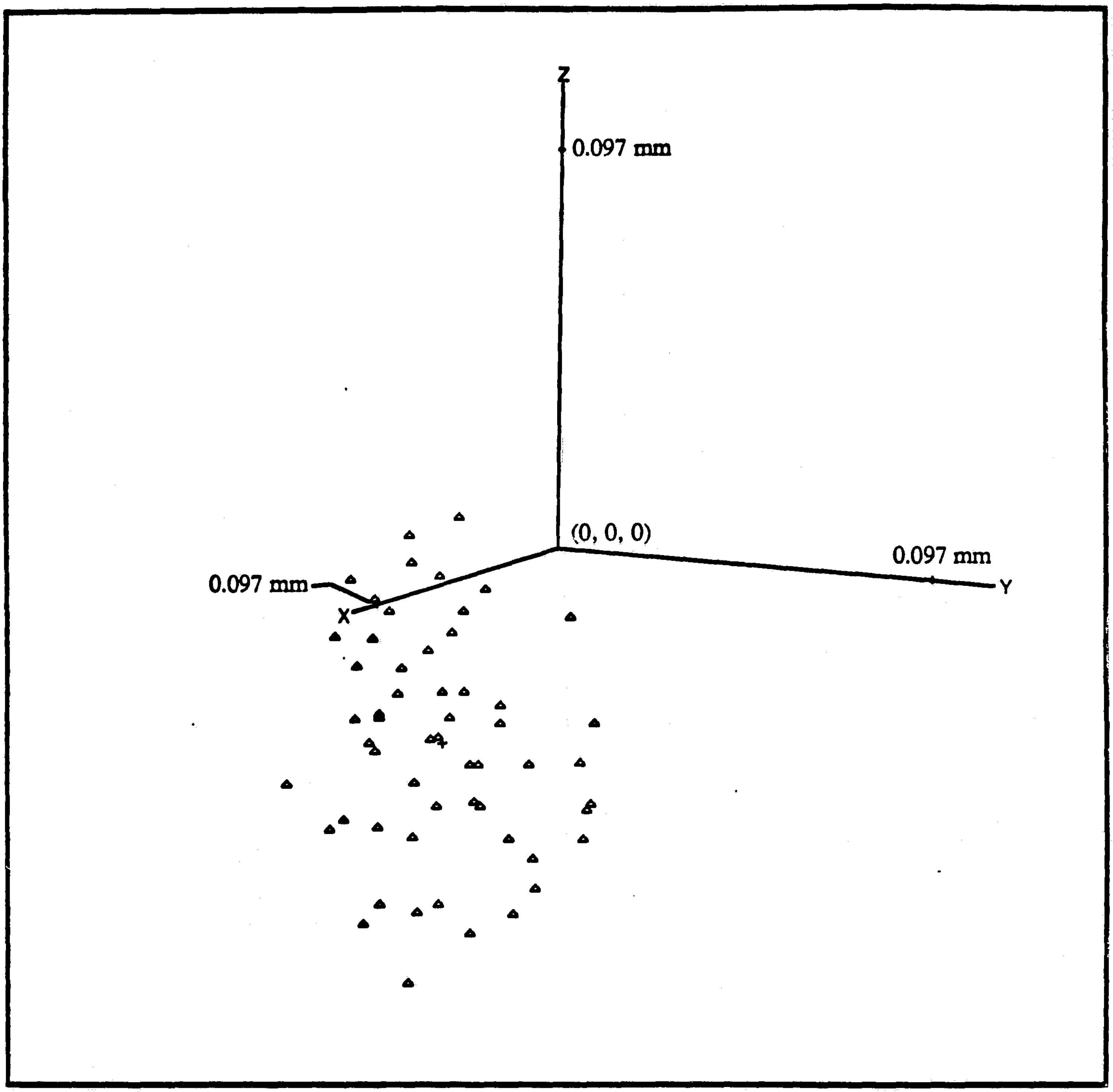

Forward Kinematics PTP Testing Errors
The cross marks the mean of the errors

Figure 4.42 Forward kinematics (continuous operation).

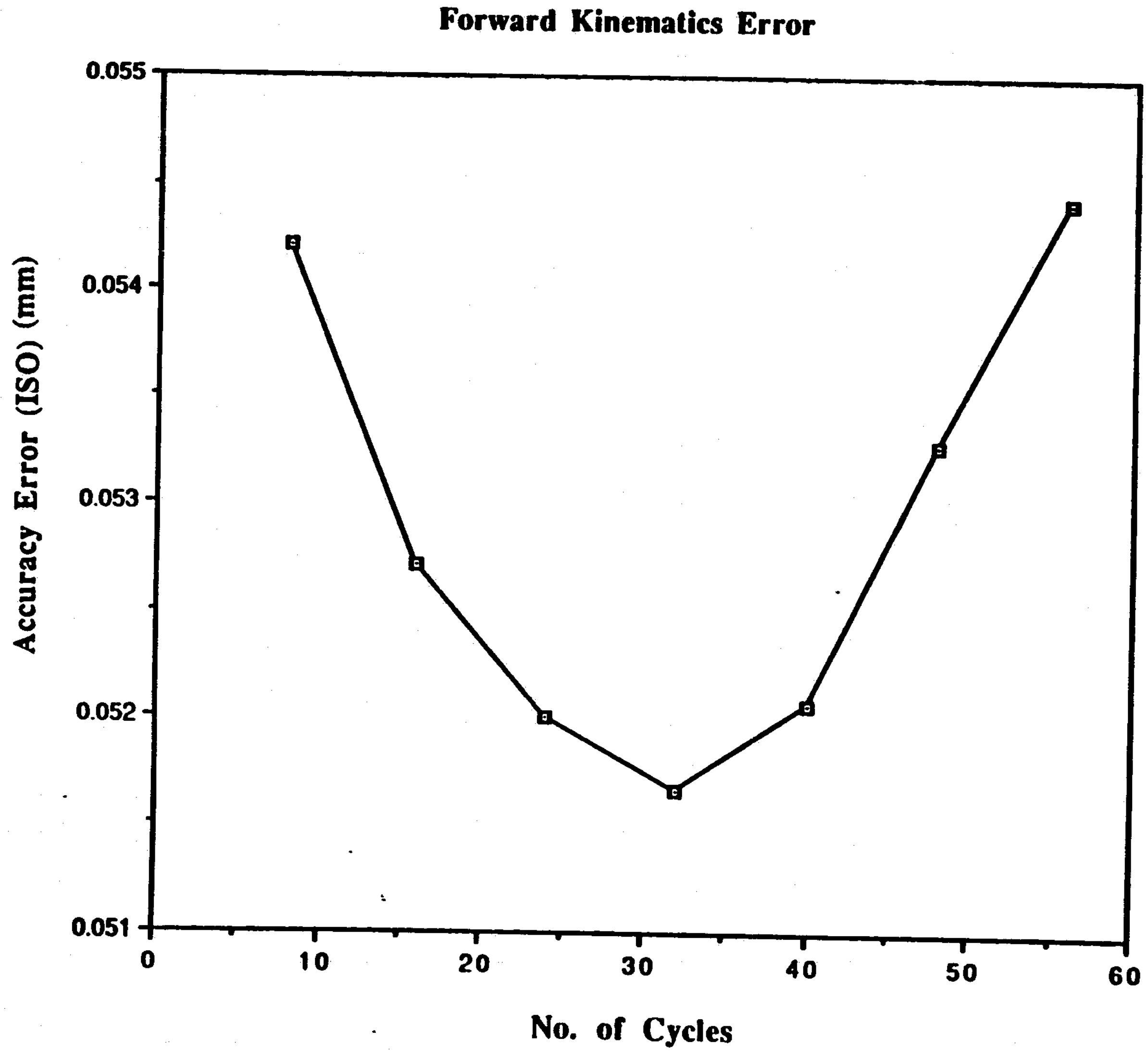

Figure 4.43 Position accuracy error plot.

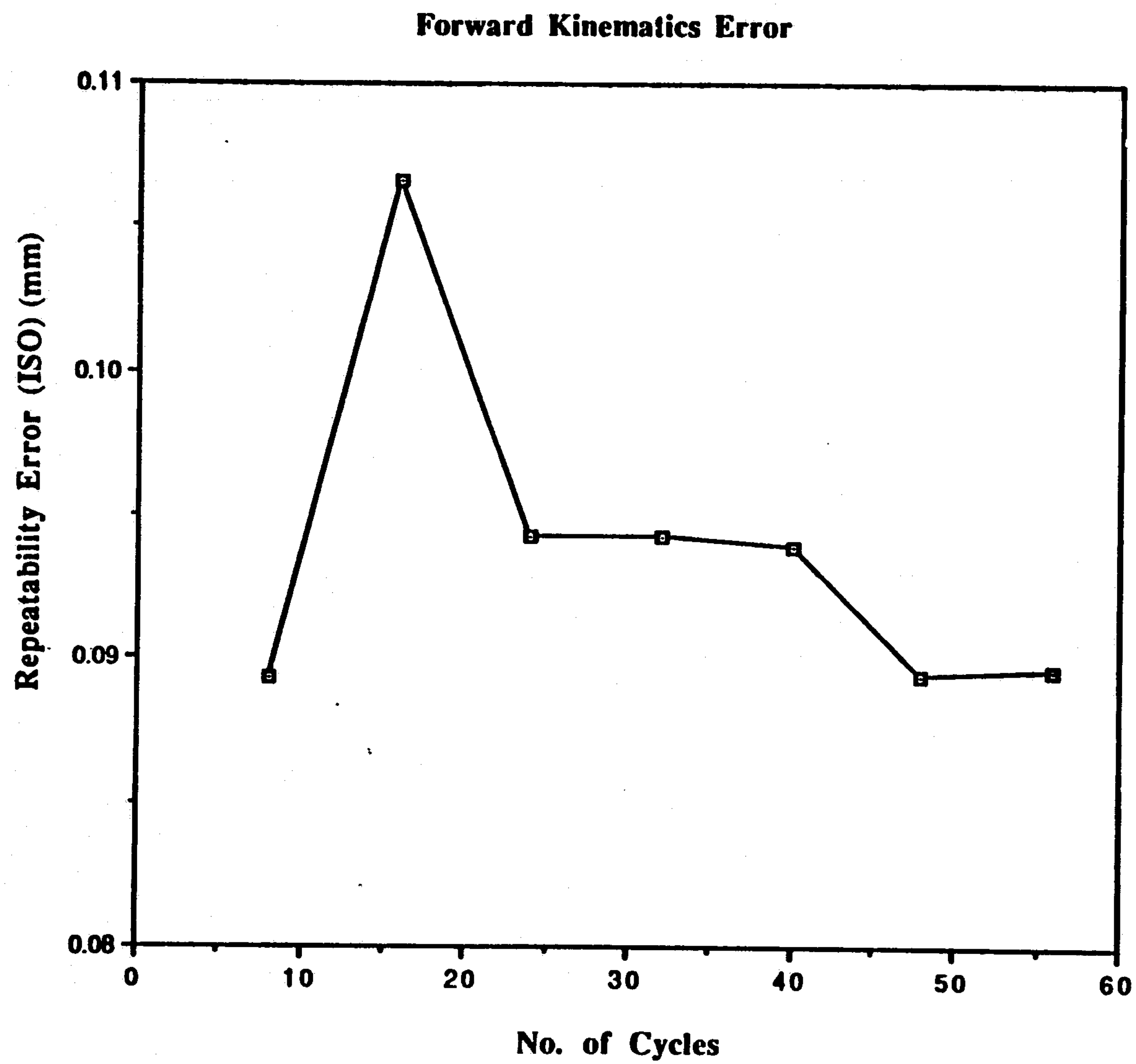

Figure 4.44 Position repeatability error plot.

Table 4.10 in the Appendix shows the results of the analysis of the last group of data which contains all 56 measured positions. Figure 4.45 is a three dimensional plot of the calculated forward kinematics errors (triangular marks), and their mean (cross mark).

Figure 4.46 is a plot of the ISO defined accuracy error versus the number of cycles contained in each analysis group. Figure 4.47 is a plot of the ISO defined repeatability error versus the number of cycles contained in each analysis group. The variation in the values of these errors as a function of the number of cycles is rather small.

Comparing Figure 4.43 with 4.46 shows that the level of the accuracy error in the case of the interrupted operation is approximately 0.49 mm higher than that of the continuous operation. Comparing Figure 4.44 with 4.47 shows that the level of the repeatability error is approximately the same. This significant increase in the value of the accuracy error is probably coming mostly from the joint position initialization error. The main source of the forward kinematics errors are computer numerical algorithm errors. The random component of these type of errors has usually a very small amplitude and that explains the small variation of these errors as a function of the number of cycles.

5.0 CONCLUSIONS

From the variety of performance tests studied in this work it is evident that such tests can be developed for most robot operations, from conventional Point-to-Point and Continuous Path to less conventional tests like Impedance Control, etc. These performance tests can evaluate general operating modes, like off-line programming and teach mode control or be specific to a particular type of operation like assembly of truss structures, etc. Existing or proposed standard tests can be used, or new ones can be devised based on the application and the knowledge of the control procedures used. The nature of the FTS sensor nest is a significant constraint in developing and conducting these tests; still, a substantial amount of data can be gathered and significant robot performance information can be obtained from them.

The teach mode joint angles kinematics control performance test is a rather simple test to perform and still can give significant information about the quality of the position servoing capability of the robot. This mode of operation gave the lowest accuracy and repeatability

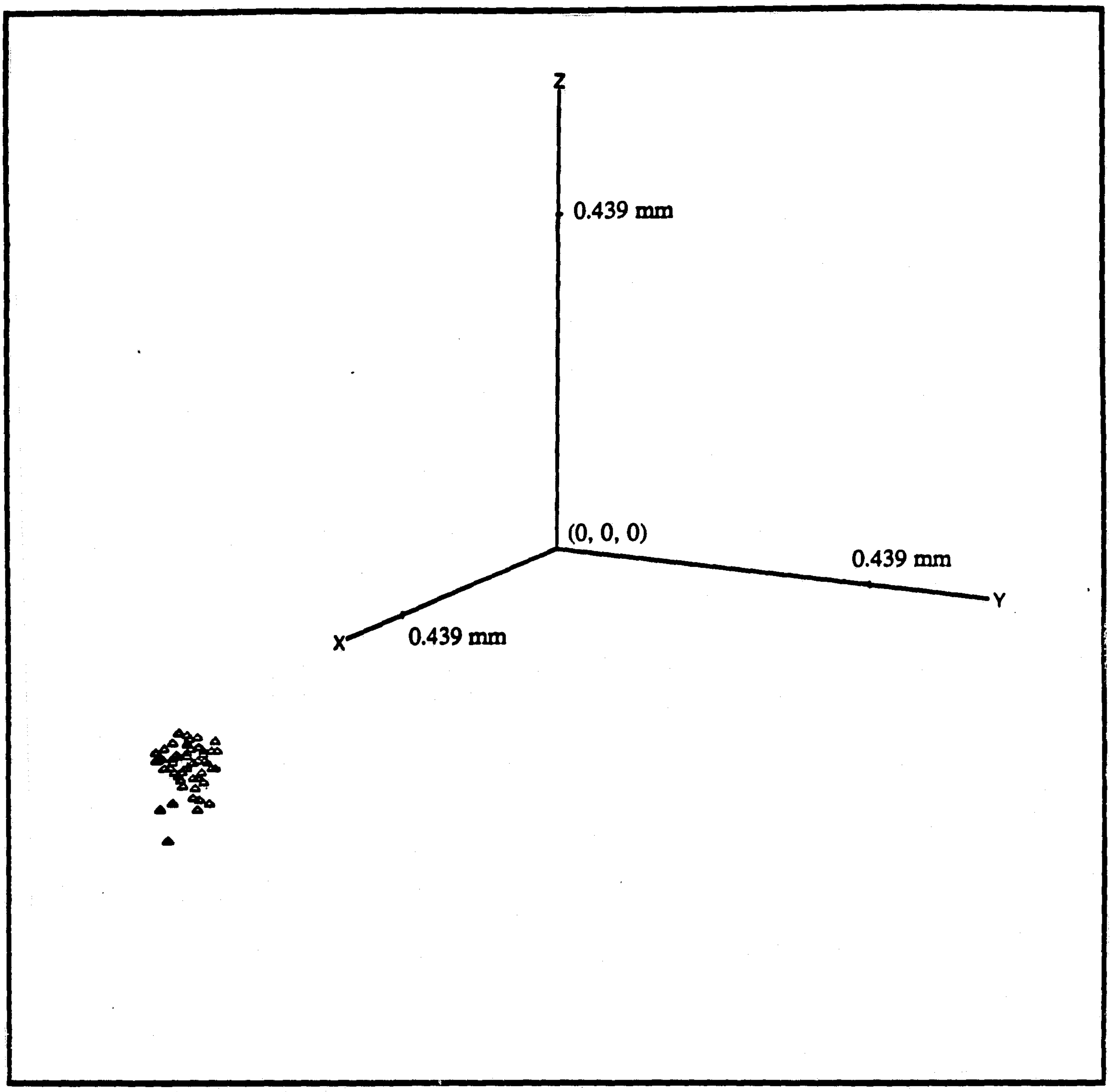

Forward Kinematics PTP Testing Errors
The cross marks the mean of the errors

Figure 4.45 Forward kinematics (interrupted operation).

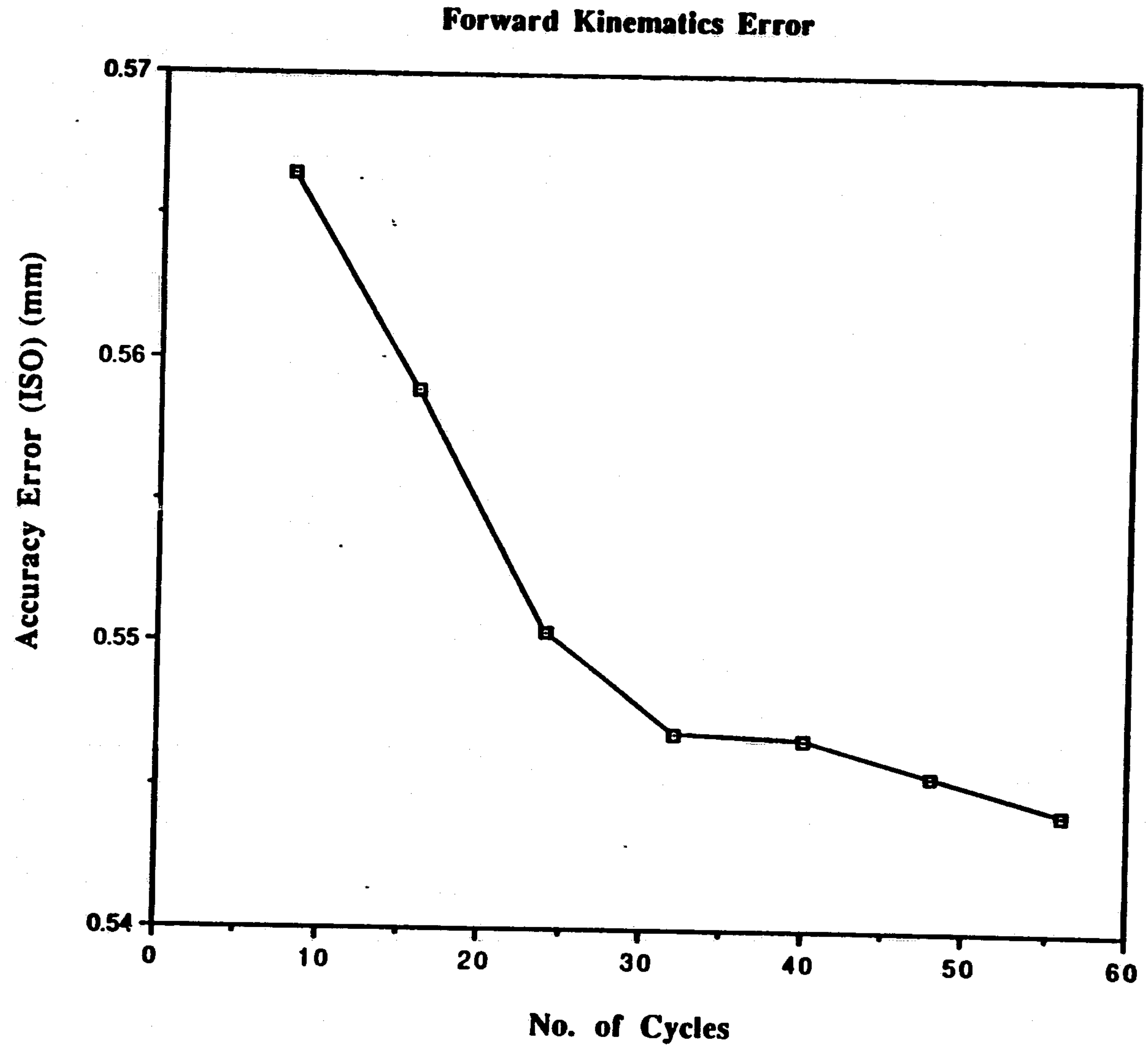

Figure 4.46 Position accuracy error plot.

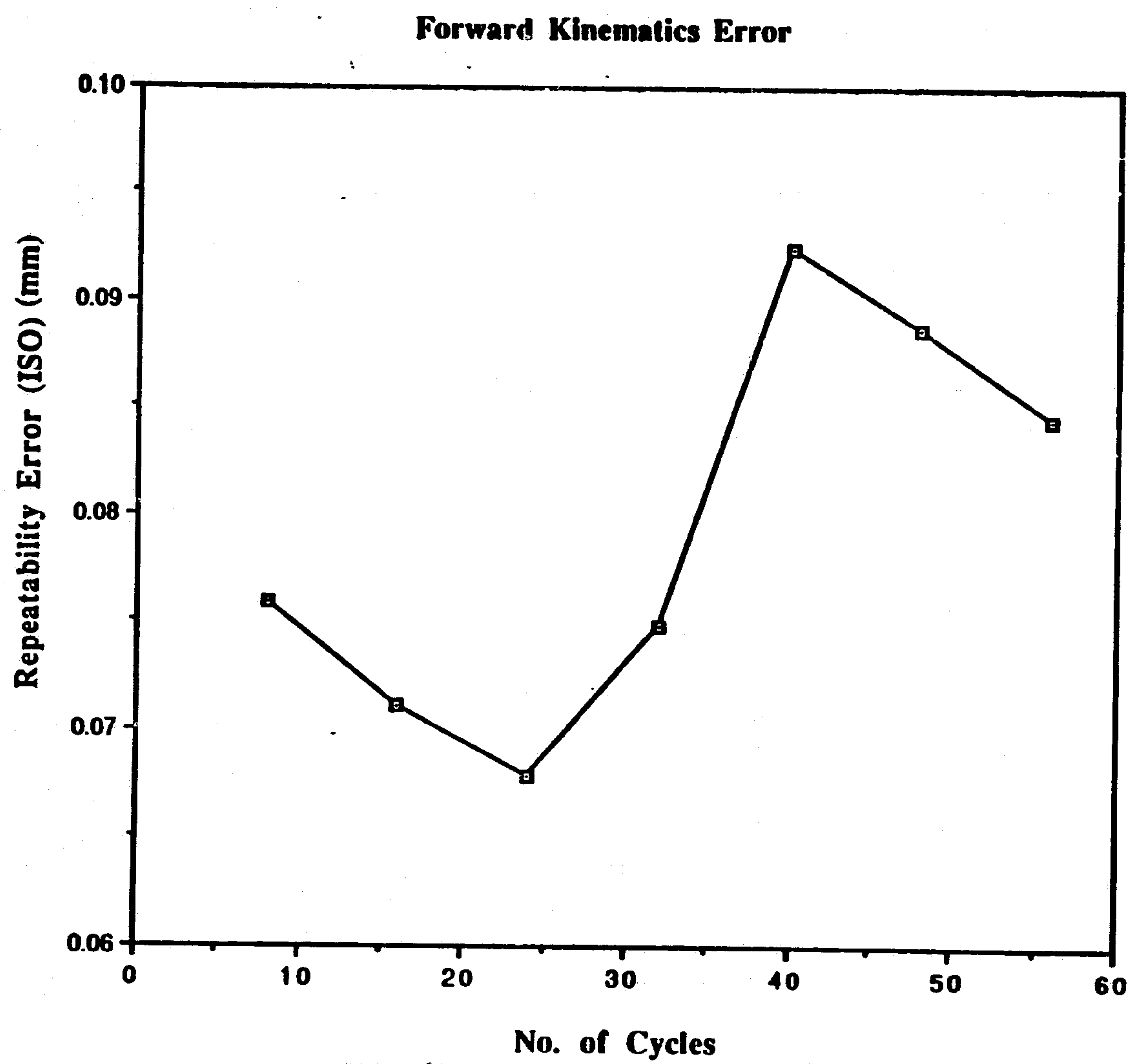

Figure 4.47 Position repeatability error piot.

errors. The teach mode inverse kinematics control errors are higher than those of the teach mode joint angles kinematics control. Thus, Cartesian interpolated motion should only be used where the requirement for a straight line path outweighs the negative affect of additional errors. Of course, the additional errors incurred with Cartesian interpolated motion are highly dependent on the particular inverse kinematics algorithm used.

Despite the small workspace available, a coordinates transformation can be determined to convert metrology instrument measured position data to robot baseframe coordinates with reasonable accuracy. Seven data positions are sufficient to estimate the parameters of the transformation, unless the transformation will be used for non-destructive testing.

The off-line programming errors are much larger than those of the teach mode operation. Since the difference is mainly due to kinematic modelling errors special care should be given to the accuracy of kinematic calibration.

Very small incremental moves along orthogonal baseframe directions seem to be difficult to perform for the RRC K-1607 robot with the control system used. This will probably be true of most serial revolute arms. In order to characterize the robot resolution performance both the magnitude and direction of the moves should be measured.

Forward kinematics error analysis is a simple and easy to perform analysis which does not require additional testing. If possible, this analysis should be applied to position data collected before and after turning the robot power off and on in order to estimate the offset error.

All the performance plots seem to be divided into two sections depending on the number of test cycles. The first section with a number of cycles less than 8 to 16 shows high values of errors, probably due to random errors, thermal drift and dynamic motion transients. The second section with a number of cycles greater than 16 to 32 shows that the errors reach asymptotic values. Although more study is needed, it is felt that the first section characterizes robot intermittent operation, while the second is representative of prolonged continuous operation. Thus the number of test cycles used for performance testing should be decided based on the type of the robot use. In the case of the FTS this will be intermittent operations.

Individual X, Y, and Z-axis plots of measured achieved positions versus the number of cycles or time may reveal cyclic positioning variation. The presence of any cyclicity should be examined carefully and the peak-to-peak amplitude measured. In several instances it was observed that this amplitude was larger than the value of the ISO-defined repeatability error. Similarly any large position differences among the first few points should be measured and studied. Although further investigation would be desirable, at this time it appears that a limited motion test should not be used as a substitute for the more complex standard path positions test. As with the intermittent versus continuous operation tests above, however, the appropriateness of the limited motion test may depend on the type of robot operation being performed.

6.0 RECOMMENDATIONS FOR FURTHER INVESTIGATION

The prototype tests presented here have provided insight as to the suitability of a number of different metrology tests for FTS performance verification. They have also provided an estimate of the positioning performance which may reasonably be expected from the current ICG lab manipulator/control system combination. In addition, they have indicated the relative importance of several factors which affect the test results. The test results also raise new questions, however, which would require further investigation to answer satisfactorily.

Questions regarding the performance of intermittent versus continuous operation have to be investigated further. During the first few test cycles the performance errors seem to increase significantly, probably because of thermal drift and dynamic motion transients. If a small number of cycles is used for the evaluation of these errors then random measurement errors could further increase the values of the performance errors. Two questions that need to be answered, then, are: 1) How many cycles does it take until transients and thermal drift have no effect on performance? 2) For a given number of test cycles, what percent of the measurement error is due to random measurement error?

The mechanism which results in large initial errors and cyclic variation position should be better understood. Is the integral control action associated with a time delay responsible for this type of behavior? Could the controller be modified to eliminate this problem without sacrificing the integrator? As part of this work the effect of time delays and distance of travel should be studied too.

The sources of the distortion during small incremental moves in specific directions should be further investigated. Precision positioning requires this type of small corrective moves. What is the primary source of the error? How can the situation be improved?

The accuracy error plot of the teach mode joint angles kinematics control tests (Fig. 4.6) shows a small rise after 40 cycles. The rise is very small but perhaps it should be investigated more thoroughly. Similarly the accuracy error plot of the teach mode inverse kinematics control tests (Fig. 4.13) is different than the rest of the accuracy error plots, which resemble a simple exponential decay and perhaps should be investigated further.

7.0 REFERENCES

Albus, J. S., Lumia, R., 1987, "NASREM -- NASA/NBS Standard Reference Model for Telerobot Control," Goddard Conf. on Space Appl. of AI and Robotics.

API, 1989, Automated Precision Inc., Gaithersburg, Maryland, U.S.A.

Craig, J. J., 1986, Introduction to Robotics: Mechanics and Control, Addison-Wesley, Reading, MA.

Eissmann, P., 1989, Servo Interface Operator's Manual, Robotics Research Corp., Milford, Ohio, U.S.A.

Fiala, J., 1988, "Manipulator Servo Level Task Decomposition," NIST Technical Note 1255, NIST, Gaithersburg, MD.

Fiala, J., 1989a, "Note on NASREM Implementation," NIST Internal Report 89-4215, NIST, Gaithersburg, MD.

Fiala, J., 1989b, "A High-Speed Serial Interface to the Robotics Research Corporation Servo Controller," Intelligent Controls Group Internal Document.

ISO (International Organization for Standardization), 1990, "Manipulating Industrial Robots - Performance Criteria and Related Testing Methods", International Standard 9283.

Kreutz, K., Long, M., Seraji, H., 1989, "Kinematic Functions for the 7 DOF Robotics Research Arm," NASA Conf. on Space Telerobotics, Pasadena.

Lau, K., Hocken, R., Haynes, L., 1985, "Robot performance measurements using automatic laser tracking techniques", Robotics & Computer-Integrated Manufacturing, Vol. 2, No. 3/4, pp. 227-236.

RIA (Robotic Industries Association), 1990, "American National Standard for Industrial Robots and Robot Systems - Point-to-Point and Static Performance Characteristics - Evaluation", Revision ANSI/RIA R15.05-1-1990.

Seraji, H., 1989, "Configuration Control of Redundant Manipulators: Theory and Implementation," IEEE Trans Robotics & Automation, Vol. 4, No. 4.

Wavering, A., 1988, "Manipulator Primitive Level Task Decomposition," NIST Technical Note 1256, NIST, Gaithersburg, MD.

8.0 ACKNOWLEDGEMENTS

We would like to thank Mr. Chuck Giaque for preparing the drawings of the retroreflector target holder and calibration fixture and supervising its construction.

We also thank Mr. John Fiala for providing additional servo control development for the metrology tests and for assisting in the performance of the tests.

9.0 APPENDIX

Table 4.1 Teach mode joint angles kinematics control analysis results.

TEACH MODE PTP ACCURACY AND REPEATABILITY ERRORS MEASUREMENT TEST

COMMANDED POSITION			# of PTP Tests
X	Y	Z	
766.024424	1554.368821	-1073.691763	56

ACHIEVED POSITIONS (Each Represents the Calculated Average Position From 1 Observation)

X	Y	Z	X	Y	Z
766.078458	1554.880623	-1073.626813	765.958049	1554.903767	-1073.784051
766.042282	1554.496745	-1073.743137	765.999853	1554.413324	-1073.775527
766.081632	1554.446924	-1073.702483	766.114853	1554.421779	-1073.681841
766.146089	1554.504260	-1073.629050	766.166000	1554.518395	-1073.634330
765.884230	1554.615005	-1073.791004	765.948985	1554.813628	-1073.801478
766.043356	1554.446858	-1073.757522	766.023978	1554.378044	-1073.753522
766.113264	1554.448968	-1073.697380	766.070512	1554.423667	-1073.692121
766.149772	1554.517655	-1073.625054	766.237044	1554.556294	-1073.560295
765.934019	1554.588574	-1073.765221	765.974645	1554.836016	-1073.787705
766.054300	1554.512493	-1073.755921	766.038840	1554.373073	-1073.759125
766.116845	1554.427987	-1073.683146	766.124442	1554.434364	-1073.662485
766.204001	1554.535331	-1073.563762	766.234674	1554.558130	-1073.567740
765.924206	1554.633662	-1073.789847	766.001622	1554.878490	-1073.776352
766.106104	1554.488634	-1073.734878	766.033132	1554.344199	-1073.764747
766.078602	1554.398114	-1073.705019	766.114086	1554.465425	-1073.681980
766.125471	1554.499700	-1073.670794	766.229186	1554.551315	-1073.578823
765.956926	1554.658467	-1073.763034	766.000968	1554.879154	-1073.785471
766.114496	1554.518983	-1073.741425	766.075306	1554.397880	-1073.761177
766.117035	1554.382286	-1073.705617	766.104459	1554.402669	-1073.732542
766.183449	1554.500292	-1073.641180	766.223321	1554.533442	-1073.594768
765.944703	1554.686038	-1073.782600	766.014160	1554.901284	-1073.794184
766.110183	1554.488831	-1073.747903	766.057220	1554.387477	-1073.781931
766.132939	1554.445344	-1073.712619	766.119729	1554.322238	-1073.703215
766.200528	1554.575282	-1073.649591	766.237563	1554.569584	-1073.606776
765.913366	1554.646957	-1073.833599	765.999188	1554.858071	-1073.806455
766.121555	1554.503069	-1073.761229	766.070124	1554.399473	-1073.764368
766.170832	1554.461352	-1073.702356	766.155713	1554.423319	-1073.682296
766.246058	1554.602996	-1073.632545	766.293513	1554.561520	-1073.561995

Table 4.1 Teach mode joint angles kinematics control analysis results.

ISO DEFINITION POSITIONING ACCURACY

DeltaL = 0.186384 DeltaLx = 0.063359 DeltaLy = 0.174348 , DeltaLz = -0.018095

ISO DEFINITION POSITIONING REPEATABILITY

r = 0.437987

RIA/ANSI DEFINITION POSITIONING ACCURACY AND ITS STANDARD DEVIATION

dPA = 0.229846, SPA = 0.143964

RIA/ANSI DEFINITION POSITIONING REPEATABILITY AND ITS STANDARD DEVIATION

rREP = 0.175931, SREP = 0.087352

TEACH MODE PTP ACCURACY AND REPEATABILITY ERRORS MEASUREMENT TEST

COMMANDED POSITION **# of PTP Tests**

X	Y	Z	# of PTP Tests
770.663152	1553.360946	-1071.547367	56

ACHIEVED POSITIONS (Each Represents the Calculated Average Position From 1 Observation)

X	Y	Z	X	Y	Z
770.244622	1553.685160	-1071.922939	770.443152	1553.933607	-1071.775477
770.818229	1553.560501	-1071.458312	770.644605	1553.365631	-1071.526830
770.895395	1553.477351	-1071.332521	770.780158	1553.447175	-1071.406512
770.875841	1553.545043	-1071.300509	770.958269	1553.597230	-1071.227522
770.730537	1554.056999	-1071.463932	770.584257	1553.998749	-1071.641573
770.857569	1553.644687	-1071.445197	770.682932	1553.352503	-1071.472249
770.801550	1553.440692	-1071.419484	770.819728	1553.484645	-1071.367358
770.798578	1553.501739	-1071.366818	770.936713	1553.597635	-1071.282187
770.439437	1553.719607	-1071.697176	770.515803	1553.953427	-1071.713169
770.795153	1553.535522	-1071.449728	770.669926	1553.337172	-1071.517070
770.851174	1553.489505	-1071.385847	770.846333	1553.433155	-1071.393377
770.852774	1553.555127	-1071.357269	770.950050	1553.611988	-1071.274051
770.443553	1553.756434	-1071.700713	770.518350	1553.932115	-1071.695589
770.718489	1553.482864	-1071.515308	770.674200	1553.399572	-1071.498173
770.801949	1553.414072	-1071.438228	770.816667	1553.433810	-1071.411664
770.781599	1553.495078	-1071.429628	770.925104	1553.629288	-1071.292503
770.431354	1553.720362	-1071.726569	770.464792	1553.873667	-1071.738180
770.742089	1553.531051	-1071.504315	770.654539	1553.369024	-1071.516271
770.855451	1553.464352	-1071.367768	770.805398	1553.416697	-1071.410872
770.849546	1553.552469	-1071.376992	770.937634	1553.567640	-1071.307864
770.739834	1554.048500	-1071.443381	770.574734	1553.970761	-1071.655896
770.812172	1553.507576	-1071.429845	770.656984	1553.384542	-1071.541372
770.886765	1553.486626	-1071.368627	770.804075	1553.460739	-1071.409068
770.855256	1553.537442	-1071.373001	770.929009	1553.581959	-1071.316484
770.473668	1553.730912	-1071.711852	770.518618	1553.871778	-1071.750677
770.812433	1553.526335	-1071.481920	770.673588	1553.391868	-1071.530246
770.848152	1553.427754	-1071.398996	770.811650	1553.443445	-1071.428391
770.828737	1553.582995	-1071.404591	770.968682	1553.590582	-1071.282654

Table 4.2 Teach mode inverse kinematics control analysis results.

Table 4.2 Teach mode inverse kinematics control analysis results.

ISO DEFINITION POSITIONING ACCURACY

DeltaL = 0.249597 DeltaLx = 0.076274 DeltaLy = 0.226682 DeltaLz = 0.071389

ISO DEFINITION POSITIONING REPEATABILITY

r = 0.673813

RIA/ANSI DEFINITION POSITIONING ACCURACY AND ITS STANDARD DEVIATION

dPA = 0.337425, SPA = 0.188322

RIA/ANSI DEFINITION POSITIONING REPEATABILITY AND ITS STANDARD DEVIATION

rREP = 0.260237, SREP = 0.137859

Table 4.3 Coordinates transformation analysis results (14 positions).

COORDINATES TRANSFORMATION ANALYSIS

ROBOT METROLOGY INSTRUMENT MEASURED POSITION COORDINATES
(Each Represents the Calculated Average Position From 1 Observation)

X	Y	Z	X	Y	Z
770.768589	1553.968453	-1071.475875	772.443358	1554.136566	-1072.244380
769.737905	1553.202187	-1072.960178	771.643109	1550.017441	-1071.970905
769.512767	1553.291974	-1073.153695	769.247171	1552.668274	-1075.481711
770.038707	1553.536206	-1072.791937	769.850088	1553.097178	-1072.620156
772.322762	1554.125659	-1071.953341	769.444396	1553.200374	-1072.906709
770.947059	1549.530172	-1072.179094	769.136865	1552.877354	-1073.070889
769.232317	1552.119536	-1075.207240	769.856757	1553.022982	-1072.613363

ROBOT CONTROLLER MEASURED POSITION COORDINATES

X	Y	Z	X	Y	Z
-725.675000	1108.206000	-614.912000	-727.157000	1108.982000	-615.764000
-724.364000	1108.249000	-616.477000	-724.172000	1111.965000	-615.495000
-724.211000	1108.034000	-616.694000	-723.632000	1108.343000	-619.061000
-724.784000	1108.122000	-616.308000	-724.363000	1108.402000	-616.120000
-727.051000	1108.921000	-615.449000	-724.085000	1108.103000	-616.420000
-723.307000	1111.994000	-615.712000	-723.643000	1108.159000	-616.622000
-723.319000	1108.790000	-618.811000	-724.333000	1108.440000	-616.157000

ROBOT METROLOGY INSTRUMENT MEASURED POSITION COORDINATES CONVERTED TO ROBOT CONTROLLER MEASURED POSITION COORDINATES

X	Y	Z	X	Y	Z
-725.641000	1108.196000	-614.996000	-727.126000	1108.965000	-615.790000
-724.349000	1108.239000	-616.472000	-724.188000	1111.965000	-615.552000
-724.209000	1108.036000	-616.661000	-723.627000	1108.366000	-618.992000
-724.785000	1108.130000	-616.305000	-724.387000	1108.395000	-616.136000
-727.021000	1108.913000	-615.497000	-724.103000	1108.080000	-616.414000

Table 4.3 Coordinates transformation analysis results (14 positions).

-723.337000	1111.983000	-615.755000	-723.667000	1108.177000	-616.577000
-723.314000	1108.821000	-618.724000	-724.351000	1108.461000	-616.130000

TRANSFORMATION TRANSLATION VECTOR

766.816000 1999.542000 450.384000

TRANSFORMATION ROTATION MATRIX

-0.834106	-0.551560	-0.007048
0.551364	-0.834051	0.018882
-0.016292	0.011863	0.999797

Table 4.4 Coordinates transformation analysis results (7 positions).

COORDINATES TRANSFORMATION ANALYSIS

ROBOT METROLOGY INSTRUMENT MEASURED POSITION COORDINATES
(Each Represents the Calculated Average Position From 1 Observation)

X	Y	Z	X	Y	Z
770.768589	1553.968453	-1071.475875	772.443358	1554.136566	-1072.244380
769.737905	1553.202187	-1072.960178	771.643109	1550.017441	-1071.970905
769.512767	1553.291974	-1073.153695	769.247171	1552.668274	-1075.481711
770.038707	1553.536206	-1072.791937			

ROBOT CONTROLLER MEASURED POSITION COORDINATES

X	Y	Z	X	Y	Z
-725.675000	1108.206000	-614.912000	-727.157000	1108.982000	-615.764000
-724.364000	1108.249000	-616.477000	-724.172000	1111.965000	-615.495000
-724.211000	1108.034000	-616.694000	-723.632000	1108.343000	-619.061000
-724.784000	1108.122000	-616.308000			

ROBOT METROLOGY INSTRUMENT MEASURED POSITION COORDINATES CONVERTED TO ROBOT CONTROLLER MEASURED POSITION COORDINATES

X	Y	Z	X	Y	Z
-725.673000	1108.207000	-614.996000	-727.142000	1108.986000	-615.807000
-724.364000	1108.236000	-616.458000	-724.183000	1111.962000	-615.541000
-724.223000	1108.032000	-616.644000	-723.613000	1108.354000	-618.969000
-724.803000	1108.131000	-616.295000			

TRANSFORMATION TRANSLATION VECTOR

762.010000 1988.994000 465.733000

TRANSFORMATION ROTATION MATRIX

-0.829325 -0.558474 -0.018092

Table 4.4 Coordinates transformation analysis results (7 positions).

0.558140	-0.829493	0.020512
-0.026463	0.006913	0.999626

Table 4.5 Standard initial positions off-line programming analysis results.

OFF-LINE PROGRAMMING PTP ACCURACY AND REPEATABILITY ERRORS MEASUREMENT TEST

COMMANDED POSITION			# of PTP Tests
X	Y	Z	56
770.663152	1553.360946	-1071.547367	

ACHIEVED POSITIONS (Each Represents the Calculated Average Position From 1 Observation)

X	Y	Z	X	Y	Z
770.671489	1554.146684	-1071.545518	770.654621	1554.136346	-1071.670477
770.908188	1553.701276	-1071.429662	770.760961	1553.518528	-1071.523032
770.901814	1553.522301	-1071.362348	770.881766	1553.595699	-1071.429883
770.904378	1553.732129	-1071.378029	771.009122	1553.743845	-1071.290177
770.551956	1553.797109	-1071.626398	770.638613	1554.070732	-1071.658842
770.882233	1553.606503	-1071.452411	770.779736	1553.528411	-1071.499111
770.849017	1553.555324	-1071.449078	770.919967	1553.604004	-1071.383732
770.897365	1553.634235	-1071.398301	771.032863	1553.728641	-1071.284001
770.593827	1553.885573	-1071.658844	770.650120	1554.050903	-1071.683837
770.898285	1553.652510	-1071.460542	770.751556	1553.513546	-1071.567118
770.910861	1553.635646	-1071.415744	770.878955	1553.569769	-1071.432780
770.956903	1553.684168	-1071.353792	770.929483	1553.779979	-1071.386303
770.584093	1553.807088	-1071.653230	770.633031	1554.049051	-1071.731620
770.879679	1553.651512	-1071.497049	770.714628	1553.539807	-1071.608276
770.901387	1553.658524	-1071.437850	770.924561	1553.660290	-1071.407177
770.941523	1553.688294	-1071.387776	771.026621	1553.766701	-1071.289593
770.591251	1553.838920	-1071.671455	770.655301	1554.080899	-1071.717886
770.811992	1553.576787	-1071.532185	770.753669	1553.504739	-1071.543754
770.884097	1553.588541	-1071.464773	770.919009	1553.601027	-1071.411615
770.947870	1553.690203	-1071.400609	770.991369	1553.793114	-1071.383835
770.598265	1553.796601	-1071.632661	770.639890	1554.025720	-1071.725905
770.914559	1553.651739	-1071.470120	770.775673	1553.518116	-1071.536824
770.953495	1553.623007	-1071.436206	770.921611	1553.655669	-1071.433459
770.949335	1553.694744	-1071.406518	770.940192	1553.713586	-1071.400824
770.580286	1553.770379	-1071.662241	770.655310	1554.069723	-1071.719938
770.902849	1553.615941	-1071.484397	770.733687	1553.523159	-1071.609974
770.967487	1553.612701	-1071.431749	770.904751	1553.548763	-1071.435949
770.954340	1553.697893	-1071.386609	771.046944	1553.749942	-1071.320047

Table 4.5 Standard initial positions off-line programming analysis results.

ISO DEFINITION POSITIONING ACCURACY

DeltaL = 0.396616 DeltaLx = 0.165649 DeltaLy = 0.356144 DeltaLz = 0.055009

ISO DEFINITION POSITIONING REPEATABILITY

r = 0.562162

RIA/ANSI DEFINITION POSITIONING ACCURACY AND ITS STANDARD DEVIATION

dPA = 0.443328, SPA = 0.161175

RIA/ANSI DEFINITION POSITIONING REPEATABILITY AND ITS STANDARD DEVIATION

rREP = 0.229508, SREP = 0.110885

Table 4.6 Limited motion off-line programming analysis results.

OFF-LINE PROGRAMMING PTP ACCURACY AND REPEATABILITY ERRORS MEASUREMENT TEST

COMMANDED POSITION / **# of PTP Tests**

X	Y	Z	# of PTP Tests
770.663152	1553.360946	-1071.547367	56

ACHIEVED POSITIONS (Each Represents the Calculated Average Position From 1 Observation)

X	Y	Z	X	Y	Z
771.945162	1553.802401	-1069.761015	771.092653	1553.928324	-1071.026967
770.964225	1553.796102	-1071.179942	770.808221	1553.668638	-1071.332264
770.762278	1553.482464	-1071.353532	770.750430	1553.468839	-1071.336661
770.771696	1553.538931	-1071.316048	770.758468	1553.504196	-1071.328372
770.969802	1553.783502	-1071.142117	770.938459	1553.652256	-1071.208114
770.843538	1553.558037	-1071.305288	770.845576	1553.593601	-1071.294993
770.819897	1553.540118	-1071.323898	770.764314	1553.481008	-1071.386687
770.817331	1553.516746	-1071.318096	770.840222	1553.634493	-1071.347919
770.936182	1553.794261	-1071.188044	770.907186	1553.715527	-1071.241519
770.865324	1553.630840	-1071.296019	770.824647	1553.601856	-1071.340226
770.819727	1553.612231	-1071.356717	770.766528	1553.556298	-1071.373752
770.740675	1553.534090	-1071.391140	770.815946	1553.549043	-1071.338783
770.919975	1553.835802	-1071.224357	770.890353	1553.681097	-1071.246968
770.867537	1553.655808	-1071.306686	770.796529	1553.621573	-1071.371901
770.809156	1553.556758	-1071.331880	770.794882	1553.619551	-1071.399196
770.792590	1553.566918	-1071.366392	770.847925	1553.581472	-1071.324740
770.976383	1553.888945	-1071.179538	770.905633	1553.682996	-1071.291022
770.876134	1553.632159	-1071.302584	770.864002	1553.564866	-1071.314976
770.839837	1553.588050	-1071.334868	770.847151	1553.582032	-1071.345557
770.815023	1553.522310	-1071.352927	770.840622	1553.583049	-1071.358715
770.963260	1553.876410	-1071.193315	770.938479	1553.692224	-1071.253399
770.855923	1553.627458	-1071.327255	770.834795	1553.548605	-1071.347833
770.826837	1553.571535	-1071.370277	770.815154	1553.598182	-1071.397237
770.819249	1553.616615	-1071.345586	770.793920	1553.514205	-1071.374143
770.958405	1553.897139	-1071.197753	770.932947	1553.723933	-1071.264980
770.890168	1553.626415	-1071.268604	770.819001	1553.603741	-1071.357208
770.737657	1553.573335	-1071.431825	770.798316	1553.572306	-1071.378240
770.785305	1553.637871	-1071.375607	770.821362	1553.531596	-1071.370421

Table 4.6 Limited motion off-line programming analysis results.

ISO DEFINITION POSITIONING ACCURACY

DeltaL = 0.430560 DeltaLx = 0.205473 DeltaLy = 0.269746 , DeltaLz = 0.265329

ISO DEFINITION POSITIONING REPEATABILITY

r = 0.899830

RIA/ANSI DEFINITION POSITIONING ACCURACY AND ITS STANDARD DEVIATION

dPA = 0.438390, SPA = 0.283825

RIA/ANSI DEFINITION POSITIONING REPEATABILITY AND ITS STANDARD DEVIATION

rREP = 0.163639, SREP = 0.245397

ROBOT POSITION RESOLUTION ANALYSIS

No. of incremental moves = 55

MEASURED POSITIONS

X	Y	Z
Movement in the X-Axis direction		
769.828688	1552.123009	-1072.240768
770.012846	1552.347347	-1072.017640
769.741931	1552.670747	-1072.149516
769.609515	1552.928975	-1072.218508
769.499419	1552.956698	-1072.189112
769.482532	1552.856120	-1072.160166
769.453115	1552.796014	-1072.207286
769.439476	1552.732104	-1072.234757
769.584114	1552.651597	-1072.179883
769.533557	1552.731483	-1072.230981
769.398620	1552.860820	-1072.363012
769.304717	1552.907489	-1072.436461
769.141093	1552.921388	-1072.543312
769.186203	1552.806332	-1072.479741
769.274922	1552.668315	-1072.428045
769.373427	1552.593812	-1072.371752
769.515844	1552.587620	-1072.321519
769.514290	1552.755287	-1072.381117
769.416616	1552.899018	-1072.477586
769.291403	1552.997660	-1072.573093
769.165273	1553.046840	-1072.646451
769.186331	1552.945844	-1072.618253
769.267106	1552.860580	-1072.554508
769.343767	1552.767194	-1072.489527
769.530598	1552.677238	-1072.376896
769.487515	1552.751413	-1072.410448
769.362265	1552.920291	-1072.537185
769.268833	1552.989916	-1072.600192
769.149583	1553.019984	-1072.679752
769.192606	1552.935061	-1072.641090
769.270564	1552.842614	-1072.566315
769.380349	1552.737912	-1072.487641
769.546438	1552.648958	-1072.367089
769.514448	1552.726733	-1072.417537
769.403209	1552.873356	-1072.514440
769.317809	1552.949127	-1072.568207
769.199455	1552.982046	-1072.638194
769.213539	1552.907020	-1072.615572
769.291861	1552.817134	-1072.555462
769.365641	1552.749103	-1072.489806
769.526753	1552.663010	-1072.404463
769.497855	1552.749564	-1072.438777
769.402814	1552.867680	-1072.517230
769.299292	1552.954236	-1072.584011

Table 4.7 Robot position resolution analysis results (commanded incremental moves of 0.15 mm).

769.209451	1552.946267	-1072.656674
769.246736	1552.875085	-1072.603428
769.287038	1552.810661	-1072.544846
769.368220	1552.722823	-1072.483016
769.569030	1552.670203	-1072.363411
769.569296	1552.725478	-1072.384205
769.448119	1552.875181	-1072.487997
769.379350	1552.954982	-1072.541138
769.247404	1552.974879	-1072.624706
769.245821	1552.920193	-1072.596496
769.341893	1552.813947	-1072.517878
769.411202	1552.725134	-1072.462664

Movement in the Y-Axis direction

769.606637	1552.786055	-1072.387552
769.777505	1552.652785	-1072.291611
769.882724	1552.530691	-1072.230492
769.921646	1552.461085	-1072.252513
769.997520	1552.423168	-1072.277282
769.910480	1552.531586	-1072.399886
769.770853	1552.671252	-1072.520693
769.603269	1552.860272	-1072.679352
769.453743	1553.017973	-1072.817439
769.552360	1552.897746	-1072.701608
769.678249	1552.759357	-1072.577447
769.809317	1552.595639	-1072.453135
769.949718	1552.422266	-1072.330650
769.875640	1552.489055	-1072.406199
769.761861	1552.623411	-1072.517640
769.621229	1552.775439	-1072.648589
769.440563	1552.961474	-1072.775819
769.544106	1552.851164	-1072.671856
769.689685	1552.702293	-1072.535210
769.843817	1552.559834	-1072.412861
770.000221	1552.497469	-1072.310282
769.925016	1552.592083	-1072.419420
769.785076	1552.757798	-1072.540917
769.646207	1552.907815	-1072.653669
769.478523	1553.091674	-1072.793672
769.551282	1553.010469	-1072.716252
769.708669	1552.835546	-1072.550536
769.889324	1552.652655	-1072.413572
769.994249	1552.508125	-1072.338230
769.931215	1552.571180	-1072.403442
769.808169	1552.713770	-1072.497592
769.670361	1552.849155	-1072.630774
769.546372	1552.987431	-1072.724870
769.606618	1552.926359	-1072.633883
769.736900	1552.780944	-1072.532363
769.883221	1552.612237	-1072.404313
770.026759	1552.456541	-1072.298467
769.942606	1552.535830	-1072.374886
769.813815	1552.666692	-1072.479321

Table 4.7 Robot position resolution analysis results (commanded incremental moves of 0.15 mm).

769.656425	1552.762674	-1072.585300
769.479090	1552.907238	-1072.727502
769.552307	1552.830785	-1072.646475
769.658991	1552.692456	-1072.530593
769.816772	1552.526042	-1072.408142
769.909129	1552.416012	-1072.333371
769.848400	1552.474677	-1072.397265
769.731534	1552.586166	-1072.501032
769.611098	1552.721467	-1072.608937
769.445826	1552.903986	-1072.758775
769.532323	1552.833166	-1072.667886
769.676123	1552.663666	-1072.524202
769.797027	1552.493368	-1072.404380
769.911406	1552.374403	-1072.309295
769.865877	1552.434522	-1072.377612
769.728256	1552.576002	-1072.474208
769.591258	1552.718960	-1072.602752

Movement in the Z-Axis direction

769.464073	1552.919976	-1072.694283
769.450420	1552.912704	-1072.616605
769.408882	1552.955548	-1072.573248
769.419722	1552.973582	-1072.489754
769.416974	1552.996548	-1072.382401
769.431527	1552.941817	-1072.326139
769.464747	1552.865209	-1072.331459
769.456738	1552.829557	-1072.335314
769.532865	1552.755819	-1072.356795
769.521339	1552.759626	-1072.355645
769.463507	1552.831741	-1072.389231
769.404349	1552.902866	-1072.370476
769.423666	1552.929203	-1072.296225
769.419958	1552.904981	-1072.273227
769.461396	1552.853113	-1072.283728
769.443185	1552.838722	-1072.311924
769.520245	1552.735936	-1072.339020
769.505617	1552.766842	-1072.333026
769.458865	1552.863041	-1072.358362
769.411082	1552.933367	-1072.346732
769.434586	1552.974137	-1072.299388
769.457342	1552.950880	-1072.289078
769.459966	1552.904166	-1072.298920
769.489168	1552.839364	-1072.292430
769.557342	1552.758639	-1072.293954
769.546264	1552.808036	-1072.326891
769.517216	1552.879178	-1072.346342
769.444782	1552.963723	-1072.357068
769.446615	1552.990513	-1072.295905
769.460806	1552.975444	-1072.284694
769.495995	1552.910917	-1072.259680
769.541870	1552.836604	-1072.245074
769.584177	1552.767582	-1072.275575
769.591928	1552.794329	-1072.277584

Table 4.7 Robot position resolution analysis results (commanded incremental moves of 0.15 mm).

769.539407	1552.876441	-1072.318746
769.478738	1552.996060	-1072.349014
769.485672	1553.082875	-1072.310918
769.484718	1553.066398	-1072.306300
769.499071	1553.029320	-1072.315422
769.544371	1552.953509	-1072.295583
769.596184	1552.855515	-1072.318826
769.584502	1552.891079	-1072.320811
769.531099	1552.975657	-1072.356023
769.489331	1553.056010	-1072.364341
769.471603	1553.105682	-1072.315345
769.476364	1553.066330	-1072.313296
769.524465	1553.011374	-1072.293721
769.537640	1552.964339	-1072.294652
769.579964	1552.862863	-1072.312309
769.592567	1552.890475	-1072.326722
769.550440	1552.951797	-1072.343921
769.496166	1553.039819	-1072.363942
769.491034	1553.077694	-1072.301344
769.491565	1553.053668	-1072.303886
769.498711	1553.010178	-1072.297397
769.543929	1552.938461	-1072.286121

Table 4.7 Robot position resolution analysis results (commanded incremental moves of 0.15 mm).

MEAN VALUE AND STANDARD DEVIATION OF THE RESOLUTION IN THE X-AXIS DIRECTION

Resolution = 0.156625 Sigma = 0.070600

MEAN VALUE AND STANDARD DEVIATION OF THE RESOLUTION IN THE Y-AXIS DIRECTION

Resolution = 0.208025 Sigma = 0.056606

MEAN VALUE AND STANDARD DEVIATION OF THE RESOLUTION IN THE Z-AXIS DIRECTION

Resolution = 0.073010 Sigma = 0.031027

ROBOT POSITION RESOLUTION ANALYSIS

No. of incremental moves = 55

MEASURED POSITIONS

X	Y	Z
Movement in the X-Axis direction		
769.767736	1552.677351	-1072.318677
769.959476	1552.493000	-1072.404938
770.458953	1553.186239	-1072.681214
770.941056	1553.311439	-1072.497534
771.412926	1553.387432	-1072.315250
771.259507	1553.816508	-1072.530830
770.719725	1553.808064	-1072.875978
770.117304	1553.668466	-1073.128186
769.538943	1552.967463	-1072.955386
769.701115	1552.685883	-1072.768096
770.214106	1552.822927	-1072.642508
770.735293	1553.075107	-1072.576545
771.147331	1553.165604	-1072.405544
770.895156	1553.512859	-1072.674313
770.470043	1553.702783	-1072.952462
769.912160	1553.453461	-1073.189525
769.375701	1552.845273	-1072.976701
769.579580	1552.468667	-1072.799365
770.138143	1552.688213	-1072.582710
770.612609	1553.034584	-1072.622331
771.120362	1553.157121	-1072.412558
770.962985	1553.466903	-1072.605501
770.593878	1553.690057	-1072.841959
769.999646	1553.425112	-1073.105567
769.548983	1552.780151	-1072.885067
769.708927	1552.445798	-1072.699086
770.249906	1552.608840	-1072.465829
770.704245	1552.995287	-1072.546031
771.245940	1553.153799	-1072.290364
771.090819	1553.452655	-1072.483109
770.692832	1553.698073	-1072.758666
770.053177	1553.447086	-1073.075927
769.474686	1552.662117	-1072.887676
769.627103	1552.365088	-1072.740549
770.120102	1552.563536	-1072.523310
770.680202	1552.876266	-1072.525446
771.206906	1553.041724	-1072.263285
770.983367	1553.426319	-1072.531727
770.576256	1553.657190	-1072.822223
769.924041	1553.365318	-1073.130337
769.411359	1552.627876	-1072.920133
769.571407	1552.344407	-1072.765352
770.080213	1552.547627	-1072.551831
770.549522	1552.903774	-1072.604166

Table 4.8 Robot position resolution analysis results (commanded incremental moves of 0.5 mm).

771.151284	1553.042528	-1072.332503
770.999096	1553.386752	-1072.491405
770.622142	1553.617018	-1072.780980
769.972138	1553.350320	-1073.099202
769.453392	1552.678852	-1072.921105
769.595449	1552.356478	-1072.770007
770.120285	1552.518938	-1072.534224
770.585367	1552.905407	-1072.586575
771.157040	1553.053931	-1072.323580
771.004052	1553.364396	-1072.491347
770.633659	1553.624181	-1072.746394
770.006714	1553.363175	-1073.073219

Movement in the Y-Axis direction

769.382215	1552.382531	-1072.837471
769.670122	1551.785465	-1072.520563
769.985904	1551.085509	-1072.308480
770.392957	1550.835708	-1072.275849
770.616775	1550.486085	-1072.455935
770.137064	1550.840529	-1072.919218
769.705667	1551.597002	-1073.277772
769.667907	1552.495141	-1073.231095
769.620962	1552.899021	-1072.841426
770.044574	1552.387264	-1072.355602
770.426979	1551.897803	-1072.140927
770.579473	1551.292038	-1072.308221
770.790747	1550.625984	-1072.311913
770.351972	1551.015693	-1072.745408
769.938660	1551.604850	-1073.089681
769.667537	1552.335897	-1073.233661
769.559194	1552.717889	-1072.844626
769.969812	1552.338095	-1072.426043
770.353091	1551.801435	-1072.163639
770.437077	1551.137935	-1072.381601
770.748777	1550.433674	-1072.273395
770.312096	1550.874401	-1072.694122
769.799915	1551.473179	-1073.120961
769.487891	1552.135257	-1073.315887
769.477775	1552.697316	-1072.916869
769.921150	1552.318997	-1072.448942
770.342649	1551.788632	-1072.170431
770.534507	1551.130885	-1072.273409
770.871600	1550.643714	-1072.241673
770.429076	1551.090447	-1072.676286
769.914130	1551.635197	-1073.138502
769.509611	1552.317202	-1073.371535
769.518032	1552.877008	-1072.955832
769.950891	1552.516358	-1072.466577
770.371810	1551.988918	-1072.209229
770.535588	1551.338018	-1072.368815
770.829730	1550.657179	-1072.276041
770.400691	1551.085855	-1072.718035
769.904694	1551.653545	-1073.134964

Table 4.8 Robot position resolution analysis results (commanded incremental moves of 0.5 mm).

769.550576	1552.259359	-1073.335997
769.528740	1552.722984	-1072.849480
769.972289	1552.350940	-1072.453771
770.356424	1551.895099	-1072.203052
770.488519	1551.202329	-1072.349169
770.788064	1550.513671	-1072.253582
770.362193	1550.933777	-1072.691269
769.859391	1551.511742	-1073.091928
769.462330	1552.121523	-1073.346262
769.511870	1552.669589	-1072.897079
769.926480	1552.354113	-1072.451404
770.361831	1551.851081	-1072.192529
770.544471	1551.204854	-1072.294493
770.847983	1550.519134	-1072.190887
770.428509	1550.916555	-1072.616864
769.921437	1551.474946	-1073.050447
769.498539	1552.111628	-1073.317790

Movement in the Z-Axis direction

769.433704	1552.520788	-1073.001668
769.359997	1552.294272	-1073.143947
769.355270	1552.326698	-1073.624622
769.519639	1552.158798	-1073.757073
769.572665	1552.095362	-1074.193889
769.568668	1552.318161	-1074.240185
769.571584	1552.465165	-1073.921433
769.688959	1552.802102	-1073.542023
769.906065	1552.784124	-1072.685931
769.866167	1552.652340	-1072.795295
769.782058	1552.742035	-1073.351839
769.703893	1552.433098	-1073.684952
769.465698	1552.058782	-1074.272030
769.408818	1552.222223	-1074.317985
769.474270	1552.366504	-1073.957806
769.589189	1552.685837	-1073.601756
769.637005	1552.742075	-1072.878837
769.601692	1552.613512	-1072.960084
769.508066	1552.658902	-1073.521923
769.465451	1552.325754	-1073.818527
769.317733	1552.031860	-1074.350854
769.273778	1552.201392	-1074.393450
769.273864	1552.365666	-1074.107382
769.406282	1552.686632	-1073.738304
769.709209	1552.748934	-1072.872415
769.696715	1552.625483	-1072.905854
769.579730	1552.678687	-1073.478285
769.596191	1552.382512	-1073.740383
769.557481	1552.013377	-1074.186928
769.503762	1552.188945	-1074.203798
769.497201	1552.352689	-1073.946330
769.565165	1552.702092	-1073.616496
769.840621	1552.780586	-1072.753952
769.856038	1552.602015	-1072.778013

Table 4.8 Robot position resolution analysis results (commanded incremental moves of 0.5 mm).

769.732632	1552.653199	-1073.382687
769.653767	1552.364817	-1073.709379
769.550292	1552.045477	-1074.180222
769.460403	1552.222444	-1074.239289
769.468064	1552.346013	-1073.972353
769.570478	1552.649251	-1073.630228
769.690804	1552.765159	-1072.884378
769.636112	1552.675951	-1072.972767
769.547664	1552.705261	-1073.479659
769.548180	1552.354671	-1073.773899
769.393213	1552.087881	-1074.310423
769.344663	1552.273207	-1074.331390
769.331633	1552.404125	-1074.072872
769.413670	1552.720594	-1073.734059
769.690657	1552.811272	-1072.892284
769.698957	1552.662814	-1072.908828
769.606612	1552.703711	-1073.450457
769.628832	1552.394758	-1073.741330
769.565476	1552.085762	-1074.177185
769.546244	1552.251706	-1074.199763
769.538448	1552.367693	-1073.922414
769.560115	1552.721383	-1073.646588

Table 4.8 Robot position resolution analysis results (commanded incremental moves of 0.5 mm).

MEAN VALUE AND STANDARD DEVIATION OF THE RESOLUTION IN THE X-AXIS DIRECTION

Resolution = 0.594424 Sigma = 0.160903

MEAN VALUE AND STANDARD DEVIATION OF THE RESOLUTION IN THE Y-AXIS DIRECTION

Resolution = 0.732857 Sigma = 0.094315

MEAN VALUE AND STANDARD DEVIATION OF THE RESOLUTION IN THE Z-AXIS DIRECTION

Resolution = 0.440251 Sigma = 0.213103

Table 4.9 Forward kinematics error analysis results (continuous operation).

FORWARD KINEMATICS PTP ACCURACY AND REPEATABILITY ERRORS MEASUREMENT TEST

The number of PTP tests was = 56

ROBOT METROLOGY INSTRUMENT MEASURED POSITION COORDINATES
(Each Represents the Calculated Average Position From 1 Observation)

X	Y	Z	X	Y	Z
770.244622	1553.685160	-1071.922939	770.443152	1553.933607	-1071.775477
770.818229	1553.560501	-1071.458312	770.644605	1553.365631	-1071.526830
770.895395	1553.477351	-1071.332521	770.780158	1553.447175	-1071.406512
770.875841	1553.545043	-1071.300509	770.958269	1553.597230	-1071.227522
770.730537	1554.056999	-1071.463932	770.584257	1553.998749	-1071.641573
770.857569	1553.644687	-1071.445197	770.682932	1553.352503	-1071.472249
770.801550	1553.440692	-1071.419484	770.819728	1553.484645	-1071.367358
770.798578	1553.501739	-1071.366818	770.936713	1553.597635	-1071.282187
770.439437	1553.719607	-1071.697176	770.515803	1553.953427	-1071.713169
770.795153	1553.535522	-1071.449728	770.669926	1553.337172	-1071.517070
770.851174	1553.489505	-1071.385847	770.846333	1553.433155	-1071.393377
770.852774	1553.555127	-1071.357269	770.950050	1553.611988	-1071.274051
770.443553	1553.756434	-1071.700713	770.518350	1553.932115	-1071.695589
770.718489	1553.482864	-1071.515308	770.674200	1553.399572	-1071.498173
770.801949	1553.414072	-1071.438228	770.816667	1553.433810	-1071.411664
770.781599	1553.495078	-1071.429628	770.925104	1553.629288	-1071.292503
770.431354	1553.720362	-1071.726569	770.464792	1553.873667	-1071.738180
770.742089	1553.531051	-1071.504315	770.654539	1553.369024	-1071.516271
770.855451	1553.464352	-1071.367768	770.805398	1553.416697	-1071.410872
770.849546	1553.552469	-1071.376992	770.937634	1553.567640	-1071.307864
770.739834	1554.048500	-1071.443381	770.574734	1553.970761	-1071.655896
770.812172	1553.507576	-1071.429845	770.656984	1553.384542	-1071.541372
770.886765	1553.486626	-1071.368627	770.804075	1553.460739	-1071.409068
770.855256	1553.537442	-1071.373001	770.929009	1553.581959	-1071.316484
770.473668	1553.730912	-1071.711852	770.518618	1553.871778	-1071.750677
770.812433	1553.526335	-1071.481920	770.673588	1553.391868	-1071.530246
770.848152	1553.427754	-1071.398996	770.811650	1553.443445	-1071.428391
770.828737	1553.582995	-1071.404591	770.968682	1553.590582	-1071.282654

Table 4.9 Forward kinematics error analysis results (continuous operation).

TRANSFORMATION TRANSLATION VECTOR

766.816000 1999.542000 450.384000

TRANSFORMATION ROTATION MATRIX

-0.834106	-0.551560	-0.007048
0.551364	-0.834051	0.018882
-0.016292	0.011863	0.999797

ROBOT METROLOGY INSTRUMENT MEASURED POSITION COORDINATES CONVERTED TO ROBOT CONTROLLER MEASURED POSITION COORDINATES

X	Y	Z	X	Y	Z
-725.045335	1108.134445	-615.438797	-725.349002	1108.039475	-615.291652
-725.458301	1108.563457	-614.985088	-725.205515	1108.628964	-615.053075
-725.477690	1108.677730	-614.861566	-725.364405	1108.637964	-614.934023
-725.498942	1108.611094	-614.828439	-725.596995	1108.614394	-614.756191
-725.658966	1108.100896	-614.983389	-725.503572	1108.065471	-615.159301
-725.537641	1108.515180	-614.971618	-725.230628	1108.662077	-614.999286
-725.378581	1108.654921	-614.947418	-725.418354	1108.629268	-614.895077
-725.410145	1108.603360	-614.893990	-725.578853	1108.601139	-614.810489
-725.228422	1108.217392	-615.215845	-725.420972	1108.064177	-615.230305
-725.425337	1108.571729	-614.976426	-725.211008	1108.666846	-615.044068
-725.447133	1108.642204	-614.914017	-725.411962	1108.686391	-614.922135
-725.484864	1108.588894	-614.884692	-725.597951	1108.596675	-614.802402
-725.252142	1108.188879	-615.219012	-725.411466	1108.083689	-615.213023
-725.331885	1108.572141	-615.041369	-725.249123	1108.617515	-615.024504
-725.364099	1108.676989	-614.966480	-725.387450	1108.669143	-614.939927
-725.391866	1108.598368	-614.956589	-725.586555	1108.568143	-614.820238
-725.221889	1108.211750	-615.245091	-725.334255	1108.102103	-615.255426
-725.378225	1108.545170	-615.030191	-725.215747	1108.631811	-615.042640
-725.436955	1108.665882	-614.896310	-725.368617	1108.677218	-614.939155
-725.480566	1108.588958	-614.904390	-725.562896	1108.626179	-614.836532
-725.662178	1108.113498	-614.963094	-725.480091	1108.083294	-615.173798
-725.424259	1108.604797	-614.957156	-725.226169	1108.619743	-615.067592
-725.475353	1108.664554	-614.897414	-725.391818	1108.639789	-614.936807
-725.477069	1108.604715	-614.900671	-725.563539	1108.609318	-614.844839

Table 4.9 **Forward kinematics error analysis results (continuous operation).**

-725.263106	1108.226559	-615.230942	-725.378021	1108.133121	-615.268820
-725.434456	1108.588311	-615.009002	-725.244137	1108.622997	-615.056652
-725.410461	1108.691793	-614.927847	-725.388461	1108.658025	-614.956455
-725.479852	1108.551504	-614.931283	-725.601625	1108.624639	-614.811560

ROBOT CONTROLLER MEASURED POSITION COORDINATES BASED ON FORWARD KINEMATICS ALGORITHMS

X	Y	Z	X	Y	Z
-724.986000	1108.215000	-615.395000	-725.360000	1108.073000	-615.294000
-725.445000	1108.589000	-614.971000	-725.219000	1108.663000	-615.023000
-725.474000	1108.732000	-614.815000	-725.397000	1108.692000	-614.877000
-725.507000	1108.641000	-614.802000	-725.601000	1108.654000	-614.718000
-725.659000	1108.132000	-614.974000	-725.477000	1108.104000	-615.160000
-725.534000	1108.541000	-614.934000	-725.214000	1108.714000	-614.977000
-725.442000	1108.670000	-614.869000	-725.416000	1108.688000	-614.868000
-725.467000	1108.631000	-614.834000	-725.631000	1108.612000	-614.729000
-725.262000	1108.249000	-615.196000	-725.427000	1108.109000	-615.215000
-725.424000	1108.600000	-614.953000	-725.255000	1108.683000	-614.979000
-725.455000	1108.653000	-614.876000	-725.443000	1108.702000	-614.839000
-725.484000	1108.617000	-614.841000	-725.598000	1108.618000	-614.739000
-725.266000	1108.236000	-615.209000	-725.434000	1108.119000	-615.172000
-725.382000	1108.594000	-614.979000	-725.245000	1108.658000	-615.017000
-725.417000	1108.657000	-614.893000	-725.388000	1108.676000	-614.887000
-725.433000	1108.571000	-614.894000	-725.597000	1108.600000	-614.762000
-725.229000	1108.233000	-615.229000	-725.382000	1108.126000	-615.211000
-725.397000	1108.566000	-614.996000	-725.242000	1108.668000	-614.996000
-725.447000	1108.707000	-614.854000	-725.441000	1108.664000	-614.857000
-725.481000	1108.609000	-614.850000	-725.562000	1108.617000	-614.775000
-725.691000	1108.131000	-614.903000	-725.501000	1108.104000	-615.129000
-725.437000	1108.621000	-614.905000	-725.256000	1108.664000	-615.000000
-725.472000	1108.681000	-614.853000	-725.405000	1108.653000	-614.875000
-725.499000	1108.600000	-614.829000	-725.557000	1108.604000	-614.781000
-725.244000	1108.232000	-615.211000	-725.398000	1108.117000	-615.221000
-725.422000	1108.584000	-614.965000	-725.252000	1108.652000	-615.009000
-725.431000	1108.694000	-614.860000	-725.450000	1108.666000	-614.859000
-725.507000	1108.588000	-614.841000	-725.620000	1108.627000	-614.725000

Table 4.9 Forward kinematics error analysis results (continuous operation).

ISO DEFINITION POSITIONING ACCURACY

DeltaL = 0.054416 DeltaLx = 0.015127 DeltaLy = -0.022612 DeltaLz = -0.047127

ISO DEFINITION POSITIONING REPEATABILITY

r = 0.089617

RIA/ANSI DEFINITION POSITIONING ACCURACY AND ITS STANDARD DEVIATION

dPA = 0.063842, SPA = 0.022006

RIA/ANSI DEFINITION POSITIONING REPEATABILITY AND ITS STANDARD DEVIATION

rREP = 0.035678, SREP = 0.017980

Table 4.10 Forward kinematics error analysis results (interrupted operation).

FORWARD KINEMATICS PTP ACCURACY AND REPEATABILITY ERRORS MEASUREMENT TEST

The number of PTP tests was = 56

ROBOT METROLOGY INSTRUMENT MEASURED POSITION COORDINATES
(Each Represents the Calculated Average Position From 1 Observation)

X	Y	Z	X	Y	Z
766.078458	1554.880623	-1073.626813	765.958049	1554.903767	-1073.784051
766.042282	1554.496745	-1073.743137	765.999853	1554.413324	-1073.775527
766.081632	1554.446924	-1073.702483	766.114853	1554.421779	-1073.681841
766.146089	1554.504260	-1073.629050	766.166000	1554.518395	-1073.634330
765.884230	1554.615005	-1073.791004	765.948985	1554.813628	-1073.801478
766.043356	1554.446858	-1073.757522	766.023978	1554.378044	-1073.753522
766.113264	1554.448968	-1073.697380	766.070512	1554.423667	-1073.692121
766.149772	1554.517655	-1073.625054	766.237044	1554.556294	-1073.560295
765.934019	1554.588574	-1073.765221	765.974645	1554.836016	-1073.787705
766.054300	1554.512493	-1073.755921	766.038840	1554.373073	-1073.759125
766.116845	1554.427987	-1073.683146	766.124442	1554.434364	-1073.662485
766.204001	1554.535331	-1073.563762	766.234674	1554.558130	-1073.567740
765.924206	1554.633662	-1073.789847	766.001622	1554.878490	-1073.776352
766.106104	1554.488634	-1073.734878	766.033132	1554.344199	-1073.764747
766.078602	1554.398114	-1073.705019	766.114086	1554.465425	-1073.681980
766.125471	1554.499700	-1073.670794	766.229186	1554.551315	-1073.578823
765.956926	1554.658467	-1073.763034	766.000968	1554.879154	-1073.785471
766.114496	1554.518983	-1073.741425	766.075306	1554.397880	-1073.761177
766.117035	1554.382286	-1073.705617	766.104459	1554.402669	-1073.732542
766.183449	1554.500292	-1073.641180	766.223321	1554.533442	-1073.594768
765.944703	1554.686038	-1073.782600	766.014160	1554.901284	-1073.794184
766.110183	1554.488831	-1073.747903	766.057220	1554.38747[illegible]	-1073.781931
766.132939	1554.445344	-1073.712619	766.119729	1554.32223[illegible]	-1073.703215
766.200528	1554.575282	-1073.649591	766.237563	1554.56958[illegible]	-1073.606776
765.913366	1554.646957	-1073.833599	765.999188	1554.858071	-1073.806455
766.121555	1554.503069	-1073.761229	766.070124	1554.399473	-1073.764368
766.170832	1554.461352	-1073.702356	766.155713	1554.423319	-1073.682296
766.246058	1554.602996	-1073.632545	766.293513	1554.561520	-1073.561995

Table 4.10 Forward kinematics error analysis results (interrupted operation).

TRANSFORMATION TRANSLATION VECTOR

766.816000 1999.542000 450.384000

TRANSFORMATION ROTATION MATRIX

-0.834106	-0.551560	-0.007048
0.551364	-0.834051	0.018882
-0.016292	0.011863	0.999797

ROBOT METROLOGY INSTRUMENT MEASURED POSITION COORDINATES
CONVERTED TO ROBOT CONTROLLER MEASURED POSITION COORDINATES

X	Y	Z	X	Y	Z
-722.217673	1104.808123	-617.060268	-722.128896	1104.719462	-617.215238
-721.974947	1105.106154	-617.180533	-721.893316	1105.151726	-617.213215
-721.980576	1105.170171	-617.141119	-721.994562	1105.209850	-617.121321
-722.066482	1105.159276	-617.068071	-722.090849	1105.158365	-617.073507
-721.908005	1104.919471	-617.224412	-722.071496	1104.789315	-617.233583
-721.948225	1105.148083	-617.195525	-721.894135	1105.194869	-617.192026
-722.063124	1105.186004	-617.136509	-721.958546	1105.183633	-617.130854
-722.076970	1105.150210	-617.063977	-722.171532	1105.167324	-617.000195
-721.935137	1104.969455	-617.199759	-722.105344	1104.785051	-617.219965
-721.993567	1105.099404	-617.193323	-721.903751	1105.20710	-617.197929
-721.999639	1105.205746	-617.122585	-722.009638	1105.20500	-617.101976
-722.132384	1105.166524	-617.003372	-722.170516	1105.16434	-617.007578
-721.951648	1104.925974	-617.223686	-722.151353	1104.764714	-617.208550
-722.023766	1105.148264	-617.173412	-721.883024	1105.227932	-617.203799
-721.951109	1105.209163	-617.144185	-722.017995	1105.173022	-617.120930
-722.046475	1105.150923	-617.109525	-722.162101	1105.166795	-617.018650
-721.992810	1104.923832	-617.197117	-722.151110	1104.763627	-617.217649
-722.047459	1105.127455	-617.179734	-721.947835	1105.206480	-617.200280
-721.974432	1105.243543	-617.145596	-721.974995	1105.219101	-617.172069
-722.095370	1105.182955	-617.080855	-722.147239	1105.178167	-617.034708
-721.997684	1104.893727	-617.216153	-722.174258	1104.752279	-617.226313
-722.027185	1105.150103	-617.186498	-721.926865	1105.204793	-617.220859
-722.022429	1105.199586	-617.152108	-721.943576	1105.295157	-617.143951
-722.150918	1105.129668	-617.088653	-722.178968	1105.155648	-617.046517

Table 4.10 Forward kinematics error analysis results (interrupted operation).

-721.949630	1104.908082	-617.267094	-722.137848	1104.779834	-617.238850
-722.044429	1105.144246	-617.199838	-721.944369	1105.202234	-617.203367
-722.062937	1105.207322	-617.142275	-722.029490	1105.231086	-617.122424
-722.204301	1105.131978	-617.072023	-722.221504	1105.194069	-617.002753

ROBOT CONTROLLER MEASURED POSITION COORDINATES BASED ON FORWARD KINEMATICS ALGORITHMS

X	Y	Z	X	Y	Z
-722.480000	1105.235000	-616.783000	-722.379000	1105.154000	-616.947000
-722.217000	1105.534000	-616.916000	-722.140000	1105.580000	-616.936000
-722.223000	1105.610000	-616.860000	-722.236000	1105.602000	-616.860000
-722.310000	1105.572000	-616.775000	-722.368000	1105.573000	-616.736000
-722.164000	1105.346000	-616.949000	-722.341000	1105.204000	-616.949000
-722.237000	1105.533000	-616.908000	-722.145000	1105.608000	-616.912000
-722.251000	1105.602000	-616.861000	-722.195000	1105.602000	-616.873000
-722.322000	1105.546000	-616.799000	-722.399000	1105.555000	-616.739000
-722.200000	1105.332000	-616.940000	-722.353000	1105.180000	-616.978000
-722.223000	1105.513000	-616.948000	-722.145000	1105.604000	-616.942000
-722.239000	1105.619000	-616.852000	-722.273000	1105.600000	-616.813000
-722.366000	1105.555000	-616.743000	-722.413000	1105.552000	-616.729000
-722.221000	1105.308000	-616.958000	-722.380000	1105.165000	-616.958000
-722.244000	1105.518000	-616.922000	-722.138000	1105.593000	-616.933000
-722.196000	1105.615000	-616.872000	-722.245000	1105.578000	-616.864000
-722.351000	1105.536000	-616.791000	-722.412000	1105.565000	-616.729000
-722.237000	1105.319000	-616.925000	-722.386000	1105.150000	-616.971000
-722.266000	1105.503000	-616.913000	-722.185000	1105.591000	-616.925000
-722.222000	1105.625000	-616.835000	-722.238000	1105.589000	-616.850000
-722.375000	1105.546000	-616.750000	-722.459000	1105.565000	-616.666000
-722.254000	1105.307000	-616.929000	-722.434000	1105.141000	-616.944000
-722.267000	1105.527000	-616.897000	-722.139000	1105.575000	-616.953000
-722.263000	1105.569000	-616.875000	-722.198000	1105.655000	-616.817000
-722.398000	1105.530000	-616.779000	-722.417000	1105.539000	-616.748000
-722.223000	1105.281000	-616.975000	-722.407000	1105.172000	-616.943000
-722.306000	1105.521000	-616.879000	-722.153000	1105.592000	-616.933000
-722.304000	1105.587000	-616.844000	-722.261000	1105.598000	-616.836000
-722.437000	1105.511000	-616.768000	-722.436000	1105.564000	-616.713000

Table 4.10 Forward kinematics error analysis results (interrupted operation).

ISO DEFINITION POSITIONING ACCURACY

DeltaL = 0.544173 DeltaLx = 0.248242 DeltaLy = -0.393385 DeltaLz = -0.282398

ISO DEFINITION POSITIONING REPEATABILITY

r = 0.084483

RIA/ANSI DEFINITION POSITIONING ACCURACY AND ITS STANDARD DEVIATION

dPA = 0.544994, SPA = 0.023630

RIA/ANSI DEFINITION POSITIONING REPEATABILITY AND ITS STANDARD DEVIATION

rREP = 0.034150, SREP = 0.016778

PB91-185090

NIST-114A (REV. 3-89)	U.S. DEPARTMENT OF COMMERCE NATIONAL INSTITUTE OF STANDARDS AND TECHNOLOGY	1. PUBLICATION OR REPORT NUMBER NISTIR 4478
	BIBLIOGRAPHIC DATA SHEET	2. PERFORMING ORGANIZATION REPORT NUMBER FEBURARY 1991
		3. PUBLICATION DATE

4. TITLE AND SUBTITLE

Recommended Fine Positioning Test for the Development Test Flight (DTF-1) of the NASA Flight Telerobotic Servicer (FTS)

5. AUTHOR(S)

Nicholas Dagalakis, Albert Wavering, Spidaliere, P.;

6. PERFORMING ORGANIZATION (IF JOINT OR OTHER THAN NIST, SEE INSTRUCTIONS)	7. CONTRACT/GRANT NUMBER
U.S. DEPARTMENT OF COMMERCE NATIONAL INSTITUTE OF STANDARDS AND TECHNOLOGY GAITHERSBURG, MD 20899	8. TYPE OF REPORT AND PERIOD COVERED

9. SPONSORING ORGANIZATION NAME AND COMPLETE ADDRESS (STREET, CITY, STATE, ZIP)

NIST CATEGORY #135

10. SUPPLEMENTARY NOTES

☐ DOCUMENT DESCRIBES A COMPUTER PROGRAM; SF-185, FIPS SOFTWARE SUMMARY, IS ATTACHED.

11. ABSTRACT (A 200-WORD OR LESS FACTUAL SUMMARY OF MOST SIGNIFICANT INFORMATION. IF DOCUMENT INCLUDES A SIGNIFICANT BIBLIOGRAPHY OR LITERATURE SURVEY, MENTION IT HERE.)

The purpose of this report is to standardize definitions and propose test procedures for the NASA DTF (Development Test Flight)-1 fine positioning tests. The unique problems associated with the DTF-1 mission are discussed, the standard robot performance tests and terminology are reviewed and a very detailed description of flight-like testing and analysis are presented.

The major technical problems associated with DTF-1 are that only one position sensor can be used, which will be fixed at one location, with a working volume which is probably smaller than some of the robot errors to be measured. Radiation heating of the arm and the sensor could cause distortions that would interfere with the test.

Two robot performance testing committees have established standard testing procedures relevant to the DTF-1. Due to the technical problems associated with DTF-1 these procedures cannot be applied as have been proposed. Although these standard tests call for the use of several test positions at specific locations, only one, that of the position sensor, can be used by DTF-1. Off-line programming accuracy might be impossible to measure and in that case it will have to be substituted by forward kinematics accuracy.

12. KEY WORDS (6 TO 12 ENTRIES; ALPHABETICAL ORDER; CAPITALIZE ONLY PROPER NAMES; AND SEPARATE KEY WORDS BY SEMICOLONS)

fine positioning tests; NASA development test flight; NASA flight telerobotic servicer; robot performance test

13. AVAILABILITY	14. NUMBER OF PRINTED PAGES
[X] UNLIMITED	124
[ ] FOR OFFICIAL DISTRIBUTION. DO NOT RELEASE TO NATIONAL TECHNICAL INFORMATION SERVICE (NTIS).	
[ ] ORDER FROM SUPERINTENDENT OF DOCUMENTS, U.S. GOVERNMENT PRINTING OFFICE, WASHINGTON, DC 20402.	15. PRICE A06
[X] ORDER FROM NATIONAL TECHNICAL INFORMATION SERVICE (NTIS), SPRINGFIELD, VA 22161.	

ELECTRONIC FORM